Biogenic Emission of Halocarbons

Dissertation
zur Erlangung des Grades
„Doktor der Naturwissenschaften“
im Promotionsfach Chemie

am Fachbereich der Chemie, Pharmazie und Geowissenschaften
der Johannes Gutenberg-Universität Mainz

vorgelegt von
Sarah Gebhardt
geboren in Düren
Mainz, 2008

Since Karl Wilhelm Scheele, Joseph Priestley and Antoine de Lavoisier discovered in the late 18th century that air is not an element but consists of several gases, scientists of the following centuries spared no effort to determine its components in detail.

This is one more attempt.

Abstract

Within this doctoral thesis, biogenic emissions of several globally relevant halocarbons have been investigated in different environments. An airborne and a shipborne field campaign were performed as well as a laboratory study, to investigate the release of selected halocarbons namely, methyl chloride, methyl bromide, methyl iodide, dibromomethane, chloroform and bromoform to the atmosphere. The airborne study was focused on the tropical rainforest ecosystem while the shipborne measurements investigated naturally occurring oceanic plankton blooms. The laboratory experiments using dried plant material were made to elucidate abiotic production mechanisms occurring in organic matter.

Airborne measurements over the tropical rainforest of Suriname and French Guyana (3 - 6 °N, 51 - 59 °W) revealed net fluxes of 9.5 (± 3.8 2σ) μg m^{-2} h^{-1} methyl chloride and 0.35 (± 0.15 2σ) μg m^{-2} h^{-1} chloroform emitted in the long dry season (October) 2005. No significant flux was observed for methyl bromide within the limits of these measurements. An extrapolation of these numbers to all tropical forests around the globe helped to narrow down the range of the recently discovered and poorly quantified methyl chloride source from tropical ecosystems. The value for methyl chloride obtained (1.5 (± 0.6 2σ) Tg yr^{-1}) is at the lower end of the range of current best estimates, which is reasonable, since a net flux inherently accounts for interfering sinks (e.g. soil uptake) in the same area. These results affirm that the contribution of the tropical forest ecosystem is the major source in the global budget of methyl chloride. The extrapolated global net chloroform flux from tropical forests (56 (± 23 2σ) Gg yr^{-1}) is of minor importance (5 - 10 %) compared to the global sources and might already be included in the soil emissions term. A source of methyl bromide from this region could not be verified.

A possible production pathway for halocarbons namely abiotic formation from dead plant material was tested in a laboratory study. The release of methyl chloride and methyl bromide from plant tissue representative of grassland, deciduous forest, agricultural areas and coastal salt marshes (hay, ash, tomato and saltwort) and bromide enriched pectin has been monitored. Incubations at different temperatures (25 - 50 °C) revealed significant emissions even at ambient temperature, and that the emissions increased exponentially with temperature. The emission rates doubled approximately each 5 °C temperature step. The strength of the emission was found to be additionally dependent on the availability of halide and the methoxyl group within the plant tissue. However, high water content in the plant material was found to inhibit methyl halide emissions. The abiotic nature of the reaction yielding methyl halides was confirmed by its high activation energy calculated via Arrhenius plots.

Shipborne measurements of the atmospheric mixing ratios of methyl chloride, methyl bromide, methyl iodide, dibromomethane and bromoform have been conducted along a South Atlantic transect from the 27.01. - 05.02.2007 onboard the French research vessel *Marion Dufresne.* The main focus of this study was set on the characterization of halocarbon emissions from a large-scale natural algae bloom encountered off the coast of Argentina. Mixing ratios of methyl chloride and methyl bromide were not significantly affected by the occurrence of the phytoplankton bloom, consisting mainly of dinoflagellates and diatoms. Emissions of methyl iodide, dibromomethane and bromoform showed pronounced mixing ratio variations, triggered by phytoplankton abundance. Variation in the relative size of the peaks was attributed to inhomogeneous species specific phytoplankton emissions or contributions from coastal sources (e.g. salt marshes or macroalgae) in vicinity of the coast. Methyl iodide was strongly correlated with DMS throughout sampled region. A new technique combining satellite derived biomass marker (chlorophyll a) data with back trajectory analysis was successfully used to attribute variations in mixing ratios to air masses, which recently passed over areas of enhanced biological production.

Zusammenfassung

Im Rahmen dieser Doktorarbeit wurden die biogenen Emissionen mehrerer global relevanter Halogenkohlenwasserstoffe in unterschiedlichen Regionen der Welt untersucht. Die Freisetzung bestimmter halogenierter Kohlenwasserstoffe in die Atmosphäre (Methylchlorid, Methylbromid, Methyliodid, Chloroform, Bromoform und Dibrommethan) wurde in zwei Feldkampagnen sowie einer Laborstudie untersucht. Die erste Feldstudie konzentrierte sich auf das Ökosystem des tropischen Regenwalds, während die zweite Studie auf die Untersuchung einer natürlichen Planktonblüte ausgerichtet war. In Laboruntersuchungen von getrocknetem Pflanzenmaterial wurde die Temperaturanhängigkeit eines möglichen abiotischen Bildungsmechanismus halogenierter Kohlenwasserstoffe geprüft.

Bei Flugzeugmessungen über dem tropischen Regenwald von Suriname und Französisch-Guyana (3 - 6 °N, 51 - 59 °W) in der Trockenzeit (Oktober 2005) konnte ein Nettofluss von 9.5 (± 3.8 2σ) μg m^{-2} h^{-1} Methylchlorid und 0.35 (± 0.15 2σ) μg m^{-2} h^{-1} Chloroform bestimmt werden. Für Methylbromid wurde innerhalb der Messungenauigkeit kein signifikanter Fluss festgestellt. Eine Extrapolation dieser Daten auf alle tropischen Wälder der Erde ergab eine globale Methylchloridquelle von 1.5 (± 0.6 2σ) Tg yr^{-1}. Dadurch konnte der Bereich der kürzlich endeckten, aber bislang unzureichend quantisierten, Methylchloridquelle innerhalb tropischer Ökosysteme eingeschränkt werden. Der erhaltene Wert befindet sich im unteren Bereich der bisherigen Abschätzungen. Dies erscheint sinnvoll, da er als Nettofluss alle eventuell auftretenden Senken (z.B. Aufnahme durch den Boden) beinhaltet. Trotzdem stellt eine Emission dieser Größenordungn die Hauptquelle des globalen Methylchloridhaushaltes dar. Der extrapolierte globale Netto-Chloroformfluss aus tropischen Wäldern (56 (± 23 2σ) Gg yr^{-1}) ist dagegen von geringer globaler Bedeutung (5 - 10 % der Gesamtquellen) und könnte schon durch andere Quellen im globalen Budget (z.B. Bodenemission) erfasst sein. Die Region konnte nicht als Quelle von Methylbromid bestätigt werden.

Innerhalb einer durchgeführten Laborstudie wurde ein möglicher Bildungsmechanismus von halogenierten Kohlenwasserstoffen, die abiotische Freisetzung aus Pflanzenmaterial, untersucht. Die Abgabe von Methylchlorid und Methylbromid aus pflanzlichen Gewebe und mit Bromid angereichertem Pectin sowie deren Temperaturabhängigkeit wurden ermittelt. Als Material dienten dabei ausgewählte Pfanzenarten repräsentativ für Wiesen und Weiden, Laubwald, landwirtschaftlich genutzte Flächen und Küstengebiete (Heu, Esche, Tomate und Salzkraut). Inkubationen der Proben bei unterschiedlichen Temperaturen (25 – 50 °C) ergab eine exponentielle Temperaturabhängigkeit. Die Emissionsrate verdoppelte sich ca. alle 5 °C. Bemerkenswert ist, dass schon bei

Umgebungstemperaturen von 25 °C signifikante Emissionen festgestellt werden konnten. Die Stärke der Emission war zusätzlich von dem Halogen- und Methoxylgruppengehalt des Materials abhängig. Ein hoher Wassergehalt des Gewebes dagegen, verhinderte die Reaktion. Über die Höhe der Aktivierungsenergie konnte bestätigt werden, dass es sich um eine abiotische Reaktion ohne Enzymbeteiligung handelt.

Währen einer Atlantiküberquerung auf dem französichen Forschungsschiff *Marion Dufresne* vom 27.01. – 05.02.2007 wurden die atmosphärischen Mischungsverhältnisse von Methylchlorid, Methylbromid, Methyliodid, Dibrommethan und Bromoform aufgezeichnet. Das Ziel dieser Studie war es, den Einfluss einer großflächigen Algenblüte vor der Küste Argentiniens auf die Emissionen von halogenierten Kohlenwasserstoffen zu charakterisieren.
Im Gebiet der Phytoplanktonblüte, die hautsächlich aus Dinoflagellaten bzw. Diatomeen bestand, konnte keine signifikante Veränderung der Mischungsverhältnisse von Methylchlorid und Methylbromid beobachtet werden. Methyliodid, Dibrommethan und Bromoform allerdings zeigten ausgeprägte Variationen ihrer atmosphärischen Mischungsverhältnisse, die wahrscheinlich durch das Vorhandensein der Algenblüte zustande kamen. In Küstennähe konnte andere Quellen, wie z.B. Salzwiesen oder Makroalgen, nicht ausgeschlossen werden. Variationen in der relativen Größe der Peaks zueinander sind auf unterschiedlich starke Emissionen verschiedener Algenspezies zurückzuführen. Methyliodid zeigte durchgehend eine gute Korrelation mit DMS. Mit Hilfe einer neuen Technik, die Satellitenbilder des Phytoplanktonmarkers Chlorophyll a mit Rückwärtstrajektorien der untersuchten Luftmassen kombiniert, konnten die Variationen der Mischungsverältnisse von Methyliodid, Dibrommethan und Bromoform Emissionen aus biologisch aktiven Gebieten zugeordnet werden.

Contents

Chapter 1

Current state of knowledge on atmospheric halocarbons

"Halocarbon" is the short form for halogenated hydrocarbon, i.e. a molecule consisting of a hydrocarbon in which one or more hydrogen atoms are substituted by halogen atoms.

Within this chapter the basic properties of the halocarbons investigated are introduced and the effects on atmospheric chemistry are described. Particular emphasis is placed on the impact of halocarbons on the stratospheric and tropospheric ozone cycles. In addition, halocarbons influence Earth's radiation budget directly by absorption of infrared radiation or indirectly by their contribution to the depletion of ozone, which is itself a greenhouse gas. Suppression of particle forming processes in the marine boundary layer is yet another potential interference with the Earth's radiation budget. Degradation products of halocarbons, so called reactive halogen species, modify the oxidation capacity of the atmosphere directly and indirectly by their interaction with reaction cycles of the main atmospheric oxidants such as ozone, the hydroxyl radical and the nitrogen oxides.
The second section of this chapter provides an overview on the sources and sinks of the investigated halocarbon compounds. Their global distribution as well as its seasonal and spatial variation is described.
The third section is dedicated to the production pathways of mono- and polyhalogenated hydrocarbons. Several possible biotic or abiotic processes leading to the formation of halocarbons are presented.

Possibly the most widely known halocarbons are the chlorofluorocarbons (CFCs). These anthropogenic species gained notoriety in the 1980s when they were shown, by virtue of their long atmospheric lifetimes, to deliver significant chlorine to the stratosphere and thereby cause the stratospheric ozone hole. Fortunately, the anthropogenic contribution to the organohalogen budget is now regulated by the Montreal Protocol and the ambient concentrations of many man-made halogenated compounds are stabilizing or declining. Thus, the relative influence of naturally produced halocarbons is becoming more important for the budgets of ozone depleting substances.

Within the scope of this PhD-thesis biogenic emissions of several globally relevant halocarbons were investigated in different environments. In two field campaigns and one laboratory study the release of a set of halocarbons - namely, methyl chloride, methyl bromide, methyl iodide, dibromomethane, chloroform and bromoform - from tropical ecosystems, oceanic plankton blooms and dried plant material was studied.

Halocarbon emissions from the tropical rainforest presented in Chapter 2 are not only interesting because the rainforest represents one of the largest and most biodiverse ecosystems, but also because the proximity to the Intertropical Convergence Zone (ITCZ) means that any emission there will have an enhanced chance of being transported rapidly into the upper troposphere/stratosphere by regionally prevalent deep convection. The large-scale airborne experiment was designed specifically to gauge the net effect of this rainforest ecosystem and to obtain data that could be extrapolated to all tropical rainforested regions. The airborne study inherently accounted for all sources and sinks, the measured result being the present net effect of halocarbon emissions from the rainforest. In reality this net effect is the result of the multitude of processes within the rainforest e.g. soil microbes, fungi, leaves and litter, living plants and animals and abiotic reactions within the canopy. In particular for prognostic purposes, it is of interest to know how these individual processes contribute to the net effect with changing ambient parameters. If the future Earth warms, as it is predicted to do, assessing the change in the effectiveness of the various halocarbon contributing processes with temperature will be particularly important.
One of the possible production pathways for halocarbons, namely abiotic formation from dead plant material, was tested in a laboratory study. Results are presented as Chapter 3 of this thesis. The observed emission of monohalocarbons was found to be highly dependent on temperature. It is noteworthy, that this abiotic production took place even at ambient temperature (25 °C). Thus, the abiotic degradation of plant litter might be responsible for a significant part of the emissions observed over the rainforest. With increasing temperature due to global warming, this production pathway will become more important.
Another source term included in the global budget of many halocarbons is the ocean. Covering more than two third of the Earth's surface the importance of such a source is obvious. Nevertheless, the term ocean is rather vague because, similar to the "rainforest ecosystem", it summarizes a myriad physical, chemical and biological processes occurring in the seawater as one net effect. In a second field campaign, described in Chapter 4, the halocarbon mixing ratios over the South Atlantic Ocean were investigated. An attempt was made to link the variations in the mixing ratios to parameters such as the phytoplankton abundance or the abundance of certain phytoplankton species, by using newly available calculations based on satellite data.
The overall goal has been to find an easily accessible parameter (e.g. the vegetation index or chlorophyll abundance as marker for phytoplankton abundance), which exhibits a significant correlation with halocarbon emissions. This relationship then could be used to better parameterize the global emissions of specific halocarbons, particularly if it is based on satellite measurements. Emission maps derived in this way could be implemented in global models to help simulate the present and future developments in halocarbon distribution more accurately.

1 Atmospheric chemistry of halocarbons

The halocarbons investigated within this thesis are: methyl chloride (CH_3Cl); methyl bromide (CH_3Br); methyl iodide (CH_3I); dibromomethane (CH_2Br_2); bromoform ($CHBr_3$) and chloroform ($CHCl_3$). As each species has only one carbon they can be considered as derivates of methane, with one or more hydrogen atoms being replaced by halogen atoms. Their molecular shape is therefore approximately tetrahedral as shown in Fig. 1.1.

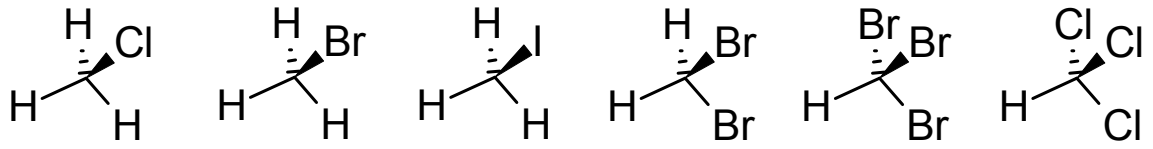

Figure 1.1: Structural formula of CH_3Cl, CH_3Br, CH_3I, CH_2Br_2, $CHBr_3$ and $CHCl_3$.

CH_3Cl and CH_3Br are gaseous at ambient temperature, whereas CH_3I, $CHCl_3$, CH_2Br_2 and $CHBr_3$ are liquids. A summary of the physical properties and safety data for these halocarbons is given in Table 1.1.

Compound	Molar mass / g mol^{-1}	Melting point / °C	Boiling point / °C	Danger Symbol
CH_3Cl	50.5	-97.6	-24.2	F^+, X_n
CH_3Br	94.9	-94	4	T, N
$CHCl_3$	119.38	-64	62	X_n
CH_3I	141.94	-66.5	42.5	T
CH_2Br_2	173.85	-52.7	97	X_n, N
$CHBr_3$	252.73	8.3	149-152	T, N

Table 1.1: Physical properties of selected halocarbon compounds (source: ILO, 2008), Danger symbols refer to the standard symbols labeling convention (F^+: highly flammable, X_n: harmful, T: toxic, N: environmentally dangerous).

As can be seen from the warning symbols the pure substances are rather noxious, being at least harmful (symbol X_n), if not not toxic (T). Some of them are identified as exhibiting a serious threat to the environment (N). However, in the mixing ratio ranges usually encountered in the atmospheric environment (circa one molecule per 10^9 - 10^{12} molecules of air) they have no direct harmful effects to animals, plants or the environment. In fact some of them are even produced by plants (see section 1-3.2 – "Biogenic production").
Nevertheless, their effect on Earth's climate is not negligible, even at these low mixing ratios. Their influence on Earth's radiation budget and atmospheric chemistry is described in the following sections.

1.1 The influence of halocarbons on the radiation budget

The radiation budget of the Earth can be considered to be in steady state, a balance between the incoming short-wave radiation from the sun in the UV and visible, and the long wave radiation reemitted from the Earth mainly in the infrared region of the spectrum. The atmosphere as a whole is relatively transparent to incoming solar radiation, and large amounts penetrate the atmosphere and heat the Earth's surface (circa 100 - 800 W m^{-2}). When a gas molecule absorbs radiation, the energy is transformed into internal molecular motion, which is detectable as a rise in temperature; i.e. by absorbing radiation a gas molecule heats its surrounding. The absorption of UV radiation in the stratosphere by molecular oxygen (O_2) and ozone (O_3) causes the temperature to rise with increasing altitude in this region of the atmosphere (Lutgens and Tarbuck, 2007). The main absorbing gases for outgoing infrared radiation from the Earth are water vapour and carbon dioxide (CO_2), which combine to produce a natural "greenhouse effect". Through reabsorption of about 60 % of the radiation emitted by the Earth, water vapour accounts for the warm temperatures in the lower troposphere, where it is most highly concentrated. The two main absorbers, H_2O and CO_2, leave a very small wavelength range, the so-called atmospheric "window", at which outgoing radiation is not absorbed. Any chemical species present in the atmosphere, which can absorb outgoing radiation within this "window" (e.g. halocarbons), intensifies the natural greenhouse warming. The extent to which a substance influences the radiation budget of the Earth is determined by its atmospheric mixing ratio and its ability to absorb radiation in the relevant range of the spectrum.

A measure of a compounds contribution to global warming is given by the global warming potential (GWP). This parameter is a relative scale, which compares the effect of a particular amount of the compound of interest with the same mass of CO_2. The global warming potential of CO_2 is 1 by definition. It depends on the following factors: the absorption of infrared radiation by the given species, the spectral location of its absorption and the atmospheric lifetime of the species. The GWP is calculated over a specific time interval, usually 100 years. A gas, which is quickly removed from the atmosphere, may initially have a large effect, but integrated for longer time periods it becomes less important.

The duration of an atmospheric perturbation is dependent on the atmospheric lifetime of the species in question and thus trace gases are generally categorized into "long lived" (lifetime > 0.5 yr) and "very short lived substances" (VSLS) (lifetime < 0.5 yr). VSLS are defined as trace gases, whose local tropospheric lifetimes are comparable to, or shorter than, tropospheric transport time scales, such that their tropospheric distributions are non-uniform. In practice, VSLS are considered to have atmospheric lifetimes of less than 6 months (WMO, 2007b). In contrast long lived substances have lifetimes of more than 6 month and are therefore usually well distributed around the globe.

The lifetimes of the halocarbon compounds investigated in this study are rather short compared to CO_2 or the CFCs (e.g. lifetime CFC-11 45 yrs, CFC-12 100 yrs (WMO, 2007a), CO_2 adjustment time ~ 100 yrs (IPCC, 2007). As shown in Table 1.2 the

atmospheric lifetimes of these naturally emitted halocarbons span a range of several days up to one year.

	Compound	Lifetime / days	Reference
Long lived	CH_3Cl	365	WMO, 2007a
	CH_3Br	255	WMO, 2007a
Very short lived	$CHCl_3$	150	WMO, 2007a
	CH_2Br_2	120	WMO, 2003b
	$CHBr_3$	26	WMO, 2003b
	CH_3I	7	WMO, 2003b

Table 1.2: Lifetimes of investigated halocarbons.

For very short lived species (i.e. lifetime less than half a year) one of the assumptions in the calculation of GWP, namely that the species is well mixed throughout the troposphere like CO_2, no longer holds and therefore the concept of giving a single value for GWP is not appropriate (WMO, 2007c). CH_3Cl and CH_3Br both have moderate direct global warming potentials. The dependence of their GWP on the time horizon chosen is shown in Table 1.3. However, due to CH_3Br's ability to destroy O_3 (see section 1-1.2.1 - "Effects on the ozone chemistry"), a greenhouse gas itself, the direct effect of CH_3Br is outweighed and a slightly negative indirect GWP results overall (100 years indirect GWP of CH_3Br: -2.2 ± 1.5 (WMO, 2007c)).

Compound	GWP for 20 years	GWP for 100 years	GWP for 500 years	Reference
CH_3Cl	45	13	4	WMO, 2007c
CH_3Br	17	5	1	WMO, 2007c

Table 1.3: Direct GWPs of CH_3Cl and CH_3Br for various timeframes.

1.2 A transport mechanism for halogen atoms

Volatile organic halocarbons represent an important means of transporting halogen atoms to the upper layers of the atmosphere, most importantly to the stratosphere. The effectiveness with which a halocarbon species can transfer halogen atoms depends on the atmospheric lifetime, emission rates (and hence mixing ratio), and the number of halogen atoms per molecule.

Halogens are transported to the stratosphere by a variety of anthropogenic and biogenic gases. The primary sources of chlorine in the stratosphere in 2004 were dominated by anthropogenic compounds. The CFCs (e.g. CFC 11 and CFC 12) and carbon tetrachloride make up most of the man-made sources. CH_3Cl is considered the most important natural source accounting for about 16 % of stratospheric chlorine. Very short lived chlorinated

gases like CH_2Cl_2 or $CHCl_3$ contributed only up to 3 % to the stratospheric chlorine budget (WMO, 2007d). Total bromine in the atmosphere is 160 times less abundant than chlorine. The amount of natural and human-made bromine reaching the stratosphere is in the same range, with halons and CH_3Br being the largest sources. The 2006 "Scientific Assessment of Ozone Depletion" showed that CH_3Br contributed 37 % of the total bromine amount (with 7 % being attributed to human-made emissions). Very short lived brominated gases e.g. $CHBr_3$ made up to 24 % of the total stratospheric bromine (WMO, 2007d).

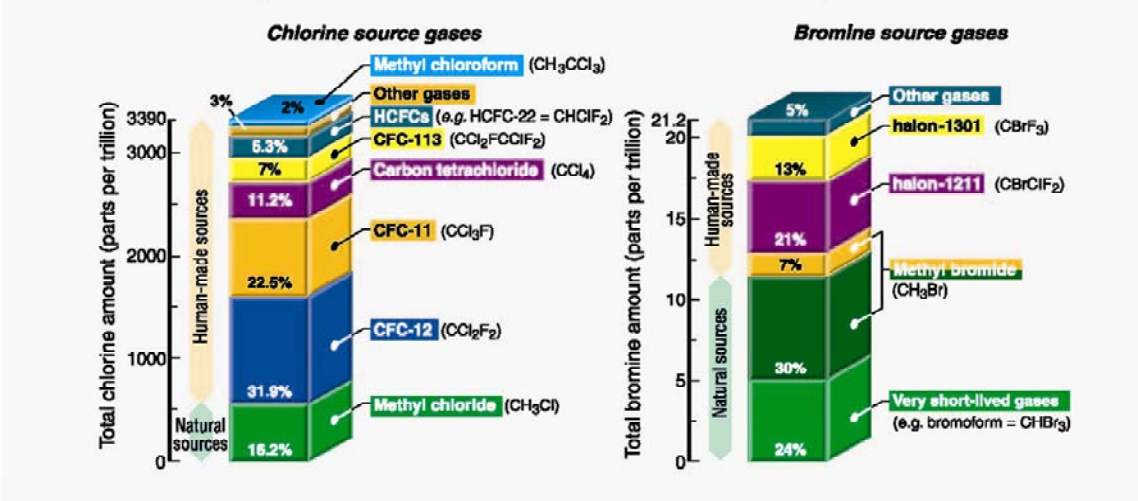

Figure 1.2: Sources of chlorine and bromine to the stratosphere (source: WMO, 2007d).

Although bromine and iodine in the stratosphere are much less abundant than chlorine, their concentrations are still of great interest, since the O_3 removal efficiency of bromine is 60 times higher than the one of chlorine (WMO, 2007b), while iodine is even 150 - 300 times more effective than chlorine in depleting O_3 on per atom basis (WMO, 2003b).

However, both iodine and fluorine have been found not to play a role in stratospheric O_3 depletion. Fluorine atoms react rapidly with water or methane to form the stable reservoir species hydrogen fluoride (HF), while iodine containing organic molecules, react so rapidly in the lower atmosphere that they do not reach the stratosphere in significant quantities (WMO, 2007b; WMO, 2007c).

Since the anthropogenic contribution to the organohalogen budget was regulated by the Montreal Protocol, the average atmospheric concentrations of many such halogenated compounds are stabilizing or declining (WMO, 2003a). Therefore the relative influence of naturally produced halocarbons is becoming more important for stratospheric O_3 depletion. CH_3Cl and CH_3Br are both in part naturally emitted. In fact they are the most abundant chlorine and bromine containing gases in the troposphere. Currently CH_3Cl contributes up to 16 % to the tropospheric organic chlorine and CH_3Br up to about 50 % to the organic bromine (WMO, 2003a). It is estimated that the contribution of natural CH_3Cl and CH_3Br to the equivalent effective stratospheric chlorine will rise to more than 50 % by 2050 (currently 23 %) (WMO, 2007c).

1.2.1 Effects on the ozone chemistry

Chemical/photochemical degradation of halocarbons in the gaseous phase leads to the formation of reactive halogen atoms. These take part in many reaction cycles involving the major oxidants O_3, its photolysis product the hydroxyl radical (OH), and nitrogen oxides ($NO + NO_2 = NO_x$). In order to understand the influence exerted by these halogen atoms we must first briefly consider the natural cycles involved in stratospheric ozone.

1.2.1.1. Stratospheric ozone

O_3 is formed in the stratosphere via the photodissociation of molecular oxygen (O_2) and the recombination of the resultant oxygen atoms (O) with other O_2 molecules. This process leads to a maximum of O_3, the so-called ozone layer, between 15 and 30 km height, where both UV radiation and O_2 abundance are sufficient to maintain O_3 formation. This layer is crucial to life on Earth, because O_3 absorbs potentially harmful UV radiation from the sun and thereby shields the plants and animals at the Earth's surface.
The simplest idea for the formation and degradation of O_3 in the stratosphere is the Chapman-Cycle (proposed in 1930 by Sidney Chapman):

$O_2 + h\nu$	$\rightarrow 2\,O$	$(\lambda \leq 242\ nm)$[1]	R 1
$2\,[O + O_2 + M$	$\rightarrow O_3 + M]$		R 2
Net: $3\,O_2 + h\nu$	$\rightarrow 2\,O_3$		

$O_3 + h\nu$	$\rightarrow O + O_2$	$(\lambda \leq 310\ nm)$[1]	R 3
$O + O_3$	$\rightarrow 2\,O_2$		R 4
Net: $2\,O_3$	$\rightarrow 3\,O_2$		

This natural O_3/O_2 cycle may be perturbed by the presence of halogens atoms (X) as follows.

$X + O_3$	$\rightarrow XO + O_2$		R 5
$O_3 + h\nu$	$\rightarrow O + O_2$	$(\lambda \leq 310\ nm)$[1]	R 6
$O + XO$	$\rightarrow X + O_2$		R 7

Or via halogen oxide recycling by reaction with the hydroperoxyl radical (HO_2) and subsequent photolysis:

$X + O_3$	$\rightarrow XO + O$	R 5
$XO + HO_2$	$\rightarrow HOX + O_2$	R 8
$HOX + h\nu$	$\rightarrow X + OH$	R 9
$OH + CO + O_2$	$\rightarrow CO_2 + HO_2$	R 10

[1] reference: Finlayson-Pitts and Pitts (1999)

Net: $CO + O_3 \rightarrow CO_2 + O_2$

The reactions (R5 - R10) in which chlorine atoms act as a catalyst was introduced by Stolarski and Cicerone (1974). A year later, in 1975 the respective reactions for bromine were confirmed by Wofsy et al. (1975). If not transformed in a non-reactive form, halogen radicals keep running through this cycle repeatedly, destroying more and more O_3 molecules. The catalytic cycle may be stopped by the conversion of the free radicals X or XO to reservoir species, which are inert to reaction with O_3, e.g. HX or $XONO_2$ (Solomon et al., 1986). However, the halogens can be reactivated if the reservoir species are broken down releasing free radicals again (e.g. by photolysis or reaction with OH). A real removal of the halogen catalysts from the atmosphere occurs if air or particles containing reactive halogens returns to the troposphere and these gases are removed from the air by moisture and rain (WMO, 2007d).

The halogen monoxide (XO) produced via halocarbon oxidation also has an impact on tropospheric ozone cycles. A detailed description of the chemistry involved is given in section 1-1.2.1.2 – "Tropospheric ozone".

The halogen radical reaction cycles occur, at least in part, naturally, since the catalyzing species may result from biogenic emissions (OH from water vapour, NO from the reaction of O (^1D) with N_2O, which mainly results from microbial processes within the soil, and halogen atoms from the photolysis of natural emitted halocarbons). On the other hand these compounds can also be introduced into the stratosphere by human activities, e.g NO from air plane exhaust or nuclear explosions (Graedel and Crutzen, 1994). Halogen catalysed O_3 depletion attracted huge scientific and public interest since Molina and Rowland (1974) linked the increasing emission of man-made CFCs to atmospheric destruction of O_3. The photodissociation of these presumed inert substances in the stratosphere produces significant amounts of chlorine, contributing to the catalytic cycles described above.

The Antarctic "ozone hole"

Stratospheric O_3 depletion by CFCs takes place all over the world. However, in polar regions, especially over Antarctica increased O_3 depletion occurs due to special meteorological conditions. These result in the springtime Antarctic ozone hole, which was first reported by Farman et al. (1985) for the period from 1980 to 1984.

The meteorological conditions requisite for the "ozone hole" consist of a polar vortex, a circumpolar circulation pattern emerging over the Antarctic continent during austral winter, which isolates polar air from surrounding air masses creating a closed atmospheric reactor. In addition, very low temperatures over the Antarctic during polar winter (up to -80 °C) allow the formation of polar stratospheric clouds (PSCs). These unusual clouds contain frozen water or a mixture of water and HNO_3, and provide a reaction site for heterogeneous reactions. At the surface of the PSCs, chlorine reservoir species (e.g. HCl and $ClONO_2$) are activated forming HNO_3 and molecular chlorine

(Cl_2). The heterogeneous reaction at the surface of the ice particles happens to be much faster than within the gas phase (Solomon et al., 1986). The resultant HNO_3 is implemented into the ice matrix, whereas the molecular chlorine is released to the gas phase. As the clouds grow, these ice particles may sink out of stratosphere due to gravitation. This process leads to a net removal of nitric acid from the stratosphere.

Therefore Cl_2 is formed by a heterogeneous reaction at the surface of the PSC particles during the polar night and accumulates in the Antarctic stratosphere due to the lack of vertical and horizontal mixing and the absence of light. When in the austral spring sunlight returns to the Antarctic region, the photolysis of Cl_2 starts the catalytic destruction cycle of O_3 destruction (R5 – R10). In the absence of other reaction possibilities, ClO is able to recycle halogen atoms by forming a dimer (ClOOCl) which can photolyse to release free Cl radicals again. Unlike Cl_2, HNO_3 bound at the ice particles does not photolyse. Therefore NO_2, the reactant which could have transformed ClO again into a reservoir species namely $ClONO_2$, is lacking. The catalytic destruction proceeds causing the springtime stratospheric ozone hole over Antarctica. As the polar vortex breaks up and the Antarctic stratosphere warms in summer, PSCs can no longer form, and the heterogeneous chemistry shuts down. The O_3 over the Antarctic then returns to near "normal" levels.

Essentially the same processes also happen in the Arctic stratosphere. However, the O_3 depletion there is much less pronounced than in the Antarctic. Since the Arctic winter atmosphere is generally warmer, PSC formation is less effective. Furthermore, temperature and wind conditions are much more variable and during fall and winter the poleward and downward transport of O_3 rich air from lower latitudes is stronger, i.e. the Arctic vortex is less distinct. Thus, total O_3 values are higher in the Arctic than in the Antarctic at the beginning of winter. All these factors combined cause Arctic O_3 depletion to be more variable and less pronounced.

1.2.1.2 Tropospheric ozone

While stratospheric O_3 shields the Earth from harmful UV radiation, tropospheric O_3 is a pollutant. It is phytotoxic, destroys rubber and other polymers possessing double bonds, and contributes to urban smog. O_3 can irritate the human respiratory system and even harm lung cells at high concentration (WHO, 2003).
The high energy wavelength UV radiation required for O_2 photolysis is not available at ground level. However, O_3 can still be formed via a more complicated process involving oxides of nitrogen (NO_x), volatile organic compounds (VOCs) or carbon monoxide (CO) and the presence of sunlight.
The basic tropospheric O_3/NO_x cycle rapidly reaches a photostationary state in which ozone is neither formed nor destroyed (see reactions R11 - R13)

$NO_2 + h\nu \rightarrow NO + O$ R 11

$O + O_2 \rightarrow O_3$ R 12

$NO + O_3 \rightarrow NO_2$ R 13

The steady state may be disturbed by the presence of peroxy radicals (produced through the oxidation of CO or VOCs), which transform NO to NO_2 without consuming O_3. The result is a net production of O_3 during daylight.

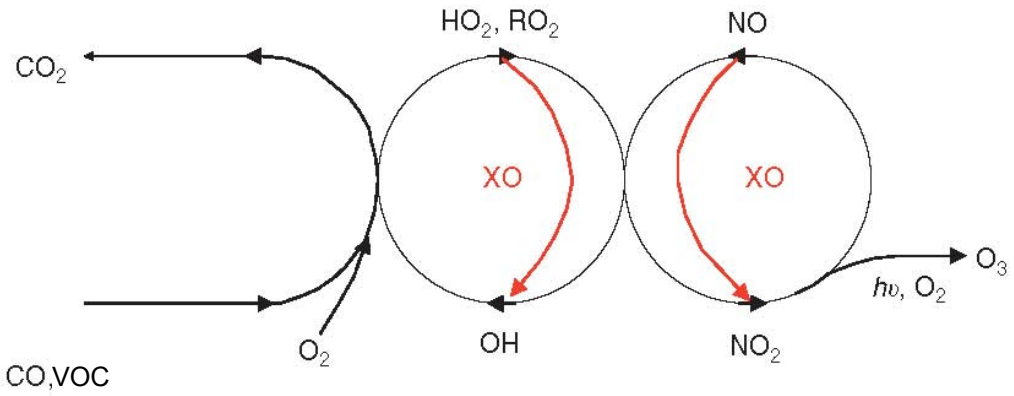

Figure 1.3: Interaction of halogen monoxides with tropospheric O_3 production (source: von Glasow and Crutzen (2007)).

Halogens can influence the aforementioned tropospheric O_3 cycle by short cutting two major reactions responsible for O_3 production (red arrows in Fig. 1.3). Under high NO_x conditions the reaction of XO with NO shifts the NO/NO_2 ratio to lower values. However, this reaction does not lead to net O_3 destruction since XO and NO_2 are both part of the odd oxygen family, i.e. potential precursors of O_3. But the reaction of XO with NO competes against the reaction of a peroxy radical with NO. The latter reaction transforms a non-odd oxygen species to a possible O_3 precursor, therefore leading to O_3 production (see Fig. 1.3). By bypassing this reaction XO suppresses O_3 production.
Secondly, the reaction of XO with HO_2 destroys one member of the odd oxygen family (von Glasow and Crutzen, 2007), leading to a net reduction in O_3 production. The formation of halogen nitrate ($XONO_2$) from XO and NO_2 and successive uptake on aerosols or cloud droplets removes NO_2 from the gas phase and reduces thereby O_3 formation.

In summary, O_3 in the troposphere is destroyed directly via the X/XO catalytic cycle as described in section 1-1.2.1.1 - "Stratospheric ozone", or indirectly by influencing the HO_2/OH and NO/NO_2 ratios, and thereby their contribution to the O_3 cycle.
Bromine related reactions have been reported to reduce zonal annual mean O_3 mixing ratios by up to 18 % (von Glasow et al., 2004). Yang et al. (2005) found a significant O_3 destruction of 4 - 6 % due to bromine chemistry in most of the troposphere, whereas larger reductions up to 30 % were found at high latitudes. Although organic emissions of bromine are relatively small compared to sea salt derived bromine, in their model, bromocarbons provided the main source of upper tropospheric Br_x. Davis et al. (1996) found that estimated tropospheric reactive iodine mixing ratios of 1.5 or 7 pmol mol^{-1}, respectively, originating from volatile organic iodine compounds may account for 6 to up to 30 % of the total column O_3 destruction. A recent study investigating the impact of

halogen oxide radicals on O_3 depletion over the open ocean (Read et al., 2008) showed that halogen-mediated O_3 loss contributed on average 56 % to the total daily O_3 loss. Monoxides of bromine and chlorine in the marine atmosphere stem mainly from sea salt (von Glasow, 2008b), whereas formation of IO in the marine boundary layer is initiated by the air-sea exchange of volatile organoiodine compounds being rapidly photolyzed within the atmosphere (Carpenter et al., 2003).

Ozone depletion events "bromine explosion"

Severe surface "ozone depletion events" (ODEs), have been observed in the Arctic at polar sunrise under special meteorological conditions, i.e. when the boundary layer is capped by an inversion layer (Oltmans, 1981;Oltmans and Komhyr, 1986; Bottenheim et al., 1986). The underlying mechanism can be summarized as follows. At high levels of BrO, the BrO self reaction represents a highly effective pathway to recycle Br radicals (Barrie et al., 1988) and destroys O_3 via the mechanism described in section 1-1.2.1.1 – "Stratospheric ozone". A special feature of this cycle is a heterogeneous reaction of HOBr, which is able to catalyze the release of halide ions from the aqueous phase (e.g. brine layer on top of fresh sea ice) as gaseous halogens (Fan and Jacob, 1992; Vogt et al., 1996). This autocatalytic cycle leads to an exponential release of bromine, a so-called "bromine explosion", if sufficient bromide is available and gas phase losses of bromine are less than 50 % (von Glasow and Crutzen, 2007).
Although it is widely accepted that the main source for reactive bromine during ODEs are reactions in the snowpack and the aforementioned release from young sea ice (von Glasow and Crutzen, 2007), the starting pulse might stem from volatile organic compounds like $CHBr_3$ released by algae. Their oxidation products may provide the initial reactive bromine to start the autocatalytic cycle of O_3 destruction at polar sunrise (Barrie et al., 1988).

1.2.2 Influence on the atmospheric oxidation capacity

As described in the previous sections halogen mediated destruction of O_3 removes the primary precursor of atmospheric oxidation. Loss of O_3 decreases the formation of OH and thus indirectly affects the oxidation capacity of the atmosphere. Besides influencing the oxidation power of the atmosphere by interacting with the cycles of the major oxidants, halogens also act as oxidizing agents themselves.

Halogen atoms have the potential to oxidize hydrocarbons like alkanes, alkenes, aldehydes and aromatics by H-abstraction or addition to unsaturated bonds. In the marine boundary layer, where Cl atoms are formed from seasalt, chlorine oxidation may under certain circumstances become significant (Wingenter et al., 1996; Finlayson-Pitts and Pitts, 1999).

Fluorine and chlorine atoms react readily with alkanes, aldehydes and HO_2 by abstracting a hydrogen atom (Platt and Janssen, 1995). Via this reaction, hydrocarbon radicals and highly water soluble HX are formed.

$Cl + CH_4 \rightarrow HCl + CH_3$ R 14

It should be noted that peroxy radicals (ROO) formed by the successive reaction of hydrocarbon radicals with O_2 lead to O_3 formation in the presence of NO_x (see Fig. 1.3). Thus, in polluted air (at high NO_x and alkane abundance) halogen atoms favour ozone production (von Glasow, 2008a).

Within the troposphere, HX may be irreversibly removed by wet or dry deposition, lowering the amount of active halogen available for O_3 depletion. Furthermore, heterogeneous reactions can recycle active halogen species from HX. The only important gas phase removal for HX is given by reaction with OH, which returns the halogen atom to the gas phase (Platt and Janssen, 1995).

$HX + OH \rightarrow X + H_2O$ R 15

For heavier halogens the reactivity towards hydrogen abstraction decreases. Bromine atoms can only abstract hydrogen from aldehydes or HO_2, while iodine is even less reactive, reacting significantly only with HO_2 ((Platt and Janssen, 1995). This is one reason why more bromine and iodine remain in a reactive form and thus are more effective destroying O_3, see section 1-1.2 – "Transport mechanism for halogen atoms".

Compounds containing unsaturated bonds generally react with chlorine atoms by addition, resulting in chlorine-containing peroxy radical products after addition of O_2. A reaction with aromatic compounds can become significant if they contain saturated side chains from which the chlorine atom can abstract hydrogen, or unsaturated bonds, to which it can add (Finlayson-Pitts and Pitts, 1999).

1.2.3 Effects on particle formation

Interaction with the DMS cycle

Within the marine boundary layer the oxidizing capability of BrO impacts the chemistry of dimethyl sulphide (DMS). The mixing ratio of DMS is strongly reduced when BrO is present, and this rapid reaction then dominates over the "usual" oxidation pathway by OH or NO_3. An increase in DMS oxidation by BrO leads to enhanced production of dimethyl sulfoxide (DMSO), which is rapidly taken up by clouds. This reduces the DMS to SO_2 conversion efficiency, which is key to the formation of new cloud condensation nuclei, but increases the size of already present cloud condensation nuclei. The result is a reduction of cloud albedo, mitigating the cooling effects of DMS on the climate (von Glasow et al., 2004).

Particle formation by iodine

Several nucleation bursts in the coastal atmosphere have been observed and attributed to iodine chemistry (O'Dowd et al., 1998; O'Dowd et al., 2002). The self-reaction of IO leading to OIO is thought to be responsible. The OIO then proceeds through self-reaction to I_2O_4 and further to a polymeric structure, which condenses forming a condensation nucleus. Since these oxides are produced during the photochemical oxidation of organic iodocarbons like CH_3I and CH_2I_2, initially the rapidly photolyzing CH_2I_2 was thought to play a major role as iodine source. However, the primary source of condensable iodine vapour is now thought to be molecular iodine (O'Dowd and Hoffmann (2005) and references therein).

In conclusion, halocarbons or halogen atoms released from them have a profound effect on the chemistry of the atmosphere. They influence the radiation budget of the Earth and the oxidation power of the atmosphere directly as well as indirectly by interaction with reaction cycles of several important compounds (O_3, HO_2, NO/NO_2, DMS). Their major impact on atmospheric chemistry is their contribution to tropospheric and stratospheric O_3 depletion.
Generally, longer lived chlorine containing compounds contribute more to O_3 depletion in the stratosphere, whereas the shorter lived bromine containing halocarbons influence tropospheric ozone destruction. Since iodocarbons are formed by marine organisms and very short lived, they primarily impact the marine boundary layer. However, deep convection events are occasionally able to transfer even short-lived substances rapidly upward, so that non-negligible amounts make it to the upper troposphere and stratosphere before being destroyed (Dvortsov et al., 1999). Model studies suggest, that short lived brominated trace gases, in particular $CHBr_3$, may contribute significantly to the stratospheric halogen budget (Dvortsov et al., 1999; Nielsen and Douglass, 2001). In contrast to bromine the contribution of iodine to the stratospheric O_3 loss is likely relatively small. A fact that is attributed to the much shorter lifetimes of iodinated compounds (WMO, 2007b).

2 Global distribution, sources and sinks

Many halomethanes have both, natural and anthropogenic sources. Among those investigated here, the majority are emitted by natural processes.
A summary on the present understanding of the sources and sinks of the investigated compounds is provided in Table 1.4. The range of these numbers is an indication of how well these terms are currently determined. For example the recently discovered CH_3Cl source from tropical plants and decaying plant material is still rather poorly defined. Its huge range makes it hard to tell whether or not the global CH_3Cl budget is closed. A more precise estimate of the tropical contribution is presented in Chapter 2 of this thesis.

	Source type	Source strength /Gg yr^{-1} min	Source strength /Gg yr^{-1} max	Sink type	Sink strength /Gg yr^{-1} min	Sink strength /Gg yr^{-1} max
CH_3Cl [a]	Tropical/subtropical plants	820	8200	OH reaction	3800	4100
	Tropical senescent/dead leaves	30	2500	Soils	100	1600
	Biomass burning	325	1125	Cl reaction	180	550
	Oceans	380	500	Loss to stratosphere	100	300
	Fungi	43	470	Loss to polar oceans	93	145
	Salt marshes	65	440			
	Fossil fuel burning	5	205			
	Waste incineration	15	75			
	Wetlands	48	48			
	Industrial processes	10	10			
	Rice Paddies	2.4	4.9			
	Total	**1743**	**13578**	**Total**	**4273**	**6695**
CH_3Br [b]	Oceans	23	119	Soils	32	154
	Fumigation	28.2	64.4	Oceans	37	133
	Biomass burning	10	40	OH and photolysis	60	100
	Salt marshes	7	29			
	Gasoline	0	10			
	Wetlands	2.3	9.2			
	Rapeseed	4.8	8.4			
	Fungi	0.5	5.2			
	Peatlands	0.1	3.3			
	Shrublands	0.5	2			
	Rice paddies	0.5	2.5			
	Total	**77**	**293**	**Total**	**129**	**387**

[a] after WMO (2007a) and references therein
[b] after WMO (2003a) and references therein

Table 1.4: Sources and sinks of investigated long lived compounds.

	Source type	Source strength /Gg yr^{-1} min	max	Sink type	Sink range /Gg yr^{-1} min	max
$CHCl_3$ [c]	Open Oceans	270	450	OH reaction	370	830
	Soil processes	120	320	Soils	not quantified	
	Pulp and paper manufacture	26	42			
	Water treatment	8	34			
	Volcanic and geological sources	9	15			
	Other industrial sources	9	13			
	Anaerobic fermentation	2	4			
	Biomass burning [d]	2	2			
	Total	**446**	**880**	**Total**	**370**	**830**
CH_2Br_2	Ocean [e]	304		OH and Photolysis [h]	60	73
	Total	**304**		**Total**	**60**	**73**
$CHBr_3$	Ocean [e, f]	843		OH and Photolysis [h]	158	264
	Water chlorination [f]	29				
	Rice paddies [g]	0.04				
	Total	**862**		**Total**	**158**	**264**
CH_3I	Ocean [e]	610		Photolysis [h]	134	179
	Rice paddies [i]	16	29			
	Vegetation and Soils [m]	33				
	Biomass burning [j]	< 10				
	Wet lands [k]	7.3				
	Salt marshes [n]	3.0				
	Peat lands [k]	1.4				
	Total	**670.7**	**693.7**	**Total**	**134**	**179**

[c] after McCulloch (2003)
[d] (Lobert et al., 1999)
[e] (Butler et al., 2007)
[f] (Quack and Wallace, 2003)
[g] (Redeker et al., 2003)
[h] (WMO, 2003b)
[i] (Lee-Taylor and Redeker, 2005)
[j] (Andreae et al., 1996)
[k] (Dimmer et al., 2001)
[m] (Sive et al., 2007)
[n] (Manley et al., 2006)

Table 1.4 continued: Sources and sinks of the short lived compounds investigated.

On close inspection, total global sources and sinks of CH_2Br_2, $CHBr_3$ and CH_3I show a significant discrepancy: namely, the ocean sources exceed the sinks by more than a factor of three. For example, the global atmospheric sink of $CHBr_3$ amounts to 158 - 264 Gg yr^{-1}, whereas the sources add up to 862 Gg yr^{-1}, dominated by an average oceanic source of 843 Gg yr^{-1}. The large numbers for oceanic emissions stem from a recent survey of Butler

et al. (2007), including emissions from highly productive estuarine and coastal areas. Whereas the sink estimates stem from the latest Scientific Assessment of Ozone Depletion (WMO, 2007b), adopted unchanged from a former version (WMO, 2003b). The latter numbers are calculated from the estimated burden divided by the lifetime. An underestimated burden, i.e. by not taking into account elevated mixing ratios over strong biogenic hot spots (coastal and shelf areas), may lead to an underestimated global atmospheric sink. On the other hand, the oceanic sources reported by Quack and Wallace (2003) and Butler et al. (2007) are based on saturation anomalies and might be overestimated due to the approximations used for the flux calculations (e.g. overestimated transfer coefficients) (pers. com. B. Quack, IfM-GEOMAR, Kiel, Germany, 2008). This substantial bias in source and sink calculations emphasizes the need to further investigate the global distribution of the strongly variable sources of these compounds.

The atmospheric loss of organohalogens in the gas phase occurs primarily via reaction with OH or photolysis. Chlorinated very short lived substances tend to be predominantly removed in the troposphere through reaction with OH; whereas the brominated VSLS are removed by a combination of UV photolysis and OH reaction depending on the degree of halogen substitution (increased importance of photolysis with higher bromine substitution) and iodine containing VSLS are removed almost exclusively by photolysis (WMO, 2007b).
Lifetimes given in Table 1.2 provide the combined lifetime with respect to OH reaction and photolysis. However, they should be seen as approximate estimates, since they do not take into account regional variations in the OH concentration, solar flux and the spatial and seasonal distribution of the halomethanes.

2.1 Methyl chloride - CH_3Cl

The global average concentration of CH_3Cl is approximately 550 ± 30 pmol mol^{-1} with higher mixing ratios observed at low latitudes (Thompson et al., 2004). Small downward trends have been reported recently from the AGAGE (Advanced Global Atmospheric Gases Experiment) measurement sites (Simmonds et al., 2004). According to the assessment provided by WMO (2007a) and references therein, the sources and sinks of CH_3Cl are as shown in Table 1.4. Earlier global budget estimates indicated that biomass burning was its main source (WMO, 1999). However, after Keene et al. (1999) and Butler (2000) highlighted an imbalance in the budget of this species, a new dominant source of CH_3Cl from tropical vegetation was discovered by Yokouchi et al. (2002) and subsequently verified by airborne field measurements of Scheeren et al. (2003). Although the sources of CH_3Cl appear to balance the sinks, large uncertainties remain regarding the nature of the tropical source since few measurements are available from this region.
The latitudinal variation of CH_3Cl in annually averaged atmospheric mixing ratios within the marine boundary layer shows a maximum in the tropics exceeding mixing ratios at the poles by about 40 pmol mol^{-1} (Khalil and Rasmussen, 1999b). The seasonal cycle can be explained mostly by the cycles of OH radicals, which are the major sink for CH_3Cl in the atmosphere. It exhibits maximum concentrations in late-winter/early-spring falling to

a minimum in late-summer/early-autumn (Khalil and Rasmussen, 1999b; Cox et al., 2003; Simmonds et al., 2004). Spikes of very high mixing ratios up to 1400 and 2750 pmol mol^{-1} have been reported by Li et al. (1999) and Yokouchi et al. (2007) from the coast of sub-/tropical islands during calm nights, pointing to a (coastal) source located in the tropics. This is in agreement with previous model calculations. Lee-Taylor et al. (2001) found that the observed mixing ratios of CH_3Cl can be reproduced by the addition of a tropical terrestrial source of 2330 - 2430 Gg yr^{-1} and the reduction of Southeast Asian biomass burning emissions. The inverse model study of Yoshida et al. (2006) suggested a seasonally invariant additional source of 2900 Gg yr^{-1} located in the tropics (30 °N – 30 °S) to explain the observed distribution.

2.2 Methyl bromide - CH_3Br

Although 50 - 60 times less abundant than CH_3Cl, CH_3Br concentrations are of great interest. It has a 25 times higher ozone depletion potential than CH_3Cl, caused by the fact that on a per atom basis bromine is 60 times more effective in destroying O_3 than chlorine (WMO, 2007c). The main global sources are oceanic production and escape when used as a fumigation agent. Due to emission restrictions related to the Montreal Protocol the global average concentration is decreasing from peak values of 9.2 pmol mol^{-1} in 1999 to currently about 7.9 pmol mol^{-1} (WMO, 2007a). Although balanced within the uncertainties, sinks seem to outweigh the sources, pointing to an underestimated or yet unknown source term. Furthermore, model calculations of Lee-Taylor et al. (1998) found that the annual observations of CH_3Br are best represented if an additional terrestrial net source of 89 – 104 Gg yr^{-1} is assumed, which is located to 50 - 71 % in the southern hemisphere. A later 3-D global chemical transport model run performed by Warwick et al. (2006) used increased biomass burning emissions (+20 Gg yr^{-1}) and an additional source of 45.6 Gg yr^{-1} CH_3Br from tropical (40 °N – 40 °S) vegetation to reproduce the annual observations. Conversely, it is also conceivable that the atmospheric lifetime of methyl bromide has been underestimated, which would help to explain the imbalance between sources and sinks (Reeves, 2003).
Wingenter et al. (1998) recorded a pronounced seasonal CH_3Br cycle exhibiting an autumn minimum and a maximum in early spring, consistent with strong seasonal removal by OH radicals, although for the southern hemisphere no well-defined seasonal cycle could be observed. These results were confirmed by measurements of Simmonds et al. (2004) in Mace Head, Ireland and Cape Grim, Tasmania during the years 1998 - 2001. Wingenter et al. (1998) found the same seasonal variation (maximum in late boreal winter, minimum in later boreal summer) in the CH_3Br interhemispheric ratio and calculated a seasonally weighted average of NH/SH = 1.2, caused by industrial sources mainly located in the northern hemisphere.

2.3 Chloroform - $CHCl_3$

The budget of $CHCl_3$ is reasonably balanced within the uncertainties and was recently summarized by McCulloch (2003) (see Table 1.4 for summary).
Antarctic firn air measurements (Trudinger et al., 2004) showed a steady increase from 4 pmol mol^{-1} around 1940 to peak values of 6.5 pmol mol^{-1} in 1990. After 1990 global observations showed a downward trend. Global average mixing ratios of 18.5 pmol mol^{-1} between 1985 and 1995 (Khalil and Rasmussen, 1999a) decreased to average background levels of 8.9 (± 0.1) pmol mol^{-1} in the years 1994 - 1998 (O'Doherty et al., 2001). The global distribution of $CHCl_3$ is strongly biased between the two hemispheres with 1.7 times higher mixing ratios found in the northern hemisphere, mirroring the uneven distribution of significant terrestrial based sources (Khalil and Rasmussen, 1999a). The main natural sources are oceanic production and soil processes. Anthropogenic emissions are thought to contribute about 10 % of the global emissions (McCulloch, 2003). However, a recent model study suggests that a higher anthropogenic contribution (41 – 50 % of the global sources) before 1990, versus 25 – 29 % in 2001, would better explain the global observations (Worton et al., 2006).
The seasonal cycle of background $CHCl_3$ mixing ratios shows a maximum in late-winter/early-spring falling to a minimum in late-summer/early-autumn (Khalil and Rasmussen, 1999a; O'Doherty et al., 2001; Cox et al., 2003), corresponding to the inverse of the OH cycle, which is the dominant atmospheric sink for $CHCl_3$.

2.4 Dibromomethane - CH_2Br_2

CH_2Br_2 has no known anthropogenic sources. Accordingly, Worton et al. (2006) found no significant trend in firn air profiles collected during the North Greenland Icecore Project at Greenland (75 °N, 82 °W). Constant mean atmospheric values over 40 years (1950 - 1990) implied that non-natural sources are insignificant. Firn air measurements from two Antarctic stations (Sturges et al., 2001) showed essentially invariant concentrations since the 1930s confirming the thesis that CH_2Br_2 is entirely of natural origin around the globe.
CH_2Br_2 is reasonably well mixed throughout the troposphere because of its wide spread marine sources and its lifetime of about 4 months (WMO, 2003b). Typical values over the open ocean range from 0.3 to 1.3 pmol mol^{-1} CH_2Br_2 (Yokouchi et al., 2005 and references therein; Butler et al., 2007).
Coastal macroalgae seem to play a major role in the atmospheric supply of CH_2Br_2. Mixing ratios up to 4 pmol mol^{-1} were observed in coastal air by Carpenter et al. (2003) at Mace Head, Ireland. Yokouchi et al. (2005) found up to 7.6 pmol mol^{-1} on a tropical island. Close to the source region a good correlation between the molar source strength of CH_2Br_2 and $CHBr_3$ could be observed pointing to a similar source. Carpenter et al. (2003) confirmed this correlation and estimated the molar source strength $CH_2Br_2/CHBr_3$ ratio to range between 15 and 25 %.

2.5 Bromoform - $CHBr_3$

$CHBr_3$ is mainly produced from natural sources in the marine environment (WMO, 2007b). However, it is also formed as a byproduct of water chlorination (Rook, 1974; Quack and Wallace, 2003) and may have a minor source from urban/industrial processes in the northern hemisphere (Blake et al., 2003).
Sturges et al. (2001) reported no significant trends in southern hemispheric $CHBr_3$ mixing ratios since about 1950 deduced from firn air measurements in Antarctica. Whereas firn air measurements conducted by Worton et al. (2006) in the northern hemisphere showed evidence for an increase in the atmospheric burden of on average 16 ± 6 % from 1950 to 1990. This increase was suggested to be predominantly the result of chlorination of seawater used to cool coastal power plants, mainly located in the northern hemisphere.
The background values for the marine boundary layer lie in the range of 0.5 - 1.5 pmol mol^{-1} (Quack and Wallace, 2003). Numerous studies (Carpenter et al., 2003; Chuck et al., 2005; Yokouchi et al., 2005; Butler et al., 2007) have reported widely different mixing ratios highlighting the fact that the ocean is by no means a homogenous source. The coastal areas (i.e. coastal macroalgae) are very important contributors to the global budget of $CHBr_3$. Mixing ratios are more variable and reach higher maximum values at the coast. Up to 22 pmol mol^{-1} were reported by Carpenter et al. (2003) in Mace Head, Ireland measuring air from coastal areas covered with macroalgae and Yokouchi et al. (2005) found up to 43 pmol mol^{-1} of $CHBr_3$ along the coast of tropical islands under a sea breeze. Regarding the open ocean, Butler et al. (2007) and Quack et al. (2004) reported highest $CHBr_3$ fluxes in areas of upwelling water, such as near the equator, and at oceanic fronts.

2.6 Methyl iodide - CH_3I

CH_3I has mixed sources; its global emissions are dominated by marine natural emissions, but it is also released by some terrestrial biomes (wet lands, peat lands (Dimmer et al., 2001) and rice paddies (Lee-Taylor and Redeker, 2005), as well as it is partly man-made (biomass burning (Andreae et al., 1996)). Sturges et al. (2001) conducted firn air measurements at two Antarctic stations and found depth profiles being generally in line with constant annual average values since the mid twentieth century.
Average oceanic background values vary with latitude and distance from the coast. Several field studies report values ranging from 0.3 to 2.4 pmol mol^{-1} (Lovelock and Maggs, 1973; Rasmussen et al., 1982; Happell and Wallace, 1996; Moore and Groszko, 1999; Chuck et al., 2005; Butler et al., 2007). Average marine background values of 1.4 pmol mol^{-1} (1998 - 2001) were reported by Cox et al. (2005) from the coastal site Cape Grim, Tasmania. The mixing ratios peaked during summer despite faster photolysis loss, and showed significantly enhanced local emissions from the ocean during summer time (Cohan et al., 2003). This seasonality showing highest concentrations in summer is observed in the mid latitudes as well (Campos et al., 1996; Blake et al., 1999; Yokouchi et al., 2001).

The latitudinal variation of CH_3I shows no equatorial maxima in the atmospheric mixing ratios, where solar radiation is highest, but at about 10 – 20 ° north and south the equator (Moore and Groszko, 1999; Blake et al., 1999; Blake et al., 2003 and Butler et al., 2007). This likely reflects the complex atmospheric (photo)chemistry of this gas. Elevated values (10 - 20 pmol mol^{-1}) were found in oceanic regions with high biological activity (Rasmussen et al., 1982) and in air passing by coastal areas covered with macroalgae (Lovelock and Maggs, 1973, Carpenter et al., 2003).

2.7 Spatial and seasonal variation of CH_3I, CH_2Br_2 and $CHBr_3$

Atmospheric mixing ratios of VSLS dominated by marine sources (CH_3I, CH_2Br_2 and $CHBr_3$) are typically higher where marine influence is significant. Oceanic emissions constitute by far the largest source of iodinated and brominated VSLS, contributing 90 – 95 % of the total global flux to the atmosphere (WMO, 2007b). Since they are mostly of marine origin, these compounds show very small or no significant interhemispheric differences in mixing ratios.

However, such compounds do exhibit high temporal and spatial variability. Highest mixing ratios occur near coastal areas, oceanic fronts and in the tropics or subtropics (e.g. Quack and Wallace, 2003; Carpenter et al., 2003; Chuck et al., 2005; Yokouchi et al., 2005 and Butler et al., 2007). Mixing ratios vary significantly because of localized sources and short atmospheric lifetimes of these compounds. The combined effect is, that it is quite difficult to calculate an overall global oceanic flux to the atmosphere.

There are some common contributors determining the global distributions: frequently occurring microalgae blooms in springtime and coastal macroalgae emitting at maximum rates when solar radiation is highest i.e. during summertime (Klick, 1993; Goodwin et al., 1997). This results in a seasonal maximum emission in summer in regions influenced by marine air masses (Cohan et al., 2003; Carpenter et al., 2005). However, different photolysis rates of these compounds lead to different latitudinal patterns. CH_2Br_2 and $CHBr_3$ show the highest mixing ratios around the equator, whereas CH_3I peaks at high tropical and subtropical latitudes (Blake et al., 2003; Butler et al., 2007).

3 Production pathways

Most of the halomethanes investigated in this study have both - anthropogenic and biogenic sources, as can be seen from Table 1.4. Since this work is focused on the biogenic production of monohalomethanes, the anthropogenic production pathways are mentioned for the sake of completeness, but not discussed further in detail.
There is a general distinction that can be made between mono- and polyhalomethanes since they are produced via the different production mechanisms. These two kinds of production pathways require different conditions, use different substrates and are catalyzed by different enzymes.

3.1 Anthropogenic production

Biomass burning

Although this mechanism involves plant tissue (as the name implies), it is listed as an anthropogenic production, because 90 % of today's biomass burning is due to human activities (Koppmann et al., 2005). Andreae et al. (1996) reported elevated CH_3Cl, CH_3Br and CH_3I mixing ratios in the smoke from savanna fires in South Africa, highly correlated with CO and with each other. Furthermore it was shown that especially in the smouldering phase of a fire, a significant part of the fuel halide content was released in form of methyl halide species.
Hamilton et al. (2003) showed that abiotic chloride methylation by plant pectin was an efficient, environmentally significant process yielding CH_3Cl. Chloride ions, which are plentiful in the leaf, react with pectin during leaf senescence and an abiotic substitution reaction yields CH_3Cl.

$$\text{Org-O-CH}_3 + X^- \rightarrow \text{Org-O}^- + CH_3X \qquad (X: Cl, Br, I) \qquad \text{R16}$$

This mechanism could account for the release of CH_3Cl, CH_3Br and CH_3I from a variety of plant sources and terrestrial ecosystems during biomass burning, since it has been shown to work most effectively at high temperatures. This mechanism is restricted by the halogen content available in the plant tissue. Nevertheless, literature also reports emission of higher chlorinated compounds like CH_2Cl_2 and $CHCl_3$ emitted during incomplete combustion (Lobert et al., 1999).

Oxidative water treatment

Oxidative water treatment, e.g. the chlorination of drinking water, cooling water for power plants or the use of bleaching agents in pulp and paper production is another important man-made source of polyhalogenated methanes (Rook, 1974; Helz and Hsu, 1978). In this case the oxidizing agent is hypochlorite (ClO^-). Oxidation leads to the breakdown of complex organic molecules (e.g. peptides, humic substances) and a multitude of smaller oxidized molecules is generated (e.g. ketones). ClO^- reacts with

ketones substituting the H-atoms of the alkyl groups adjacent to the keto-group (α-activation) with chlorine. If one of the alkyl moieties is a methyl group, di- or trichloromethane can be split off according to the haloform reaction, as shown in the following reaction scheme. Higher ketones will result in α-halogenated ketones. Rook (1977) described the degradation of fulvic acids by fast chlorination of the carbon atoms that are activated by ortho-OH-substituents.

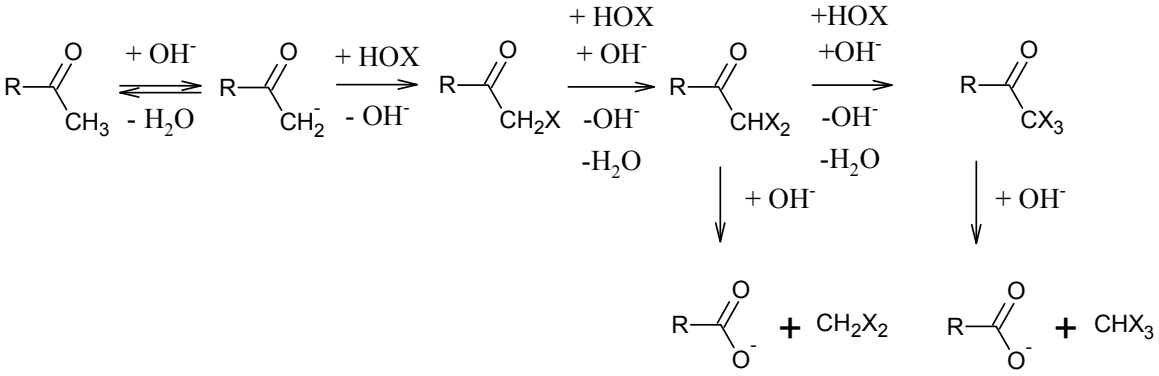

R 17 R 18

If the haloform reaction takes place in the presence of bromine (e.g. seawater) ClO^- is converted to BrO^- and brominated halomethanes are formed (Helz and Hsu, 1978). Helz and Hsu (1978) reported the production of $CHCl_3$, $CHBrCl_2$, $CHBr_2Cl$ and $CHBr_3$ from estuarine and coastal waters induced by adding NaOCl. In the presence of iodine, iodination will occur as well (Rook, 1977).

This process virtually yields no monohalomethanes since the first substitution favors additional substitutions by further activating the α-C. As a result the second step dominates over the first.

3.2 Biogenic production

Regarding the direct biosynthesis of the halomethanes two underlying production pathways need to be considered. Monohalomethanes are produced by a methylation of the respective halide ion. Di- and trihalomethanes are formed via the haloform and/or sulfo-haloform reaction. Both processes involve enzymatic catalyzation.

Enzymatic methylation via halide ion methyl transferase

The most important way to form monohalomethanes in vivo is an enzyme catalyzed transfer of a methyl group to a halide ion. This mechanism proceeds via a methyl donor (e.g. S-adenosyl-L-methionine (SAM)), and a halide ion transferase to carry the methyl group over to the halide ion. As a substrate, several compounds within the plant, containing activated methyl groups might be considered. Sulfur-activated methyl groups provide an electrophilic carbon site for halide ion attack; and sulfur containing amino acid methionine have been reported as a suitable substrate (Harper et al., 1999). Alternatively modified methionine compounds, like methionine methyl sulfonium chloride (MMSCl) (Urhahn and Ballschmiter, 1998) and SAM (Itoh et al., 1997) may serve as the methyl group source.

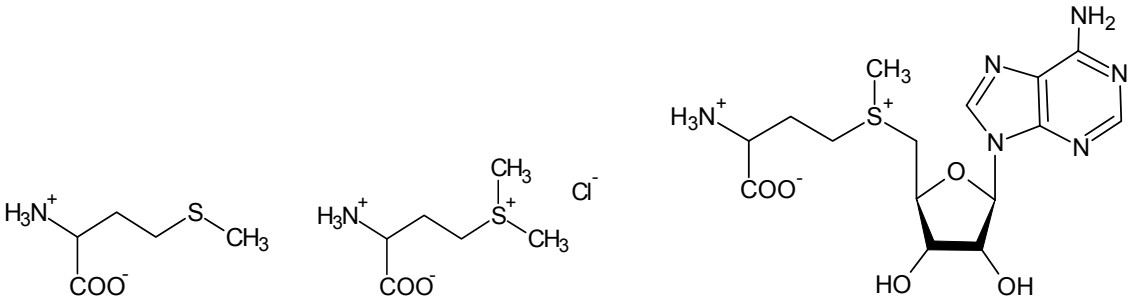

Figure 1.4: Possible sulfur-activated substrates: methionine, MMSCl, SAM.

In the marine environment dimethyl sulfonium salts like dimethyl sulfoniopropionate (DMSP: $(CH_3)_2S^+CH_2CH_2COO^-$) act as a further possible methylation agents. The formation of CH_3Br and CH_3I from dimethyl sulfonium compounds in seawater has been confirmed by White (1982) and Brinckman et al. (1985).

Several studies report halomethane formation from the SAM/methyltransferase system (Wuosmaa and Hager, 1990, Saxena et al., 1998, Attieh et al., 1995), and different kinds of methyl transferase have been found. They show rather different kinetics and substrate specificities (Harper, 2000). Some of them can catalyze the formation of just one of the monohalomethanes, while others are capable of catalyzing simultaneous production of several halocarbons (Itoh et al., 1997). In general the order of reactivity with the halide ions follows the order iodide, bromide, chloride (chloride being the poorest acceptor) consistent with their decreasing nucleophilicity (Wuosmaa and Hager, 1990).

The halide methyl transferase enzyme was detected in marine macro- and micro algae (Itoh et al., 1997), terrestrial plants (Ni and Hager, 1998, Attieh et al., 1995), bacteria (Coulter et al., 1999) and fungi (Saxena et al., 1998; Wuosmaa and Hager, 1990).

While the methyl substitution mechanism can efficiently produce monohalogenated compounds, it is most likely not the source of tri- and dihalomethanes, which would require multiple substitution.

Enzymatic halogenation via haloperoxidase

The enzymatic biohalogenation process is based on two steps. The first one produces electrophilic halogen species like XO^- or R_2NX via haloperoxidase enzymes (X stands for C, Br or I). The oxygen-based oxidant co-substrate is hydrogen peroxide (H_2O_2) as the enzyme nomenclature reflects.

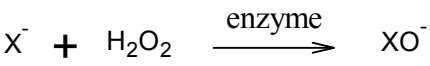

R 19

In the second step the electrophilic halogen molecule attacks a carbonyl activated methyl group and substitutes an H-atom. Subsequent H-atom substitution leads to the formation of di- or trihalogenated methanes. The mechanism is known as the haloform reaction and is described in the previous chapter (R 17 and 18). If the halogenation step does not go to completion and the halogenation is aborted after the second step, dihalomethanes are produced.
A similar reaction involving methylsulfone groups leads to the same result and is called sulfo-haloform reaction.

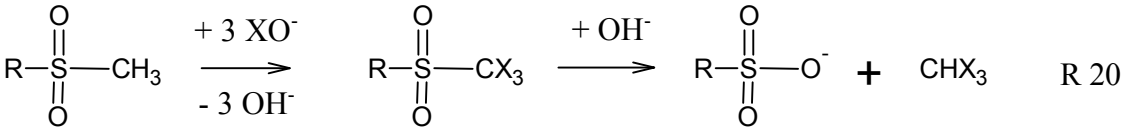

R 20

Urhahn and Ballschmiter, (1998) state that this reaction using methyl sulfur compounds like methionine, DMSO and dimethyl sulfone, serves as a possible source for the biosynthesis of di- and trihalomethanes.

The decarboxylation of trichloroacetic acid, which is formed by an enzymatic chlorination of acetic acid in soil, leads to elevated $CHCl_3$ levels in soil-air (Frank et al., 1989; Haselmann et al., 2000b) via a similar mechanism.

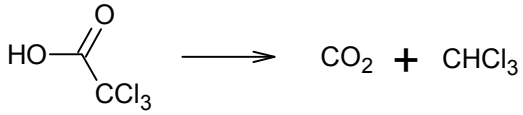

R 21

Haloperoxidase enzymes are very common in nature and characterized by their ability to oxidize halogens anions. Iodoperoxidases can only use iodide; bromoperoxidases can use

bromide and iodide, whereas chloroperoxidases can utilize chloride, bromide and iodide (Moore et al., 1996b, Urhahn and Ballschmiter, 1998). These enzymes have been found in soil extracts (Asplund et al., 1993), marine macro- and microalgae (Moore et al., 1996b, Wever et al., 1991) and fungi (Hoekstra et al., 1998b).
The reactions described above may take place inside the plant tissue (Nightingale et al., 1995) or outside the plant, i.e. activated halogen compounds (e.g. HOBr) released from extra-cellular surface bound enzymes diffuse into the surrounding seawater and react there with organic material (Wever et al., 1991). The same process was reported for fungal production of $CHCl_3$ in soils (Hoekstra et al., 1998a).

Physiological reasons to produce halocarbons

There is no clear answer to the question why organisms produce halomethanes. Ni and Hager (1998, 1999) suggested, it may come via a mechanism for halophytic plants to regulate their internal chloride ion concentrations by transforming it into a small neutral molecules which are able to diffuse through cell membranes (e.g. CH_3Cl). A SAM methyl transferase isolated from a cabbage species (Brassica oleracea) has been shown to be able to methylate halides as well as bisulfide (HS^-). Therefore it was concluded, that halide methylation is just a side reaction of the essential sulfur metabolism of these plants (Attieh et al., 1995). Physiological functions like as herbivore detergents were proposed by Itoh et al. (1997) and Gschwend et al. (1985). Several fungi species use CH_3Cl as an intermediate methyl donor for biosynthesis of larger molecules like methyl esters of monocarboxylic acids or veratryl alcohol within their metabolism (Harper et al., 1989, Harper et al., 1990).

3.3 Abiotic production

There are several production pathways, which do not directly involve enzymes or living organisms, so called abiotic processes. Although the precursors of these reactions may stem from biogenic sources the actual reactions producing the halomethanes proceed without direct biological involvement.

Nucleophilic substitution

One example already mentioned in paragraph 1.4.1 is the abiotic chloride methylation by plant pectin (Hamilton et al., 2003). This process does not only occur during biomass burning but also during leaf senescence. Wishkerman et al. (2008) recently demonstrated that CH_3Cl and CH_3Br are even released at ambient temperatures.

Another abiotic process forming monohalogenated alkanes was identified by Keppler et al. (2000). During the oxidation of organic matter (methoxy substituted phenols) by an electron acceptor like Fe (III) in soil, sediments or organic rich waters, halide ions are methylated or even make ethyl or propyl halides. Significant fluxes are likely from soil, which is rich in organic matter in highly saline environments, e.g. peat bogs near the coast.

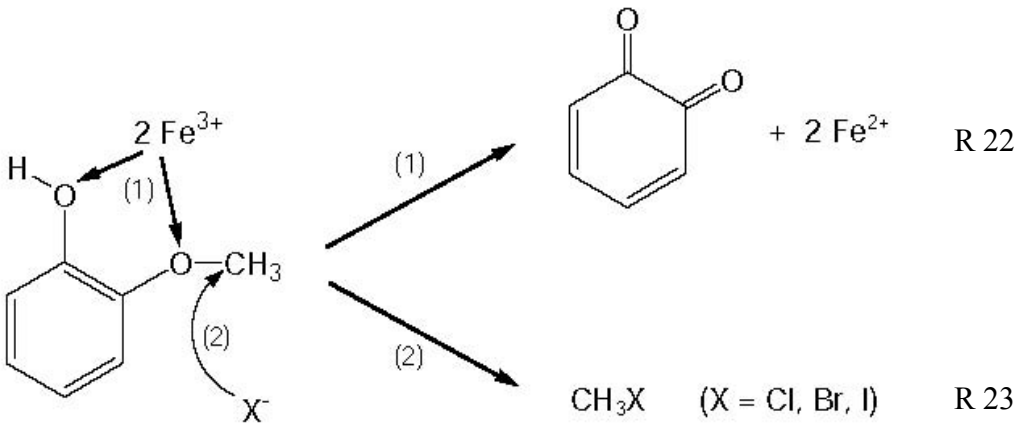

R 22

R 23

Source: Keppler et al. (2000)

A similar reaction involving seawater iodide, organic substances and Fe (III) provided by dust input was proposed to be responsible for elevated CH_3I mixing ratios related to dust events (Williams et al., 2007a).

An abiotic removal mechanism for CH_3Br and CH_3I in seawater is the nucleophilic substitution either with Cl to form CH_3Cl (Zafiriou, 1975) or with water to form methanol (hydrolysis).

$CH_3Y + Cl^- \rightarrow CH_3Cl + Y^-$ (Y: Br, I) R 24

$CH_3X + H_2O \rightarrow CH_3OH + X^- + H^+$ (X: Cl, Br, I) R 25

The former reaction does not only represent a sink for methyl bromide and iodide, it also produces methyl chloride.

Another methyl group containing molecule was proposed to act as a precursor for methyl halides by White (1982). Therein it was suggested that DMSP could react with halide ions forming CH_3X in a reversible nucleophilic substitution.

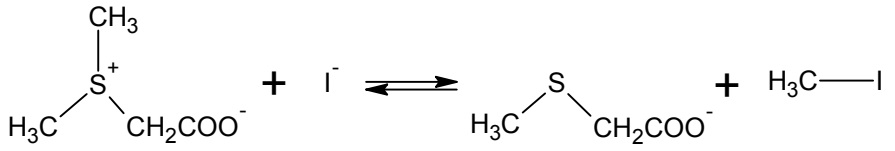

R 26

A similar conversion of CH_2Br_2 and $CHBr_3$ to chlorobromo compounds finally yielding CH_2Cl_2 and $CHCl_3$ was investigated by Geen (1992) and found to be quite slow (halflife of $CHBr_3$ against substitution is in the order of years). In any case, the process may be the source of mixed polyhalogenated products like $CHBrCl_2$ or $CHBr_2Cl$.

A photoinduced ($\lambda > 290$ nm) iodo/bromo/chloro exchange from the biogenic halomethanes CH_2I_2 and CH_2Br_2 could add to occurrence of mixed polyhalogenated methanes found in marine air and water (Class and Ballschmiter, 1987; Class and Ballschmiter, 1988).

$CH_2Y_2 + Cl^- \rightarrow CH_2ClY + Y^-$ (Y: Br, I) R 27

$\rightarrow CH_2Cl_2 + Y^-$ R 28

Photochemical production – only relevant for CH_3I

Although biological release of CH_3I by macroalgae and phytoplankton is reported for many different species, photochemical production is probably the main source of CH_3I within the ocean. Moore and Zafiriou (1994) suggested that CH_3I is produced by the interaction of sunlight and seawater via a mechanism involving photochemically produced CH_3 and I radicals.

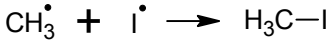

R 29

They reported higher production rates in coastal waters; a result which could be due to higher concentration of organic matter acting both as light absorber and methyl radical source. Although the presence of oxygen tends to inhibit the reaction by snatching away the methyl radicals, they stated that the reaction rate would be high enough to make this process potentially significant for the total production of CH_3I in surface ocean waters.

Chapter 2

Halogenated organic species over the tropical South American rainforest

Airborne measurements of the halogenated trace gases CH_3Cl, CH_3Br and $CHCl_3$ were made over the Atlantic Ocean and about 1000 km of pristine tropical rainforest in Suriname and French Guyana (3 - 6 °N, 51 - 59 °W) in October 2005. In the boundary layer (0 - 1.4 km), maritime air masses, advected over the forest by southeasterly trade winds, were measured at various distances from the coast. Since the organohalogens presented here have relatively long atmospheric lifetimes (0.4 - 1.0 years) in comparison to the advection times from the coast (1 - 2 days), emissions will accumulate in air traversing the rainforest. The distributions of CH_3Cl, CH_3Br and $CHCl_3$ were analyzed as a function of time the air spent over land and the respective relationship used to determine net fluxes from the rainforest for one week within the long dry season.

Net fluxes from the rainforest ecosystem have been calculated for CH_3Cl and $CHCl_3$ as 9.5 (± 3.8 2σ) and 0.35 (± 0.15 2σ) μg m^{-2} h^{-1}, respectively. No significant flux was observed for CH_3Br within the limits of these measurements.
The global budget of CH_3Cl contains large uncertainties, in particular with regard to a possible source from tropical vegetation. Our measurements are used in a large-scale approach to determine the net flux from a tropical ecosystem to the planetary boundary layer. The global net flux obtained by extrapolation, 1.5 (± 0.6 2σ) Tg yr^{-1} for CH_3Cl, is at the lower end of current estimates for tropical vegetation sources, which helps to constrain the range of tropical sources and sinks (0.82 to 8.2 Tg yr^{-1} from tropical plants, 0.03 to 2.5 Tg yr^{-1} from senescent/dead leaves, and a sink of 0.1 to 1.6 Tg yr^{-1} by soil uptake). Nevertheless, these results show that the contribution of the rainforest ecosystem is the major source in the global budget of methyl chloride. For $CHCl_3$, the extrapolated global net flux from tropical ecosystems is 56 (± 23 2σ) Gg yr^{-1}, which is of minor importance compared to the total global sources and might be already contained in the soil emission term.

The results of this study have been published as

Halogenated organic species over the tropical South American rainforest, S. Gebhardt, A. Colomb, R. Hofmann, J. Williams, and J. Lelieveld Atmos. Chem. Phys., 8, 3185-3197, 2008.

Within the ACP special issue:
The "Guyanas Atmosphere-Biosphere exchange and Radicals Intensive Experiment with a Learjet" (GABRIEL) measurement campaign in October 2005

1 Introduction

Halogenated organic compounds have been shown to be important to the chemistry of both the troposphere and the stratosphere (see section 1-1 – "Atmospheric chemistry of halocarbons"). Since CH_3Cl, CH_3Br and $CHCl_3$ have relatively long atmospheric lifetimes (CH_3Cl 1.0 yr, CH_3Br 0.7 yr, $CHCl_3$ 0.41 yr (WMO, 2007c)), they can effectively transport halogen atoms from surface sources to the stratosphere, and thereby significantly contribute to stratospheric ozone loss (Stolarski and Cicerone, 1974, Wofsy et al., 1975; Levine et al., 2007). As has been shown in section 1-1.2 – "Carrier of halogen atoms" CH_3Cl and CH_3Br represent the major natural sources to stratospheric chlorine and bromine, respectively. Since the Montreal Protocol now regulates the anthropogenic release of O_3 depleting substances, the ambient concentrations of many such halogenated compounds (i.e. CFCs) are stabilizing or declining (WMO, 2003a). Hence, the relative contribution of naturally produced halocarbons is becoming more important for the budget of stratospheric halogens. It is estimated that the contribution of natural CH_3Cl and CH_3Br to the equivalent effective stratospheric chlorine, will rise to more than 50 % by 2050 (currently 23 %) (WMO, 2007c). Despite its small total contribution to stratospheric ozone loss, $CHCl_3$ is an important natural source of tropospheric chlorine.

To be able to assess the future development of natural halocarbon emissions and their feedback on possible climate changes, it is important to determine their global sources and sinks, including distribution and strength, as precisely as possible.

Several model studies have been conducted to gain an improved understanding of the global distribution of the CH_3Cl and CH_3Br sources (Lee-Taylor et al., 2001; Yoshida et al., 2006 and Lee-Taylor et al., 1998; Warwick et al., 2006). From these studies it appears, that CH_3Cl as well as CH_3Br have tropical terrestrial sources. In the case of CH_3Cl there are some field studies, which support this thesis (Yokouchi et al., 2002; Scheeren et al., 2003) and the numbers derived from these publications are already incorporated in the global budget (see Table 1.4). However, due to the sparseness of these measurements, large uncertainties remain regarding the nature and strength of the tropical source. Regarding the global CH_3Br budget, although balanced within the uncertainties, sinks seem to outweigh the sources. This might be due to an underestimated or yet unknown (tropical) source term or an underestimation of the atmospheric lifetime of CH_3Br (Reeves, 2003).

Here we present large-scale airborne measurements of the organohalogen species CH_3Cl, CH_3Br and $CHCl_3$ over the rainforest of Suriname and French Guyana performed during one week within the long dry season (October) 2005, conducted within the Guyanas Atmosphere-Biosphere exchange and Radicals Intensive Experiment with the Learjet (GABRIEL) project. Additional information on the projects background and objectives, as well as the additionally measured parameters can be found at http://www.mpch-mainz.mpg.de/~scheeren/gabriel/ and in the supplementary material of Lelieveld et al. (2008). The vertical and horizontal distributions of these species are analyzed and fluxes from the rainforest ecosystem are determined. The influence of biomass burning and

entrained air on the derived fluxes is discussed and an extrapolation to the global scale made based on the new data. Tropical rainforest regions are important to investigate for organohalogens, not only because few measurements have been made so far but also the proximity to the ITCZ, a region of prevalent deep convection (Holton, 1992), increases the chance of emissions being transported into the stratosphere.
This study enables us to determine the net flux from a large area well suited to extrapolate to global scale, because it inherently accounts for all possible sources and sinks.

2 Sampling and analysis

2.1 Sample collection

In total 99 pressurised air samples were collected during 10 flights between 0 - 11 km over the tropical rainforest (see Fig. 2.2) using a custom-built automated air sampling system (Williams et al., 2007b). The system consisted of a module containing 18 0.8 l electropolished stainless steel canisters and was installed within an adapted wingpod on a Learjet aircraft (Learjet 35A D-CGFD operated by GFD, Hohn, Germany and Enviscope GmbH, Frankfurt, Germany). The entire sampling system was constructed from ¼" (= 0.635 cm) o.d. stainless steel tubing and connectors (Swagelok, Solon OH, USA). The inlet and outlet valves of the canisters were actuated by electric valves (Clippard–24V, Fluitronics, Düsseldorf, Germany). Thorough leak testing was carried out prior to the flights by pressurizing the sampling system with helium and looking for leaks with a helium leak detector. An aircraft metal bellows pump (Senior Aerospace, Hertfordshire, UK) was used to draw ambient air through the inlet, flush all tubing throughout the flight and, when the fill valve was activated, to pressurise the canister to at least 3 bar (3000 hPa). Canisters were filled sequentially at 10-minute intervals without any in-line drying agent. Depending on the ambient atmospheric pressure, filling took from less than 25 s at 500 m to around 60 s at 8.5 km. Prior to flight, the canister module was evacuated to 10^{-4} hPa and directly after landing the filled module was transferred to the laboratory for immediate (< 48 hours) analysis. Storage tests on similar canisters (Colomb et al., 2006) have indicated that the investigated halocarbons are stable over 60 days under dry and humid conditions.
Three identical modules were built, allowing flights to be performed in quick succession. Pressure, temperature and valve status were controlled and logged by a computer within the wingpod.

2.2 Instrumental setup

The instrumentation used for the canister analysis consisted of a gas chromatograph - mass spectrometer system (GC/MS 6890/5973, Agilent Technologies, Palo Alto CA, USA), modified from the commercial version for analysis of low-level ambient air samples (Gros et al., 2003).
Approximately 450 ml of the compressed air sample was introduced into the sampling inlet, dried by flushing through a magnesium perchlorate filled tube heated to 100 °C and prefocussed by a cryo-concentrator unit (1/16" ss line filled with glass beads, cooled to -70 °C). After the cryofocussing the line was rapidly heated to 200 °C and the target compounds were flushed into the GC. The separating column was a 60 m x 0.248 mm x 1 µm DB-5 capillary column (J&W Scientific, Agilent Technologies, Palo Alto CA, USA). The temperature profile of the GC was ramped (35 °C for 1 min, heating at 8 °C min^{-1} to 120 °C, hold 1 min, further heating at 70 °C min^{-1} to 230 °C, hold 2 min, hold 1 min at 200 °C). The chromatography parameters were optimised to enable good separation of circa 35 identified compounds; a complete run took about 18 minutes. The mass spectrometer was operated in Single Ion Mode (SIM) to achieve maximum

sensitivity. Post flight, the filled canister module was attached to the GC-MS system (see Fig. 2.1) and the analysis proceeded semi automatically within 48 h.
The detection limit was defined as three times the standard deviation of the noise (for the specific ion at its specific retention time). It was found to be 0.14 pmol mol^{-1} for $CHCl_3$, 0.51 pmol mol^{-1} for CH_3Br and 1.9 pmol mol^{-1} for CH_3Cl. The overall uncertainty was calculated based on the accuracy of the calibration standard (5 %) and its precision (CH_3Cl 3.2 %, $CHCl_3$ 6.3 %, CH_3Br 6.0 %) and resulted in 5.9 % for CH_3Cl, 8 % for $CHCl_3$ and 7.8 % for CH_3Br.

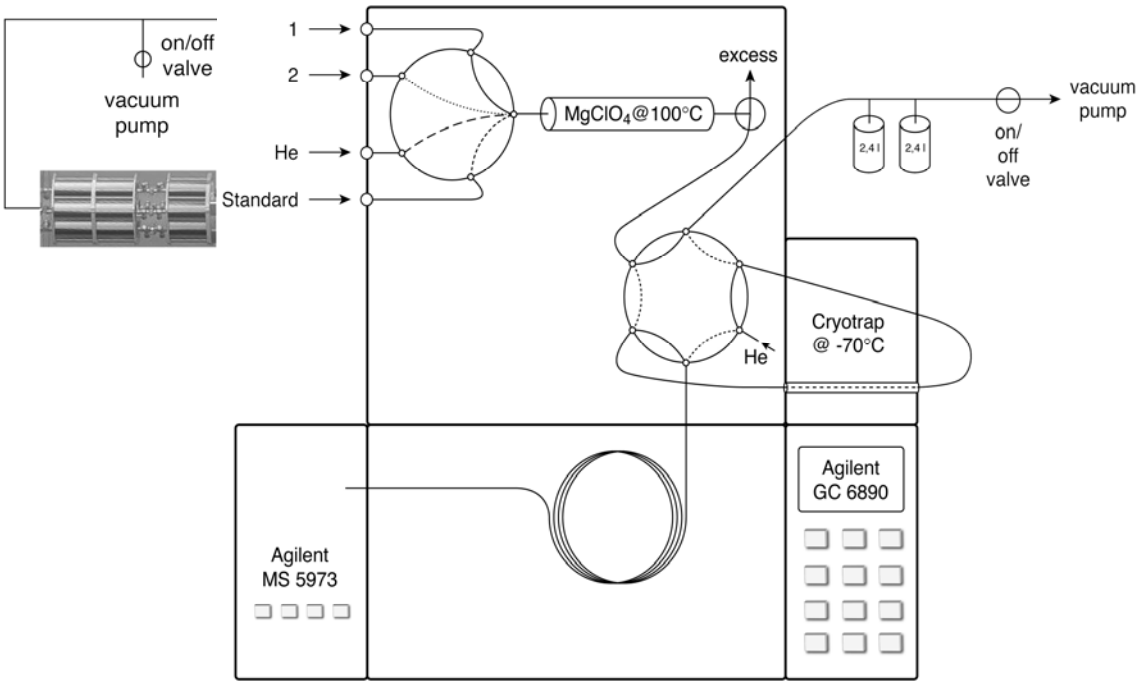

Figure 2.1: A schematic diagram of the canister sampling setup attached to port 1 of the GC-MS system inlet system.

2.3 Calibration

Calibrations were performed against a whole air working standard, prepared by filling an aluminium cylinder with ambient suburban air using a three-stage oil-free piston compressor (RIX Industries, Benicia CA, USA) modified after Mak and Brenninkmeijer (1994). This cylinder was calibrated relative to a NIST primary standard at the National Centre for Atmospheric Research (NCAR, Boulder CO, USA). The working standard was analysed every five measurements. The average response factor of these analyses was used to calibrate the samples measured in between. At least one blank (using the same analytical procedure but without collecting an air sample) was performed at the start of each measurement sequence, and showed a generally clean baseline. Linearity of the system was confirmed in the range of measured concentrations (CH_3Cl 1.9 - 1900 pmol mol^{-1}, $CHCl_3$ 0.14 - 470 pmol mol^{-1}, CH_3Br 0.5 - 25 pmol mol^{-1}). It should be noted that the $CHCl_3$ mixing ratio in the calibration gas was significantly higher than in the ambient air samples.

3 Results and discussion

3.1 Meteorological conditions in Suriname

The northeast coast of South America is an excellent location to study the effects of the tropical rainforest on atmospheric trace gas composition. Meteorological conditions in this region are controlled by the steady trade winds and the annual migration of the ITCZ. The data presented here were collected from the 6th to the 13th of October 2005 within the GABRIEL project. During this time of the year - the long dry season - the ITCZ was located a few degrees north of the Guyanas at approximately 10 - 15 °N (see Fig. 2.2). Thus, although geographically in the northern hemisphere, Suriname (3 - 6 °N, 51 - 59 °W) was atmospherically located in the southern hemisphere. The location and height of all measurements is shown in Fig. 2.2.

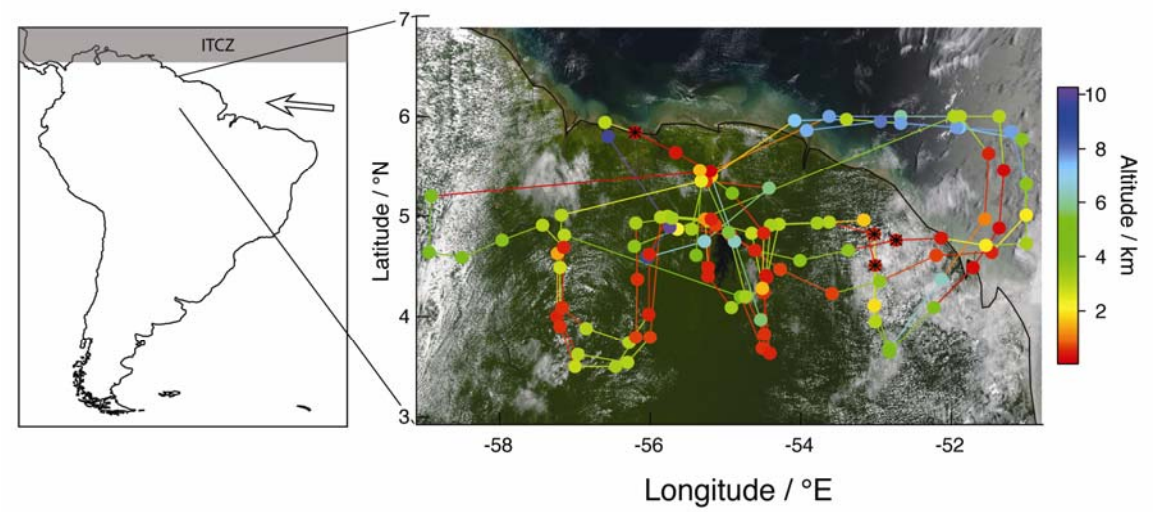

Figure 2.2: Sampling area and flight tracks: ITCZ and prevailing wind direction (arrow) are shown on the left. On the right side dots mark the position of the samples, while the colour-coding gives the height information. Black asterisks mark samples excluded from the calculation (source of satellite picture: Jacques Descloitres, MODIS Rapid Response Team, NASA/GSFC; downloaded Sep 2007 from: http://visibleearth.nasa.gov/).

During the campaign the meteorological conditions were generally constant with only occasional short thunderstorms. The cloud conditions observed were typical of tropical regions. This includes the development of shallow cumulus clouds in the morning, occasionally transforming into cumulonimbus clouds and hence thunderstorm activity in the late afternoon, before proceeding to clear sky in the evening. The prevailing wind direction in the boundary layer was easterly (95°), with average wind speeds of 5.8 m s^{-1}, which is typical of the trade winds. Closer to the surface the wind weakened and turned to a more northeasterly direction as a result of the increased friction with the surface. Wind speed and direction as a function of altitude are shown in Fig. 2.3.

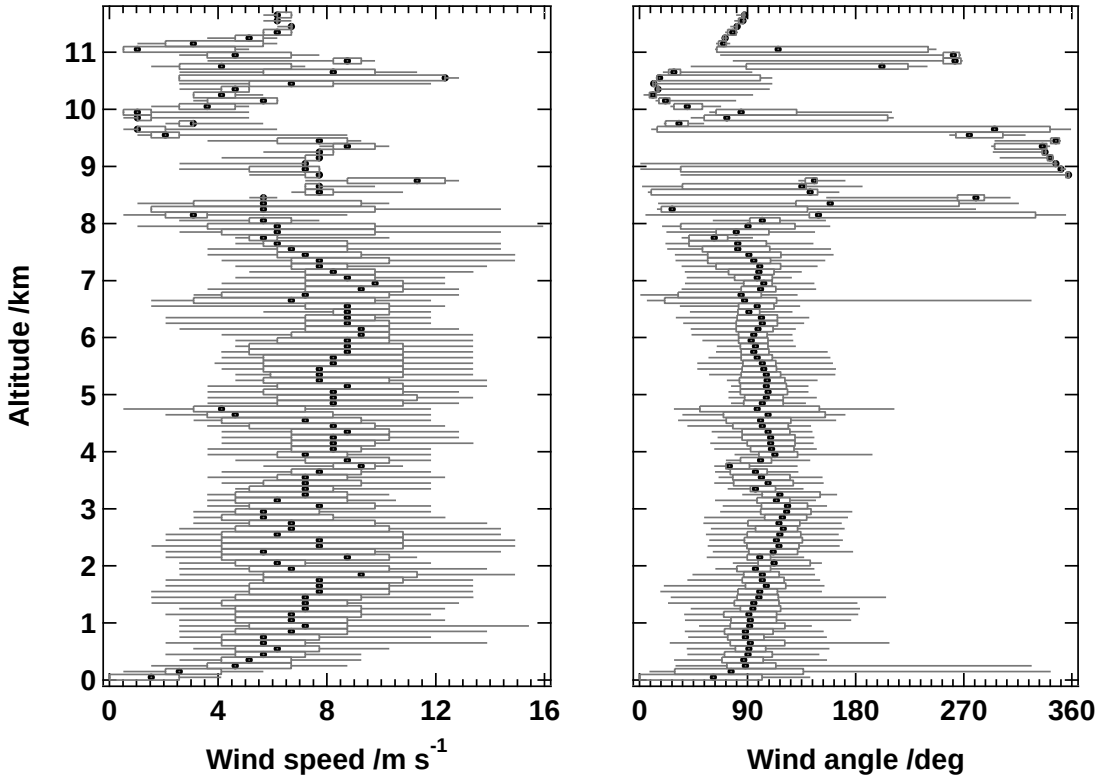

Figure 2.3: Altitude distribution of wind speed and direction (angle) binned in 100 m intervals (dots: median, boxes: 25/75 percentile, whiskers: 5/95 percentile). The data are 100 m binned average values of the 1 Hz data obtained by the aircraft flight management system.

Maritime air masses were advected from the Atlantic Ocean and then over approximately 1000 km of pristine rainforest. The 10-day back trajectories of the boundary layer samples are shown in Fig. 2.4. These indicate that air arriving at the coast of French Guyana and Suriname was transported for the most part within the southern hemisphere over the Atlantic Ocean.

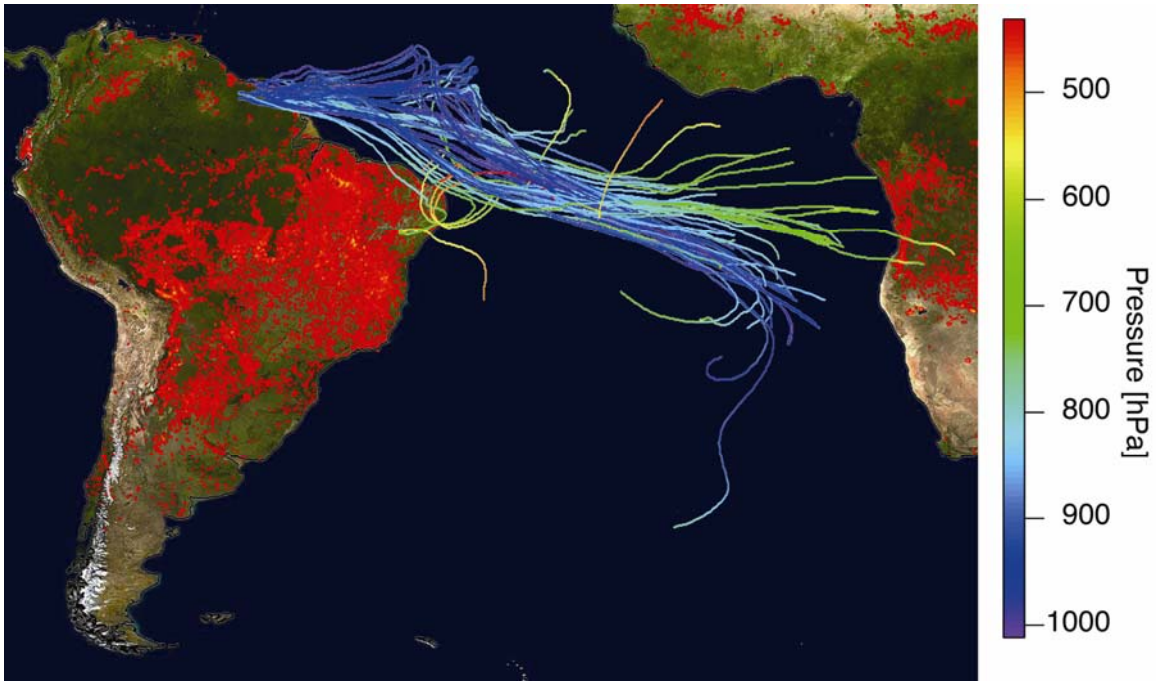

Figure 2.4: 10-day back trajectories (provided by KNMI) of the canister samples taken within the boundary layer (< 1400 m) overlaying a MODIS fire map showing all fires detected in the period from 08.10. - 18.10.2005 (Source: Fire maps created by Jacques Descloitres, MODIS Rapid Response System at NASA/GSFC; downloaded Sep. 2007 from http://rapidfire.sci.gsfc.nasa.gov/firemaps/).

The boundary layer height during the day, which is important in calculating the net flux, was determined using fluctuations in the static air temperature (corresponding to temperature inversions) measured from the aircraft when ascending (G. Eerdekens, personal communication). The temperature was recorded by the Enviscope analogue data acquisition system. Often there are a number of inversions present in the vertical profiles, and for this study we assumed that the lowest identifiable inversion delineates the top of the boundary layer. The derived boundary layer grew from about 600 m around 9:30 local time (UTC -3 h) to 1200 m at 12:30 up to about 1400 m in the afternoon. The empirically determined mixed layer height seems to be in agreement with the investigations by Krejci et al. (2005), who reported mixing layer heights from the same area in 1998. Because most of our measurements took place around midday or early afternoon, we assumed an average boundary layer height of 1400 m. The variability in the boundary layer height determinations between 12:00 and 16:00 was used to derive an uncertainty in the boundary layer height, which was determined to be ± 260 m (2σ).

3.2 Vertical distribution

The vertical profiles of CH_3Cl, CH_3Br and $CHCl_3$ are presented in Fig. 2.5. The measurements span a range from the surface up to 11 km height, although air was predominantly sampled in the boundary layer. Generally the profiles could be divided

into three different parts: The mixed boundary layer (ML) up to 1400 m, the lower free troposphere below the trade wind inversion (LFT) from 1400 to 3500 m and the free troposphere (FT) above 3500 m.

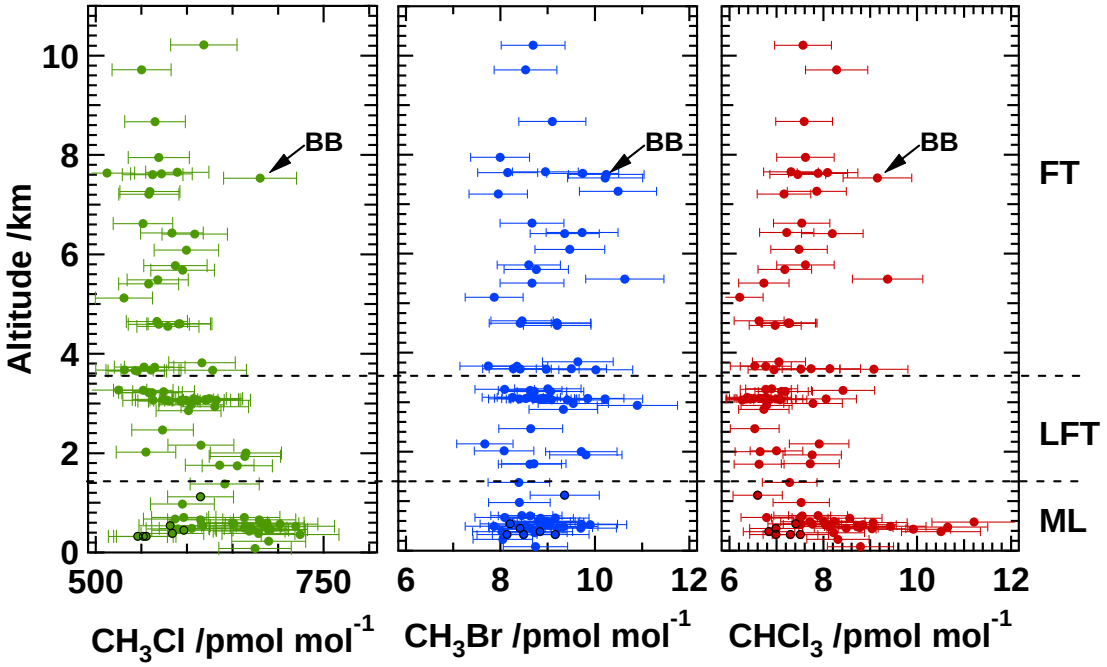

Figure 2.5: Vertical distribution of CH_3Cl, CH_3Br and $CHCl_3$ (black circles mark the mixed layer samples at TOL = 0h). The horizontal dashed lines mark the divisions referred to in the text as mixed layer (ML), lower free troposphere (LFT) and free troposphere (FT). BB marks the sample influenced by biomass burning.

The CH_3Cl profile showed higher mixing ratios near the ground decreasing with altitude. The average within the mixed layer was 643 pmol mol^{-1}, decreasing to 600 pmol mol^{-1} within the LFT and further to 575 pmol mol^{-1} on average in the FT; the one outlier (marked with BB in Fig. 2.5) is discussed further below.
The vertical distribution of CH_3Br was quite scattered, which is in part due to the 7.8 % precision error. The mixing ratios varied between 7.7 and 10.9 pmol mol^{-1} showing no significant trend with height.
The $CHCl_3$ profile showed a decrease in mixing ratio from ML (8.2 pmol mol^{-1}) to LFT (7.0 pmol mol^{-1}). The average FT values were again slightly elevated (7.5 pmol mol^{-1}). Taking into account the uncertainty of the data points, no statistically significant information on the source distribution could be obtained from the vertical profiles. Nevertheless, on average higher mixed layer mixing ratios of CH_3Cl and $CHCl_3$ pointed to a ground based source of these compounds. This surface source is further investigated in section 3-4 – "Net fluxes from the tropical rainforest".
The elevated value at 7.9 km visible in all three components corresponded to a sample taken within air strongly influenced by biomass burning, most probably originating from a distant biomass burning event in Africa. It coincided with elevated values in the

biomass burning tracers carbon monoxide (CO) and acetonitrile (CH_3CN) (H. Bozem, personal communication).

3.3 Influence of biomass burning

As can be seen from the example above, the possible influence of biomass burning has to be considered when interpreting the mixing ratios of the investigated compounds. When considering natural fluxes, care must be taken to exclude burning effects from calculated gradients. Burning is known to be a strong source of CH_3Cl and also a source of CH_3Br and $CHCl_3$ (Lobert et al., 1999; Andreae and Merlet, 2001). Since during the period September to November there is widespread burning in the southern hemisphere, it would not be surprising if some influence of this was detected during this campaign, particularly in CO, CH_3CN and CH_3Cl. However, fire maps prepared from GOES-12 satellite images (http://cimss.ssec.wisc.edu/goes/burn/wfabba.html) showed no significant burning activity in the direct vicinity of the investigated area. Furthermore, back trajectories from the measurement locations showed that the fires occurring south or west of the Guyanas had almost no impact on the investigated air masses in the boundary layer (see Fig. 2.4). Generally low levels of CO and CH_3CN in the boundary layer (Stickler et al., 2007; G. Eerdekens, personal communication) also supported the view that the measurements were not significantly influenced by local burning sources. The ratio CH_3Cl/CO can also be used to deduce source information of both gases. Previous studies have reported CH_3Cl/CO ratios of 0.85 (± 0.06) $x10^{-3}$ for South American smouldering fires and 0.57 (± 0.03) $x10^{-3}$ for African flaming fires (Blake et al., 1996). During this study a CH_3Cl/CO ratio of 2.77 (± 0.64 2σ) $x10^{-3}$ was obtained. The ratio measured here, lies clearly outside the reported range for biomass burning. Therefore we conclude that the predominant source of the observed CH_3Cl in the boundary layer is most likely not biomass burning.

Since the vertical profile showed no statistically significant mixing ratio changes in the transition zone between ML and LFT, the influence of entrainment from upper layers of air is not taken into account in the following calculations.

3.4 Net fluxes from the tropical forest

As clean marine boundary layer air was advected westwards over the pristine tropical rainforest of French Guyana and Suriname during GABRIEL, mixing occurred between the marine boundary layer air and the forest emissions. Long-lived trace gases emitted by the forest can accumulate in the mixed boundary layer so that mixing ratios of such species will increase westwards and hence be positively correlated with the time the air spent over land. Conversely uptake of gases by the forest will result in a negative correlation. The volume mixing ratios of CH_3Cl, CH_3Br and $CHCl_3$ samples in the ML (< 1660 m) (n = 35) are shown as a function of time over land (TOL) in Fig. 2.6.

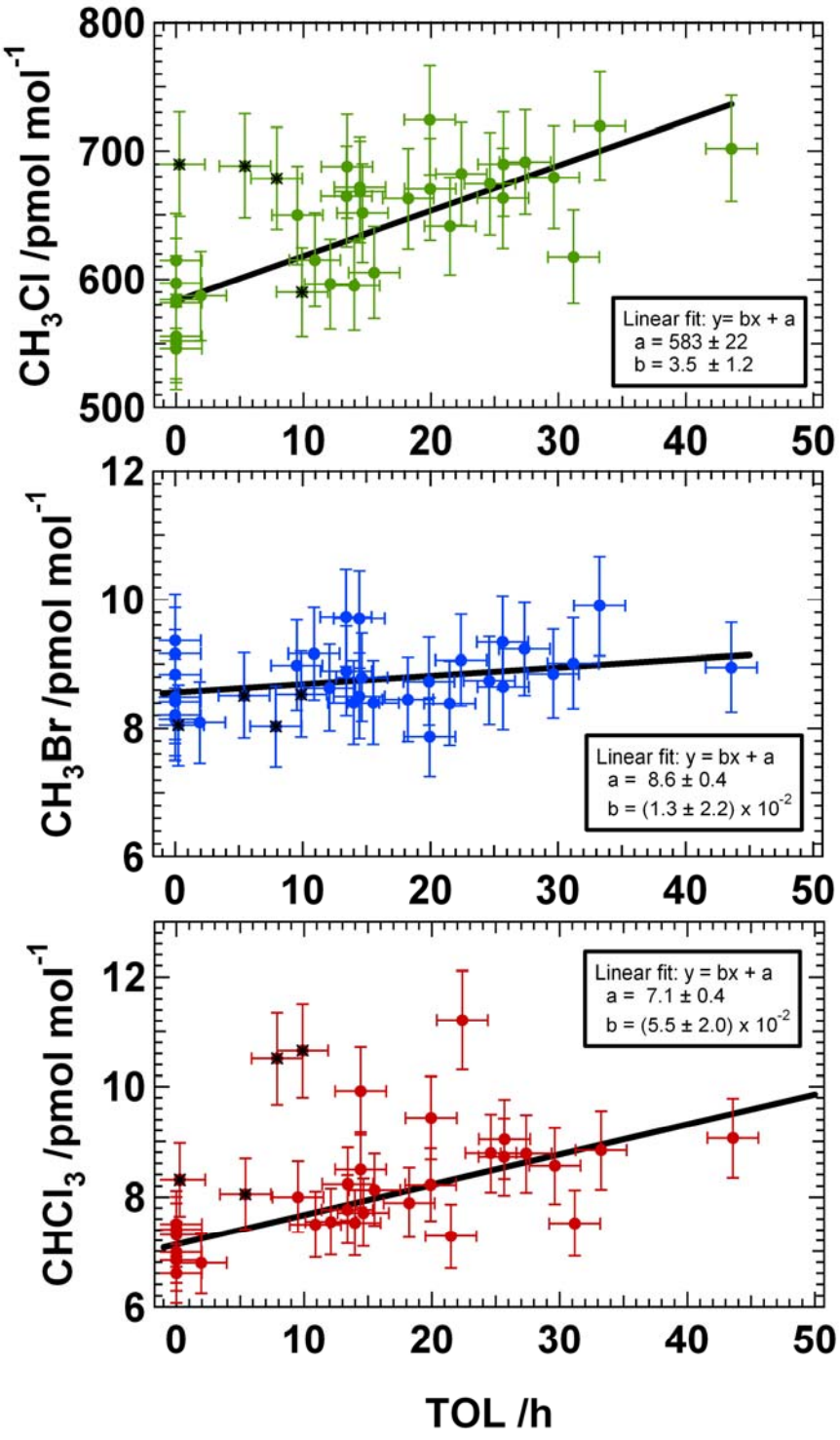

Figure 2.6: Mixing ratios of CH_3Cl, CH_3Br and $CHCl_3$ vs. TOL. Dots represent the mixed layer samples with their individual error bars. The black line indicates the regression line. Fit coefficients including their uncertainty are given in the boxes; black asterisks mark samples excluded from the calculation.

The mixing ratios in the boundary layer ranged from 546 to 724 (avg 643) pmol mol^{-1} for CH_3Cl, 6.6 to 11.2 (avg 8.2) pmol mol^{-1} for $CHCl_3$ and 7.9 to 9.9 (avg 8.8) pmol mol^{-1} for CH_3Br. These are somewhat higher than the global mean value of 550 ± 30 pmol mol^{-1} for CH_3Cl, which is expected, since generally higher concentrations are reported for lower latitudes (WMO, 2007a). For $CHCl_3$, the values reported here agree very well with the average mixing ratio for the SH tropics, 9.7 pmol mol^{-1} (Khalil and Rasmussen, 1999a). For CH_3Br the measured range fits the global average 7.9 pmol mol^{-1} (Simmonds et al., 2004). The error bars shown in Fig. 2.6 indicate the total uncertainty of the individual measurements (± 5.9 % for CH_3Cl, ± 7.8 % for CH_3Br and ± 8.0 % for $CHCl_3$).

To calculate the time the air parcel spent over land we used the following approach. Starting at the sampling position we followed the path of the air parcel along the back trajectory in distinct time steps until it reached the coastline. For this procedure we used 10-day back trajectories, provided by P. van Velthoven (Royal Netherlands Meteorological Institute (KNMI), De Bilt, Netherlands). Trajectories were calculated using the KNMI trajectory model TRAJKS based on 6 hourly ECMWF three-dimensional meteorological wind fields, interpolated to a 1° × 1° lat–lon grid.
The uncertainty associated with the trajectories is highly dependent on the meteorological parameters employed. The general weather situation in the region is quite invariant (trade wind zone) and not more than the first 48 h of the calculated trajectories are considered for TOL calculation. Nevertheless, to account for the uncertainty in the trajectories we have applied an error of ± 2 h for TOL. For the reasons stated above we feel that the trajectories can be used in this case to estimate our TOL with reasonable accuracy. Furthermore, we consider this trajectory based method to be the best currently available to determine the time the air parcel spent over land.

Samples taken above the ocean and coastline (TOL = 0 h) consisted of marine air and are used to define the boundary conditions, e.g. start mixing ratio prior to accumulation of compounds emitted from the forest. Mixed layer samples at TOL = 0 h are circled in black in Fig. 2.5. In general there is no significant difference between ocean and coastline mixing ratios. For CH_3Cl and $CHCl_3$ four data points at low TOL appear as outliers to the fit (marked with a black asterisks in Fig. 2.2 and 2.6). Interestingly, these samples were taken in somewhat different geographical circumstances than the rest of the dataset. The sample taken at 0 h TOL was deliberately collected at low altitude (200 m a.s.l.) directly above coastal salt marshes as such regions have been suggested to emit CH_3Cl (Rhew et al., 2000), although this view was recently questioned (Wang et al., 2006). The three samples at 5, 8 and 10 h TOL were taken in the vicinity of the capital of French Guyana, Cayenne, downwind of Rochambeau airport and were therefore probably influenced by anthropogenic emissions. For the aforementioned reasons these points are not included in the flux calculations given below.
An orthogonal distance regression was used to calculate the net flux from the rainforest ecosystem. Rather than minimizing the sum of squared errors this method minimizes the orthogonal distance from the data to the fitted curve. The slope of the fit gives the increase of the mixing ratio per hour the air mass spent over the jungle. The black line in Fig. 2.6 indicates the regression line, while fit coefficients including their uncertainty

(equivalent to 2σ) are given in the boxes. To calculate the fit coefficients and their confidence parameters, the total uncertainty of each individual data point (regarding mixing ratio and TOL) was used as weighting parameter. In this case the flux was statistically significant if the given deviation was not bigger than the value of the parameter itself. Two compounds showed a significant correlation with TOL ($\Delta CH_3Cl/\Delta TOL$ = 3.5 ± 1.2 (2σ) pmol mol^{-1} h^{-1} and $\Delta CHCl_3/\Delta TOL$ = (5.5 ± 2.0) $x10^{-2}$ (2σ) pmol mol^{-1} h^{-1}) and thus appear to be emitted from the forest ecosystem. For CH_3Br the slope is not significant ($\Delta CH_3Br/\Delta TOL$ = (1.3 ± 2.2) $x10^{-2}$ (2σ) pmol mol^{-1} h^{-1}) and therefore no net flux could be determined within our detection limit.

Using the slope derived from Fig. 2.6 the flux was calculated by following formula:

$$F = (\Delta MR/\Delta TOL) \times H_{ML} \times (p \times M/(R \times T))$$

Where F is the flux (µg m^{-2} h^{-1}), $\Delta MR/\Delta TOL$ the linear regression slope (pmol mol^{-1} h^{-1}), H_{ML} the mean mixing layer height (1400 ± 260 m (2σ) (n = 11)), p the mean air pressure below 1660 m (941 ± 71 hPa (2σ) (n = 34710)), M the molar weight (µg), R the gas constant (0.08314 hPa m^3 K^{-1}) and T the mean air temperature below 1660 m (296 ± 15 K (2σ) (n = 33596)).
The result is a flux of 9.5 (± 3.8 2σ) µg CH_3Cl m^{-2} h^{-1} and 0.35 (± 0.15 2σ) µg $CHCl_3$ m^{-2} h^{-1}, respectively. Using the slope uncertainty of $\Delta CH_3Br/\Delta TOL$ we determine the lowest detectable CH_3Br flux as 0.11 (2σ) µg CH_3Br m^{-2} h^{-1}.

Despite their large size and potential importance to atmospheric chemistry, the Earth's tropical forests are surprisingly poorly characterized for organohalogen species. There are only few measurement studies available for comparison and these were mainly performed in Asia (Li et al., 1999; Yokouchi et al., 2000; Yokouchi et al., 2002; Saito and Yokouchi, 2006; Yokouchi et al., 2007) measured in a tropical glasshouse and on forested islands. Scheeren et al. (2003) measured the two chlorinated compounds in Suriname in March 1998 and Moore et al. (2005) analyzed tropical fungi and soils in Brazil.

Li et al. (1999) observed a very high flux of 41 to 64 µg CH_3Cl m^{-2} h^{-1} from a coastal area at Okinawa Island, Japan. Yokouchi et al. (2002) reported a flux of 5.4 (3.8 - 8) µg CH_3Cl m^{-2} h^{-1} from a greenhouse containing vegetation typical of the lowland tropical forest of Southeast Asia and smaller though not quantified fluxes of CH_3Br and CH_3I. Recently they reported an emission rate of 12 - 33 µg CH_3Cl m^{-2} h^{-1} measured on one of the subtropical Okinawa islands (Yokouchi et al., 2007). The study performed by Scheeren et al. (2003) over Suriname in March 1998 reported fluxes of 7.6 ± 1.8 µg CH_3Cl m^{-2} h^{-1} and 1.1 ± 0.08 µg $CHCl_3$ m^{-2} h^{-1}. Moore et al. (2005) reported wood rotting fungi to be a CH_3Cl source and confirmed the soil as a sink, in agreement with previous measurements (Watling and Harper, 1998; Khalil and Rasmussen, 2000). Elevated mixing ratios above the canopy led them to the assumption that there have to be further strong sources in the rainforest beside the fungi.

The CH_3Cl fluxes of Scheeren et al. (2003) agree very well with the 9.5 (± 3.8 2σ) µg CH_3Cl m^{-2} h^{-1} derived in this study, although these results were obtained using a different measurement technique (GC-ECD). The fluxes derived by Yokouchi et al. (2002) and Yokouchi et al. (2007) are in the same range, although they were obtained surveying a different kind of tropical species in Southeast Asia, while the study of Li et al. (1999) reported much higher fluxes than all other studies. However, the latter value was obtained in a coastal area and might be influenced by coastal/marine production. It is included here for completeness, but is not expected to match the other vegetation focused studies.
These findings support previous model results (Lee-Taylor et al., 2001; Yoshida et al., 2004 and Yoshida et al., 2006), which have postulated a land based, constant source of CH_3Cl all over the tropics.

In the case of $CHCl_3$ there is to our knowledge only one comparable flux reported in literature. Scheeren et al. (2003) obtained a value approximately three times higher in March 1998 than the one measured in our study during October 2005. There are two wet seasons in Suriname associated with the passage of the ITCZ over the country. These wet seasons are bracketed by two dry seasons, one from February to April termed the short dry season, and one from August to November, the long dry season. Thus, both available fluxes were determined in dry seasons and therefore only small differences in the meteorological conditions were observed between the March and October field campaigns. The precipitation and therefore presumably soil moisture were very similar (70.3 mm during March 1998, 65.6 mm in October 2005), whereas the maximum temperature was on average higher by 1.6 °C in October 2005 (33.4 °C), while the minimum temperature was similar (23.6 °C March 1998, 23.8 °C October 2005) (C. Becker, Meteorological Service Suriname, personal communication). Meteorological parameters therefore do not provide a good explanation for the discrepancy between the two measurements.

However, the results presented here show strong differences in the $CHCl_3$ flux, but at most very small differences in the CH_3Cl emissions. This leads to the assumption that these compounds are emitted via different formation pathways.
To investigate this discrepancy in detail it is necessary to consider the different component parts of the rainforest and thereby the multitude of interacting sinks and sources, e.g. soil, decaying leaves, fungi and the plants themselves.
Besides the anthropogenic, oceanic and biomass burning sources of CH_3Cl and $CHCl_3$ several further possible formation pathways have been reported. Isidorov et al. (1985) and Isidorov and Jdanova (2002) showed that CH_3Cl as well as $CHCl_3$ are emitted by living leaves and leaf litter of some tree species (e.g. pencil cedar, evergreen cypress, northern white cedar, aspen and willow). Other higher plants such as tropical ferns, halophytes and potato tubers show significant emissions of CH_3Cl (Harper et al., 1999; Rhew et al., 2000; Yokouchi et al., 2002; Harper et al., 2003) as well as fungi (Watling and Harper, 1998).
Although there is some evidence that $CHCl_3$ is emitted directly by plants (Isidorov et al., 1985), soil processes are assumed to be the major source in the tropical ecosystem (Laturnus et al., 2002; McCulloch, 2003, see Table 1.4). Several pathways are reported in the literature (see section 1-3 – “Production pathways”): Basidiomycetous fungi are able

to synthesize $CHCl_3$ *de novo* (Hoekstra et al., 1998b). It can also be formed by chlorination of organic matter catalysed by extracellular peroxidase-like enzymes (chloroperoxidase CPO) most probably deriving from fungi (Hoekstra et al., 1998a). Another plausible mechanism is the decarboxylation of trichloroacetic acid (Frank et al., 1989; Haselmann et al., 2000b).
The metabolic origin of CH_3Cl has been identified as an enzyme catalysed halide methylation reaction, which uses either S-adenosyl-methionine (SAM) or methionine as a methyl donor (Harper et al., 1999; Harper, 2000). Hamilton et al. (2003) showed that abiotic chloride methylation by plant pectin is an efficient, environmentally significant process producing CH_3Cl. Chloride ions, which are plentiful in the leaf, react with pectin during leaf senescence and an abiotic substitution reaction yields CH_3Cl. This mechanism could account for the CH_3Cl release from leaf litter and during biomass burning. Recent results from isotopic studies of CH_3Cl (Keppler et al., 2005) support this abiotic mechanism. Another abiotic process forming monohalogenated alkanes was identified by Keppler et al. (2000). During the oxidation of organic matter by an electron acceptor like Fe (III) in soil, sediments or organic rich waters, halide ions are methylated or even build ethyl or propyl halides.
While the aforementioned substitution mechanisms can efficiently produce monohalogenated compounds they are not likely to be the source of the $CHCl_3$, which would require multiple substitution. The fact that the two molecules do not show the same variation in their emissions, strengthens the assumption that they are produced via different production pathways.
In summary it thus appears that the CH_3Cl and $CHCl_3$ are produced at different locations within the ecosystem and by different mechanisms. CH_3Cl is produced mainly by plants themselves and during their decay abiotically or by fungi. In contrast, the main $CHCl_3$ production is restricted to fungal and microbial processes within the soil and leaf litter.
Measurements of soils in temperate forests indicate $CHCl_3$ emissions of up to 0.34 $\mu g\ m^{-2}\ h^{-1}$ from soils covered with woodchips (Hoekstra et al., 2001). Haselmann et al. (2000a) report local emissions in a Danish forest up to 0.16 $\mu g\ m^{-2}\ h^{-1}$. These rates correspond very well with the flux of 0.35 ($\pm$ 0.15 2σ) $\mu g\ m^{-2}\ h^{-1}$ $CHCl_3$ derived in this study and strengthens the argument that the main fraction of $CHCl_3$ in the tropical ecosystem is produced by soil processes. This would support the assumption of Laturnus et al. (2002), who speculated on a similar or even larger input from tropical forest areas as reported from northern temperate forests.

Regarding CH_3Br the average mixing ratios reported here are slightly elevated compared to global background values (WMO, 2007a), but no significant net emission from the rainforest of CH_3Br could be determined. This is in contrast to greenhouse and small-scale experiments (Gan et al., 1998; Yokouchi et al., 2002; Saito and Yokouchi, 2006), which report CH_3Br emission from plants of the brassicaceae family, Asian lowland forest and tropical ferns. A vegetation source providing additional 45.6 Gg yr^{-1} in the tropics as postulated by Warwick et al. (2006) would correspond to a local gross flux of 0.287 $\mu g\ CH_3Br\ m^{-2}\ h^{-1}$. An emission of this order of magnitude would have been detected by this study (detection limit for CH_3Br: 0.11 $\mu g\ m^{-2}\ h^{-1}$). Since soils are known to uptake CH_3Br (see Table 1.4), one may speculate that the possible release from tropical vegetation is reduced by a local soil sink and therefore not detectable in a large-

scale experiment like this one. On the other hand, a recent modelling study suggests that the atmospheric lifetime of CH_3Br has been underestimated (Kerkweg et al., 2008), which also closes the imbalance between sources and sinks without the presumed vegetation source.

3.5 Global emissions from the tropical forest

Before extrapolating the observed net fluxes from the South American rainforest to the global scale several aspects must be noted.

Firstly, the fluxes measured here were the net effect of the "rainforest ecosystem" at one time of year. As mentioned previously there are likely several competing sources and sinks (plants, bacteria, fungi, senescencing leaves etc.) within the ecosystem each of which may vary independently in the course of a year.

Secondly, the tropical forest covers a large fraction of the globe and accounts for nearly half of the total global forest (FAO, 2001). The largest areas are found in the Amazon Basin (South America) and the Congo Basin (Africa), as well as large parts of Southeast Asia and Oceania are covered by tropical forest. For these extrapolations, the forest from these diverse regions is considered homogenous. This is obviously a simplification and therefore the derived fluxes should be regarded as a rough estimate.

Thirdly, the definition of the forest area is an important issue. Using the widely distributed number of 18.2 million km^2 of tropical forest (FAO, 2001), which refers to all kinds of forest located in the tropics, we obtained fluxes of 1.5 (± 0.6 2σ) Tg CH_3Cl yr^{-1} and 56 (± 23 2σ) Gg $CHCl_3$ yr^{-1}. Using the lowest detectable flux derived in section 2-3.4 – "Net fluxes from the tropical forest" we determine the lowest global detectable CH_3Br flux to be 17 (2σ) Gg CH_3Br yr^{-1}. A more conservative estimate using only the area of tropical rainforest (10.8 million km^2) (FAO, 2001), results in fluxes of 0.9 (± 0.4 2σ) Tg CH_3Cl yr^{-1} and 33 (± 14 2σ) Gg $CHCl_3$ yr^{-1}.

These numbers are obtained using the flux derived by this study throughout the year. Bearing in mind that $CHCl_3$ emissions seem to be varying and other studies reported higher flux rates, one should regard these flux estimates as a lower limit. Taking into account the measurements of Scheeren et al. (2003) - which were carried out in the same region - and using the average flux of both studies, the annual emission of $CHCl_3$ would be more than doubled. It should be noted that this estimate is particularly uncertain since no measurements have yet been made in the wet season.

Although these extrapolations are inherently uncertain due to the aforementioned assumptions in the calculation, they do represent our current best estimate of the rainforest contribution to the global budgets of these compounds and appear to be quite reasonable. The calculated flux of 1.5 (± 0.6 2σ) Tg CH_3Cl yr^{-1} from the tropical forest would account for half of the additional source postulated by the models (Lee-Taylor et al., 2001; Yoshida et al., 2006). In comparison with the current best estimates of global

tropical source terms, it is at the lower end of the range reported (0.82 to 8.2 Tg yr^{-1} from tropical plants, 0.03 to 2.5 Tg yr^{-1} from senescent/dead leaves and a sink of 0.1 to 1.6 Tg yr^{-1} by soil uptake). Nevertheless an emission of this order of magnitude would be the main global source for CH_3Cl, exceeding the ocean, biomass burning and anthropogenic sources. It should be noted that the studies providing the basis for current estimates (Yokouchi et al., 2002 and Hamilton et al., 2003) were restricted to the small scale (greenhouse or laboratory measurements), and therefore the large-scale approach applied here should be a more reliable assessment of the real global net flux from this ecosystem.
The $CHCl_3$ flux extrapolated to all tropical forests results in a net flux of 56 (± 23 2σ) Gg yr^{-1}. This is between 5 and 10 % of the total sources, and as previously mentioned, it could be already incorporated in the soil source term.
The global extrapolation of the lowest detectable CH_3Br flux yields 17 (2σ) Gg yr^{-1}. A source of this size would be a non-negligible contribution to the global budget, supplying between 6 and 22 % of the total global sources.
Once again it is important to recall that the global fluxes presented in this study are net sources. To compare them with the numbers listed in Table 1.4 all possible sinks and sources within the measurement area have to be combined.

To better understand the budgets of these compounds it will be necessary to examine seasonal variations of the various sources and sinks within the rainforest ecosystem. In particular, the driving parameters of the sources and sinks need to be better characterized, e.g. their dependence on ambient temperature and/or soil moisture changes. These variations will be particularly important for predicting future changes in the natural halocarbon emissions fluxes, which will become more important as the anthropogenic contribution recedes.

4 Summary and conclusions

This study presents airborne measurements of CH_3Cl, $CHCl_3$ and CH_3Br over the tropical rainforest of Suriname. Aircraft measurements of the kind reported here inherently consider the rainforest ecosystem as a whole, and are ideally suited to gauge the net effect over large areas. The fluxes are possibly the result of separate strong sinks and strong sources within the ecosystem, and represent the net flux from the rainforest to the atmosphere in October 2005. For both CH_3Cl and $CHCl_3$ a significant correlation between mixing ratio and time the air mass spent over the rainforest was found. The rainforest ecosystem produced 9.5 (± 3.8 2σ) µg m^{-2} h^{-1} CH_3Cl and 0.35 (± 0.15 2σ) µg m^{-2} h^{-1} $CHCl_3$.

No significant trend for CH_3Br could be determined from these measurements. The tropical vegetation gross source postulated by an inverse model prediction (Warwick et al., 2006) is possibly reduced to a very small net flux by concomitant sinks such as soil uptake. Our measurements over the South American rainforest agree with global observations generally, and vertical gradients between the boundary layer and free troposphere appear to be small or absent. This supports the conclusion that tropical forest ecosystem is not a significant net global CH_3Br source.

The CH_3Cl flux is in good agreement with previously measured fluxes by Yokouchi et al. (2002) and Yokouchi et al. (2007), who reported 5.4 (3.8 - 8) µg CH_3Cl m^{-2} h^{-1} and 12 - 33 µg CH_3Cl m^{-2} h^{-1} for Asian lowland tropical forest, and Scheeren et al. (2003), who derived 7.6 (± 1.8) µg CH_3Cl m^{-2} h^{-1} over Suriname. This suggests that the rainforest ecosystem appears to be a seasonally constant and important CH_3Cl source in the tropics. Extrapolating the flux to the global scale resulted in 1.5 (± 0.6 2σ) Tg CH_3Cl yr^{-1}, which would account for half the additional tropical source postulated by the previous model studies (Lee-Taylor et al., 2001; Yoshida et al., 2006). Since the soil is known to be a sink for CH_3Cl the observed total flux in this study should be considered as lower limit of the possible direct production by plants or plant decay. It ranges at the lower end of current best estimates of the global tropical source terms but nevertheless it would be the main global source.

Regarding the $CHCl_3$ emission we observed a threefold weaker flux than that derived by Scheeren et al. (2003). Our lower limit of the global extrapolated flux from the tropical forests is 56 (± 23 2σ) Gg $CHCl_3$ yr^{-1}, about 5 to 10 % of the total global sources. These fluxes may be incorporated in global models to provide an overall net source strength of the rainforest ecosystem. Since these numbers are based on a large-scale approach local phenomena tend to be averaged out and a more representative value is obtained.

From the different emission patterns we conclude that these two compounds are probably produced via different mechanisms. According to the literature, $CHCl_3$ is most probably formed by microbial processes in the soil depending on temperature and soil moisture, however, there are no clear meteorological differences between March 1998 and October 2005 to explain the flux differences observed. Performing a similar study during the wet season would provide additional information on the soil moisture dependence of the

formation pathways and the seasonal variation of the emissions, which could be incorporated in global models.

To obtain a better understanding of the role of the rainforest ecosystem as a possible sink or source of halogenated organic species, more studies on the different tropical biomes are necessary. Furthermore, a more detailed survey of the possible contributors (plants, soil, leaf litter, fungi etc.) would complement the knowledge about the separate sources and sinks within the tropical rainforest ecosystem.

Chapter 3

Abiotic methyl halide formation from vegetation

Within this study the release of methyl halides (CH_3Cl, CH_3Br) from plant tissue at ambient temperatures was examined. Bromide enriched pectin and four different plant species have been monitored. The plant species were selected as representatives for grassland (hay, reference material IAEA V-10), deciduous forest (ash, *Fraxinus excelsior*), agricultural areas (tomato, reference material NIST-1573a) and coastal salt marshes (saltwort, *Batis maritima*). Incubations at different temperatures (25 - 50 °C) revealed a strong temperature dependence. The emissions of CH_3Cl and CH_3Br approximately doubled with each 5 °C temperature step, resulting in an exponential increase with increasing temperature. The strength of the emission was found to be additionally dependent on the halide content and the methoxyl group (CH_3O) content of the plant tissue. However, water i.e. the water content of the plant material was found to reduce emissions. The abiotic nature of the reaction leading to methyl halides formation was confirmed by Arrhenius plots.

CH_3Cl and CH_3Br are the most abundant chlorinated and brominated organic gases in the troposphere and represent the major natural sources to stratospheric chlorine and bromine, respectively. The contribution of abiotic formation from vegetation to the global budget will vary geographically as a result of regional differences in both temperature and halide content of terrestrial plants. Maximum emissions are to be expected for plant material containing high amounts of halogens decaying under warm and dry conditions. If global temperatures increase further, as predicted, methyl halide emissions will not only increase due to exponential temperature dependence, but increased occurrence of extreme weather events like heat waves and droughts could cause emission hotspots as plants dry out, and new source regions may emerge in areas where historic wetlands begin to dry out.

1 Introduction

CH_3Cl and CH_3Br are the most abundant chlorine and bromine containing gases in the troposphere, respectively. Their influence on atmospheric chemistry, in particular on stratospheric ozone depletion, has been described in section 1-1.2 – "Carrier of halogen atoms".
To better gauge the present and future development of halogen input into the stratosphere, and thus the impact on stratospheric ozone depletion, it is critically important to understand the processes involved in the release of halogen containing substances to the atmosphere. Fortunately, the major anthropogenic contribution to the organohalogen budget - the CFCs - has already been well documented and the actions taken (regulations laid down in the Montreal Protocol and its amendments) are showing positive results. The atmospheric concentrations of many man-made CFCs are stabilizing or declining. Hence, the impact of naturally produced carriers of halogen atoms will become more important over the coming years. It is estimated that the contribution of natural CH_3Cl and CH_3Br to the equivalent effective stratospheric chlorine will rise to more than 50 % by 2050 (currently 23 %) (WMO, 2007c).

CH_3Cl and CH_3Br have both natural and anthropogenic sources. The globally important sources and sinks of CH_3Cl and CH_3Br are given in Table 1.4. The major man-made contributions are due to burning processes (e.g. biomass, fossil fuel and waste) and, in the case of CH_3Br, use as fumigation agent. Several terrestrial biomes have been found to emit CH_3Cl and/or CH_3Br, respectively. Salt marshes (Rhew et al., 2000; Rhew et al., 2002), wetlands (Varner et al., 1999), rice paddies (Redeker et al., 2003; Lee-Taylor and Redeker, 2005), rapeseeds (Gan et al., 1998), mangroves (Manley et al., 2007), grasslands (Teh et al., 2008; Rhew et al., 2007), peatlands (Dimmer et al., 2001) and shrublands (Rhew et al., 2001) have been identified as source regions for emissions. The most recently discovered and thus far least well characterised natural source term for CH_3Cl, tropical/subtropical plants and/or their degradation processes (Yokouchi et al., 2002; Hamilton et al., 2003; Scheeren et al., 2003), is dealt with in Chapter 2 of this thesis. However, substantial uncertainties remain regarding the strength and nature of the production pathways of these compounds.
In view of the huge variety of ecosystems releasing CH_3Cl and CH_3Br, the production mechanism does not seem to be specific to a certain plant species. Possibly, production is not related to plant metabolism at all. Previous studies have suggested several possible pathways, which are described in detail in section 1-3 – "Production pathways".
The biosynthesis of methyl halides by living plants is thought to be an enzyme catalyzed transfer of an activated methyl group to a halide ion (Wuosmaa and Hager, 1990; Saxena et al., 1998; Attieh et al., 1995). As a substrate, several molecules containing activated methyl groups, and known to exist within the plant might be considered (e.g. S-adenosyl-L-methionine (SAM)).
The oxidation of organic matter (methoxyl substituted phenols) in soil, sediments or organic rich waters by an electron acceptor like iron (Fe^{3+}) represents another pathway to form methyl halides (Keppler et al., 2000). However, the environmental importance of this process remains unknown.

A further process generating methyl halides, in particular CH_3Cl, was introduced by Hamilton et al. (2003). They reported the abiotic conversion of chloride using the widespread plant component pectin as a methyl donor, to be responsible for CH_3Cl production. The emission from senescent and dead plant material was observed even at ambient temperature (30 °C), increasing dramatically with rising temperature (tested up to 350 °C). The process was found to be additionally dependent on the tissue chloride content, and the water content of the leaves, showing higher emissions with drier leaves. They conclude, that the postulated abiotic mechanism might not only represent a significant source of CH_3Cl during weathering of plant material, but may also account for CH_3Cl release during biomass burning. The presumed methyl donor substance pectin, is a polysaccharide composed primarily of partially esterified α-(1-4) linked galacturonic acid units, which accounts usually for 7 - 23 % of plants leaf cell wall material (Hu et al., 1996). A subsequent study of Keppler et al. (2004) using carbon isotopic ratios confirmed that the predominant source of CH_3Cl and CH_3Br released from plant material by the above described abiotic process, are methoxyl groups transferred from plant own macromolecules like pectin and lignin. In a later study Keppler et al. (2005) indicated that the abiotic methylation of chloride in plant and soil organic matter might account for the bulk of CH_3Cl emitted to the atmosphere.

So far the occurrence (Hamilton et al., 2003) and the potential importance for the global budget of the abiotic formation of methyl halides from vegetation have been established (Keppler et al., 2004; Keppler et al., 2005). The process was found to be crucially dependent on the prevailing temperature (range examined 30 - 350 °C), as well as the halide and methoxyl group content of the plant tissue.

This study is focused on investigating the relevance of the abiotic formation of methyl halides at ambient temperatures. The emissions of dried leaves of several plant species representative of different terrestrial biomes have been monitored over a temperature range from 25 to 50 °C. The dependence on halogen content and methoxyl group availability within the plant material was analyzed. In light of future global warming predictions, the temperature and water dependence of the organohalogen release rates suggests increasing contributions via this mechanism.

2 Sampling and analysis

Details on the sample preparation, the determination of the halide and methoxyl content of the plant tissue and the analysis of the CH_3Cl emissions by GC-MS are described in detail by Wishkerman et al. (2008). In summary the halide content was determined via x-ray fluorescence (XRF) or instrumental neutron activation analysis (INAA) and the methoxyl content by transforming methoxyl groups to CH_3I, which was quantified by GC-MS.

2.1 Sample incubation

A certain amount of ground sample (0.1 - 1.5 g, dependent on plant tissue halogen content), was placed in a 40 ml glass vial (Fisherbrand, Pittsburgh, PA, USA) and sealed with a PTFE/silicon septum (Sigma-Aldrich, St. Louis, MO, USA). The vials were incubated for 17 h at the desired temperature. In the initial experiment, investigating pectin enriched with bromide (632 mg Br kg^{-1} dry weight), samples were incubated at temperatures of 30, 40 and 50 °C. For the plant samples, a smaller temperature step was chosen and samples were incubated in the temperature range 25 - 50 °C at 5 °C intervals. Prior to the analysis of the headspace by GC-MS the samples were allowed to equilibrate at 25 °C for 30 min.

Figure 3.1: Sample incubation.

2.2 CH_3Br analysis by GC-MS

The sample was transferred from the vial to the GC inlet line using a 10 ml gas-tight syringe (VICI Precision Sampling, Baton Rouge LA, USA). Prior to sampling the syringe was flushed with ambient air three times. The needle was inserted through the vial's septum and the plunger of the syringe was operated three times to ensure a well mixed headspace.

The GC-MS system (GC/MS 6890/5973, Agilent Technologies, Palo Alto CA, USA) used for the CH_3Br analysis consisted of a commercial MS with a modified inlet system suitable for trace gas analysis (Gros et al., 2003).
A given volume of the sample (2 to 10 ml depending on the expected concentration) was injected to a continuous helium gas flow (30 ml min^{-1}) leading to the sampling device of the instrument. A schematic diagram of the inlet and GC-MS system is shown in Fig. 3.2. The injection was performed very slowly (total injection time ~ 1 min) and afterwards sampling from that line was continued for ten more minutes, to make sure, that the sample volume was quantitatively flushed to the cryo-trap (-70 °C, on glass beads in a 1/16" ss tube). All lines prior to the cryo-trap were heated to about 60 °C to prevent wall losses of sticky compounds. Target compounds were released from the cryo-trap by rapidly heating it to 200 °C and passed onto the GC. Helium 6.0 carrier gas was pre-purified in a converter tube (Supelco, Bellefonte PA, USA).

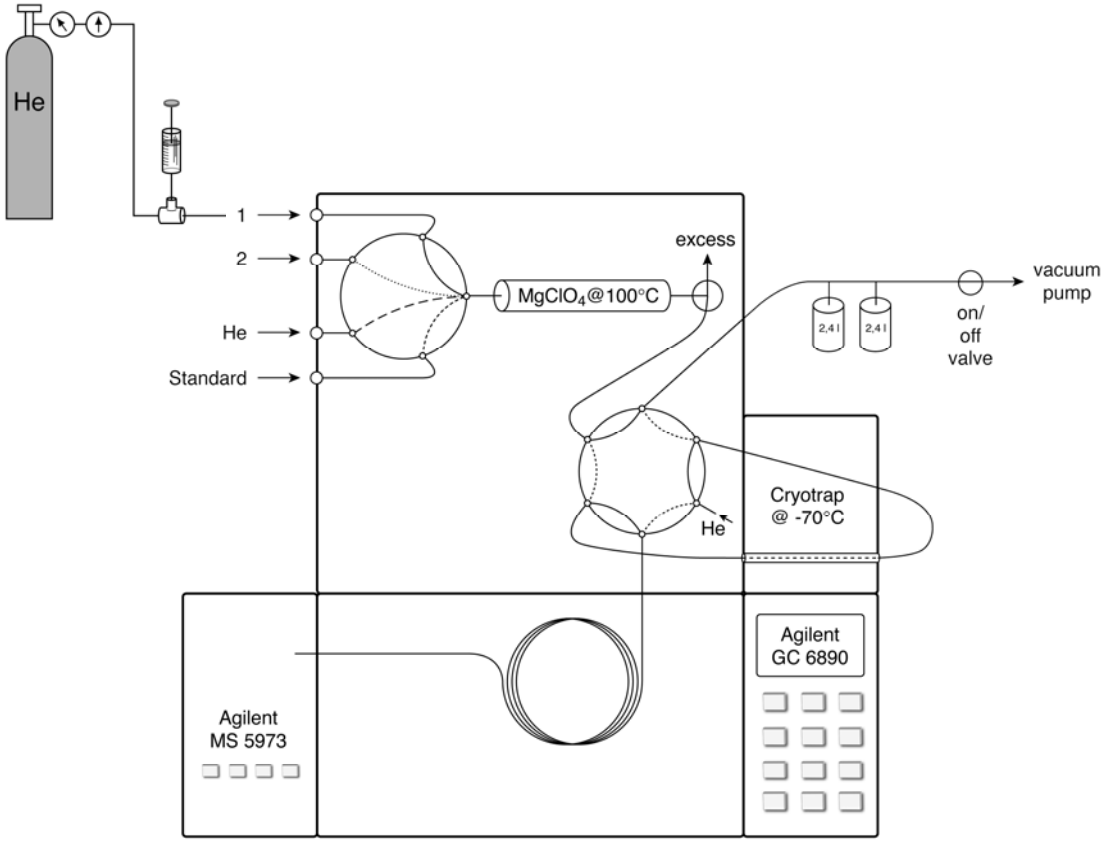

Figure 3.2: A schematic diagram of the sampling line attached to port 1 of the GC-MS system.

The chromatographic parameters were optimised to enable good separation of the methyl halides: The separating column was a 60 m x 0.248 mm x 1 µm DB-5 capillary column (J&W Scientific, Agilent Technologies, Palo Alto CA, USA) employed in constant flow mode (2.7 ml min^{-1}). The temperature program of the GC oven was as follows: temperature held at 35 °C for 4 min, ramped at 15 °C min^{-1} to 120 °C, held at this

temperature for 3 min, then ramped at 120 °C min^{-1} to 250 °C and held for a further 3 min. A complete run took about 18 minutes. The MS was operated in Single Ion Mode (SIM) to achieve maximum sensitivity monitoring the currents at m/z 94 and 96, which are specific to CH_3Br. Between the measurements, the cryo-trap was conditioned by flushing with helium at 200 °C to remove any residual trace compounds.

Calibrations were performed against a gravimetrically prepared calibration gas (Apel-Riemer Environmental, Denver CO, USA). It was analysed every four measurements using syringe injection identical to the sample procedure. The response factor of these standard analyses was used to calibrate the samples measured in between. At least one blank (using the same analytical procedure but without injecting a sample) was performed in each measurement sequence, and showed a generally clean baseline. Linearity of the system was confirmed in the range of measured mixing ratios (0 to 45 nmol mol^{-1}).

The detection limit was defined as a signal exceeding the background by at least three times the standard deviation of the noise (for the specific ion at its specific retention time) (S/N = 3). It was found to be 0.2 nmol mol^{-1}. The calibration gas precision i.e. the coefficient variation (CV) corrected for detector drift was found to be 7.2 %. Taking into account the calibration gas' uncertainty of 5 % the overall uncertainty amounted to 8.8 %. Strictly speaking these values only apply to mixing ratios close to the calibration gas value. However, care was taken by varying the injected calibration gas volume to keep the response of the detector similar for the calibration gas and sample measurements. Nevertheless, in case of very low emission (e.g. the ash samples) this could not always be attained (recorded area was lower by a factor of up to 30). This results in higher uncertainties for lower emissions (up to 20 % total uncertainty for mixing ratios < 1 nmol mol^{-1}).
It should be noted that the uncertainty of the measurements is generally lower than 10 %. Larger error bars shown in Fig. 3.5 are due to concentration variations within duplicate measurements caused by inhomogeneous plant material.

3 Result and discussion

3.1 Temperature dependence of methyl halide emissions

In a first approach the effect of different temperatures on methyl halide emissions was tested on pectin, a methoxyl group donor compound. To ensure sufficient halide availability, pectin was enriched with bromide ions (632 mg kg^{-1}). The obtained CH_3Br release rates at 30, 40 and 50 °C are plotted in Fig. 3.3. They show an exponential increase with increasing temperature. The emission rate of 26.4 (avg) ng g^{-1} dry weight (dw) d^{-1} at 30 °C rose to 286.3 (avg) ng g^{-1} dw d^{-1}, when pectin was incubated at 50 °C increasing by a factor of ~11.

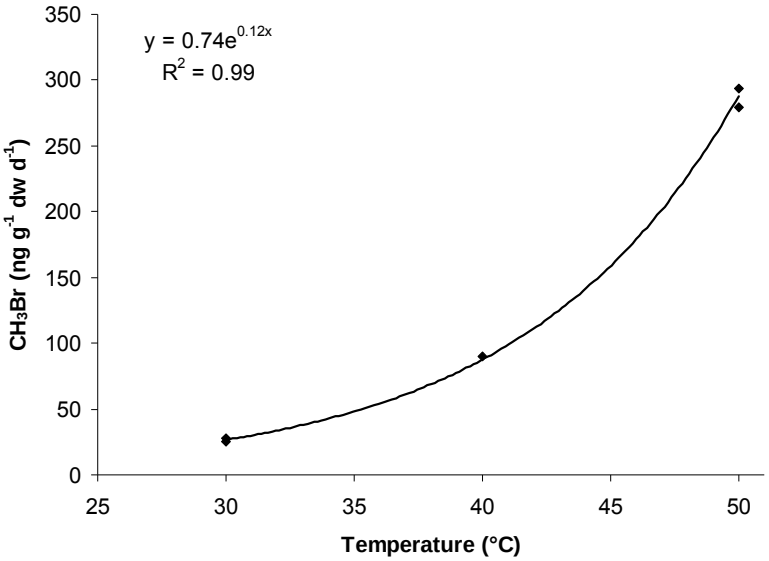

Figure 3.3: CH_3Br emission from pectin enriched in bromide.

A test on differently treated plant leaf material revealed, that regardless of sample preparation, emissions for each plant type were in the same range and increased similarly with temperature. However, with all sample types and at all temperatures the standard deviations of the measured emissions from whole leaf samples were considerably higher than those from ground leaf samples. Since sample preparation did not change the production rate significantly, ground leaf material was used for the following experiments.

Saltwort, hay, ash and tomato leaf material was incubated under the same conditions as those specified for pectin, though a smaller temperature step was employed. CH_3Br emission rates of the plant samples showed an exponential increase with temperature similar to pectin, however, the release rates of CH_3Br were found to be highly variable between the species. The temperature dependent emission rates are shown in Fig. 3.4 and 3.5. The saltwort samples showed the highest emission rates of CH_3Br. The values of 18.6 (avg) ng g^{-1} dw d^{-1} at 30 °C and 175.5 (avg) ng g^{-1} dw d^{-1} at 50 °C come closest to the values reported for pectin enriched with bromine. CH_3Br release rates decline following the order tomato, ash and hay. Tomato samples emitted on average

7.5 (avg) ng g^{-1} dw d^{-1} at 30 °C and 156.2 (avg) ng g^{-1} dw d^{-1} at 50 °C. Ash leaves showed more than an order of magnitude smaller emissions (0.23 (avg) ng g^{-1} dw d^{-1} at 30 °C and 4.6 (avg) ng g^{-1} dw d^{-1} at 50 °C). The release of CH_3Br from hay was hardly detectable (0.016 (avg) ng g^{-1} dw d^{-1} at 30 °C and 2.0 (avg) ng g^{-1} dw d^{-1} at 50 °C). However, all plant samples showed an exponential increase of the emission rates with increasing temperature. On average, a 5 ºC temperature rise doubled the amount of CH_3Br released. From the temperature dependence of the reaction rate the activation energy for CH_3Br release from the different plant species could be calculated (Wishkerman et al., 2008). Arrhenius plots revealed much higher activation energy values than reported for enzymatic processes. The emission could thus be attributed to an abiotic chemical process.

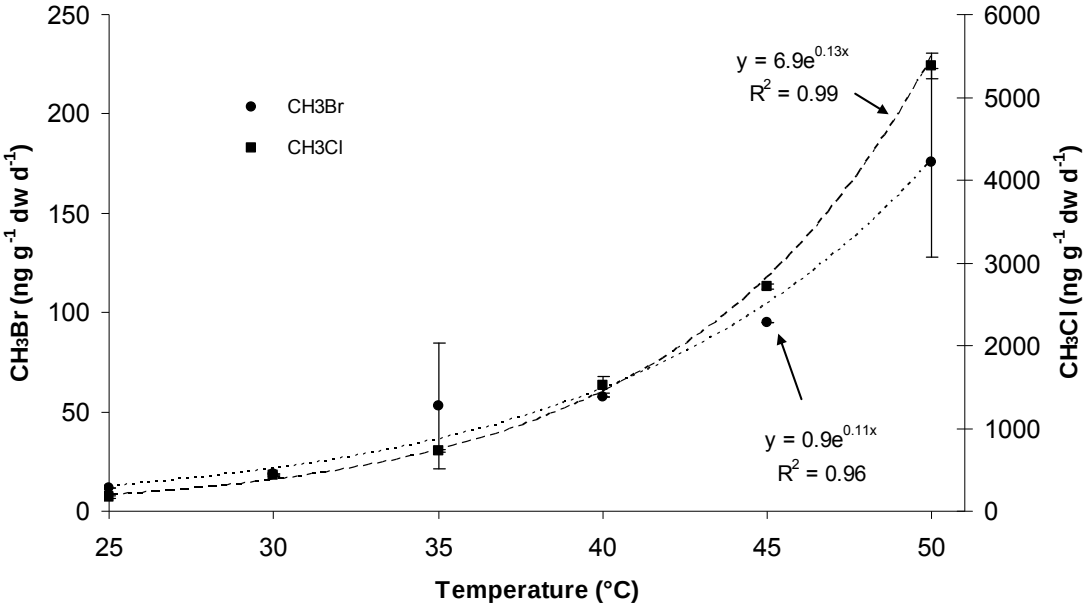

Figure 3.4: Temperature dependence of CH_3Br and CH_3Cl emissions for saltwort material (*Batis maritima*). Error bars show the standard deviation for triplicate samples ($\pm 1\sigma$).

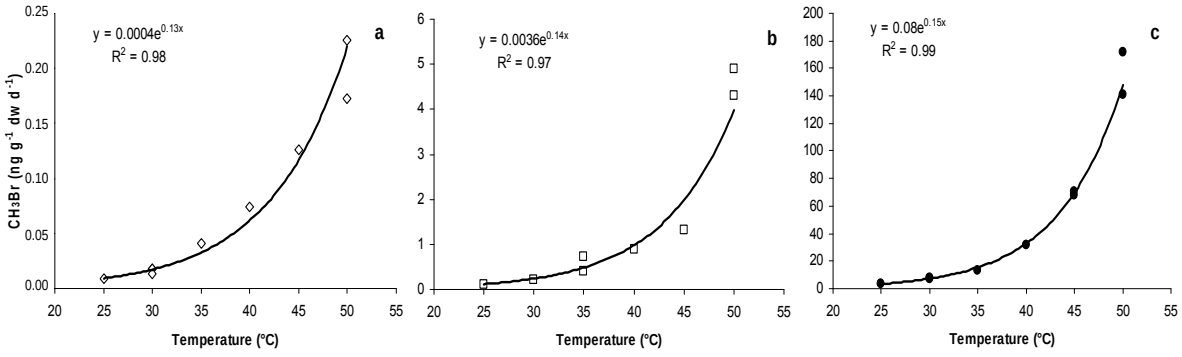

Fig. 3.5: CH_3Br emissions from hay (a), ash (b) and tomato (c) plant material.

3. 2 Halide and methoxyl content dependence of CH_3Br emission

Since methyl halides are formed by a reaction involving halide ions and methoxyl groups, the formation and therefore release rate is dependent on the availability of both precursors (Hamilton et al., 2003). The halide and methoxyl content of the investigated material is given in Table 3.1. Hay and ash contain natural levels of bromine (8 mg kg^{-1} (dw) and 34 mg kg^{-1} (dw), respectively). The bromine concentration of the tomato sample was higher than expected (1335 mg kg^{-1} (dw)), probably reflecting its growing conditions. Agriculturally grown vegetables can contain high concentrations of bromine (Mino and Yukita, 2005), due to fumigation or residual amounts of bromine from fertilizer usage. Saltwort is a typical salt marsh plant accustomed to a high saline environment. The saltwort sample showed bromine content similar to pectin, 872 mg kg^{-1} (dw), and a high chlorine content, 186 g kg^{-1}.

Sample	Bromine / mg kg^{-1} dw	Chlorine / mg kg^{-1} dw	Methoxyl groups / %
Hay (IAEA V-10)	8*	N.D.	2.38
Ash	34.4**	7800**	1.17
Tomato (NIST 1573a)	1335***	6540****	0.89
Saltwort	872***	186000***	0.81
Pectin + KBr	632***	N.D.	7.95

* IAEA laboratory data
** INAA
*** XRF
****Becker et al. (1994)
N.D. – Not determined.

Table 3.1: Content of bromine, chlorine and methoxyl groups in plant material and pectin.

If the formation of CH_3Br was just dependent on the bromine content the emission efficiency should follow the order: hay, ash, pectin, saltwort, tomato. And indeed hay and ash emitted the lowest amounts of CH_3Br. Interestingly, CH_3Br emissions from pectin were higher than those observed for saltwort and tomato, although it contained less bromine. This, however, can be explained by the higher methoxyl content of pectin (~ 8 %) compared with that of saltwort or tomato (~ 1 %) (Table 3.1). Figure 3.6 shows the fraction of bromine being converted to CH_3Br within one day. The higher efficiency of conversion observed with pectin is most likely due to its high methoxyl content. However, despite having the highest methoxyl content of all plant species investigated (2.4 %), hay showed the lowest bromine conversion rates. This may result from higher lignin contribution to the methoxyl content in the hay sample compared to the other species. As has been reported by Hamilton et al. (2003) lignin methoxyl groups are not available as methyl donors over the temperature range used in this study. Unfortunately, the analytical method employed does not distinguish between methoxyl groups derived from pectin or lignin and total methoxyl content may therefore not be an accurate measure of methylating potential at these low temperatures.

The general conversion efficiency at ambient temperature for all samples (pectin and all plant species) is very low. Even at 50 °C less than 1 % of the available bromine is converted and released as CH_3Br. This is in agreement with results from Hamilton et al. (2003) regarding the formation of CH_3Cl from chloride and pectin. They reported conversion rates of less than 2 % for temperatures below 175 °C, whereas complete volatilization was achieved at 275 °C.

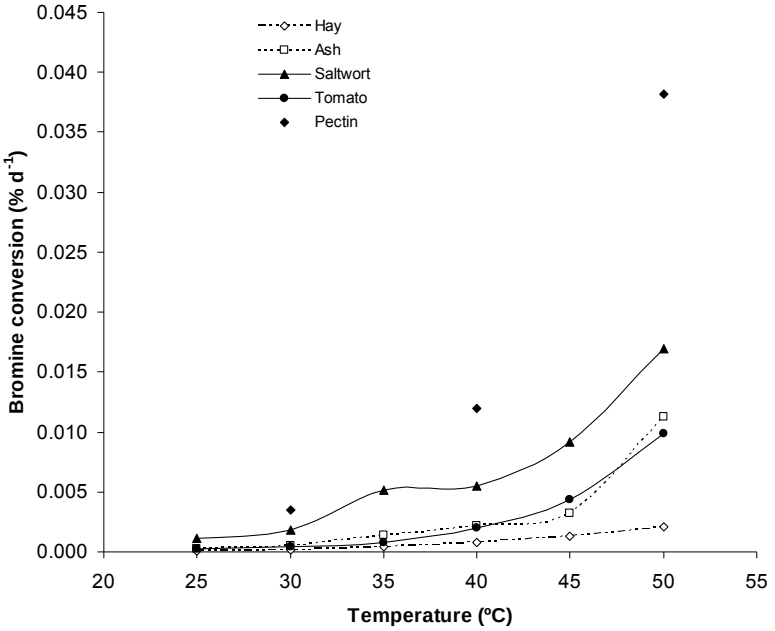

Figure 3.6: Conversion of bromine to CH_3Br at temperatures ranging from 25 to 50 °C.

As saltwort is known to emit both CH_3Br and CH_3Cl (Rhew et al., 2000; Manley et al., 2006), and exhibits a similar bromine content to pectin and a high chlorine content, pectin and saltwort were chosen to compare the emission profiles of CH_3Br and CH_3Cl (Figure 3.4). The methyl halide emission patterns in the 25 to 50 °C temperature range were analogous, showing an exponential increase with temperature, which is indicative of a similar mechanism of formation for both compounds. CH_3Br and CH_3Cl emission rates at the lowest temperature investigated (25 °C) were 12 ng g^{-1} dw d^{-1} and 173 ng g^{-1} dw d^{-1}, respectively. When samples were incubated at 50 °C CH_3Br and CH_3Cl emissions increased approximately 15 and 31 fold, respectively (see Fig. 3.4).
Comparing the halogen content of the plant material (see Table 3.2) it is clear, that chlorine is three orders of magnitude more abundant than bromine. Saltwort and ash molar halogen ratios (Cl/Br = 475 or 505, respectively) lie in the same range as usually found in seawater (~ 650) and precipitation (~ 845) (Yuita, 1994), representing a "natural" molar halogen ratio. As mentioned before, the tomato sample contains artificially high bromine concentrations. Its Cl/Br molar ratio is therefore shifted to lower values (~ 11). In contrast the molar ratios of CH_3Cl and CH_3Br emitted from the plant samples show much lower values. Depending on the incubation temperature they range from 45 to 58 (saltwort) or 47 to 134 (ash). The tomato sample at 50 °C exhibits a ratio of 4.8. This observation indicates the preference of bromine over chlorine in the formation

process. Interestingly, the activation energy of CH_3Br formation from saltwort (84.6 kJ mol^{-1}) was found to be significantly lower than for CH_3Cl formation (107.1 kJ mol^{-1}). This explains the observation, that bromide was more efficiently methylated than chloride and is in accordance with its higher nucleophilicity (Wuosmaa and Hager, 1990). Despite the higher efficiency of bromine being converted to CH_3Br the total release of CH_3Cl still exceeds the CH_3Br emission, since the abundance of Cl in the plant material is overwhelming.

Sample	Temp / ºC	CH_3Cl / ng g^{-1} dw d^{-1}	CH_3Br / ng g^{-1} dw d^{-1}	CH_3Cl:CH_3Br Molar ratio	Cl/Br ** Molar ratio	Cl:Br/ CH_3Cl:CH_3Br Molar ratio
Saltwort	30	440	18.6	44.5	475	10.7
	50	5380	175	57.8	475	8.2
Ash	30	13*	0.23	106	505	4.7
	40	64*	0.9	134	505	3.8
	50	115*	4.6	47	505	10.7
Tomato (NIST 1573a)	50	398	156	4.8	11	2.3

* Data from Hamilton et al. (2003)
** Halide concentrations in plants.

Table 3.2: Ratios of released CH_3Cl/CH_3Br at 30, 40 and 50 °C and Cl/Br ratio of the plant material.

3.3 Water content dependence of CH_3Br emission

Studying the abiotic CH_3Cl release from freshly detached intact leaves Hamilton et al. (2003) reported that water content of the leaves was important. The emission rate increased by an order of magnitude, when the water content, initially 65 %, was reduced to 40 %. They found that further drying of the sample had no significant effect on the rate of CH_3Cl emission. As the profiles for abiotic CH_3Cl and CH_3Br emissions observed in this study show an almost identical pattern, we would expect that water had a similar effect on CH_3Br formation as described for CH_3Cl formation (Hamilton et al., 2003). This was indeed the case; addition of water to milled dried ash samples was found to reduce emissions of CH_3Br by an order of magnitude, when its water content was increased to 60 %. At water concentrations of 75 % and above, emission rates dropped below the detection limit of the analytical system employed. Thus, it is necessary that additional studies are conducted to fully assess the influence of water, i.e. the water content of the leaves, on abiotic methyl halide formation.

3.4 Environmental implications

The results of this study are consistent with an abiotic mechanism yielding methyl halides from plant material. The reaction involving plant own halide ions and methoxyl groups is highly sensitive to temperature changes. It is additionally dependent on the water content of the plant material (see also Hamilton et al. (2003)). As plants dry out the evolution of CH_3Br and CH_3Cl by the abiotic process becomes more efficient. The contribution of this process will vary spatially and temporally with changing temperature, halide and water content of the plant material. Amongst the zones that might be susceptible to temperature increase are agricultural areas such as, the Mediterranean, semiarid and arid zones where enriched halide plants can be found due to use of halogen enriched brackish water (Bustan et al., 2004) or saline soils (Rengasamy, 2006). Other possible CH_3Br sources are vegetation from land reclamation areas and restored saline land (Ravindran et al., 2007).

If global temperatures increase, as has been predicted, contribution of CH_3Br by this mechanism to the CH_3Br budget will be expected to increase dramatically based on the results presented here. On average, a rise of 5 ºC in temperature increases the amount of CH_3Br emitted by hay, ash, saltwort, tomato by a factor of 1.9 ± 0.4, 2.2 ± 0.8, 1.8 ± 0.7, 2.1 ± 0.3, respectively.
This is analogous to findings on methyl chloride made previously (Hamilton et al., 2003; Keppler et al., 2005). In addition to a general increase in CH_3Br emissions from existing sources occurring as a consequence of rising global temperatures, new source regions may emerge in areas where historic wetlands begin to dry out (e.g. Siberia). Furthermore, regional short duration extreme weather events such as heatwaves and droughts could cause emission hotspots as plants dry out. Such an event was experienced in Europe and the United States during the summer of 2003 (Trigo et al., 2006).

Further investigation on methyl halide emissions from saline soils and vegetation are certainly worthwhile since the United Nation Environment Program estimates that 20 % of agricultural land and 50 % of croplands in the world is under salt stress (Flowers and Yeo, 1995).

4 Summary and conclusions

Within this study the release of methyl halides (CH_3Cl, CH_3Br) from plant tissue was examined within a range of ambient temperatures (25 - 50 °C). All materials investigated during this study (bromide enriched pectin, hay, ash, tomato and saltwort leaves) showed an exponential increase of halomethane emissions with increasing incubation temperature. The activation energy for this process, determined using the temperature dependence of the reaction rates, gave strong evidence for a chemical rather than an enzyme-catalyzed reaction being responsible for the formation.

Large differences of CH_3Br release rates amongst the different plant species could be attributed to the formation process' dependence on bromine availability within the plant tissue. Inconsistencies could be explained by the varying methoxyl group content of the samples.

Release rates of CH_3Br and CH_3Cl showed a similar dependency on temperature. Small differences based on the slightly higher activation energy needed for the chlorine conversion can be ascribed to the lower nucleophilicity of the chloride ion.

The conversion efficiency of all investigated samples was less than 1 % of available Br within one day in the temperature range from 25 to 50 °C. This leaves a high potential of further release with increasing temperature, especially interesting with respect to global warming. However, a similar study by Hamilton et al. (2003) revealed that substantial increases in conversion efficiency occur only at temperatures higher than 175 °C.

This study demonstrates that CH_3Br as well as CH_3Cl release from plant material does happen significantly at ambient temperatures. A substantial increase with increasing temperature (nearly doubling the CH_3Br release rate each temperature step of 5 °C) indicates the high relevance of this process, if global warming continues.

However, the impact of this reaction is somehow restricted by the water content of the plant material. Tests revealed (see as well Hamilton et al. (2003)) that a water content of more than 65 - 75 % in the plant material prevents methyl halide formation. Thus, the largest impact of this process is expected from dry regions in high saline environments experiencing warm ambient temperatures and emerging dry regions.

The tropical rainforest ecosystem as investigated in Chapter 2, however, experiences high precipitation throughout the year. Hence, the complete drying out of plant material in this region is unlikely. Nevertheless, Hamilton et al. (2003) and Keppler et al. (2005) proposed that abiotic methylation in plants and soil organic matter primarily located in tropical/subtropical areas (30 °N - 30 °S) may account for the major global source of CH_3Cl (see Table 1.4). Their and our observations point to the possibility that methyl halide emissions from a variety of plants and terrestrial ecosystems (tropical plants, rice paddies, dry shrublands, peatlands and salt marshes) may be at least in part be derived from abiotic methylation resulting from senescent or water-stressed vegetation.

Chapter 4

Atmospheric halomethane measurements during a phytoplankton bloom at the Argentinean shelf break

Shipborne measurements of the atmospheric mixing ratios of CH_3Cl, CH_3Br, CH_2Br_2, $CHBr_3$, and CH_3I have been conducted along a South Atlantic Ocean transect from the 27th of January to the 5th of February onboard the French research vessel *Marion Dufresne.* The main focus of this study was on the characterization of halocarbon emissions from an algal bloom encountered off the coast of Argentina. Correlations within this halomethane dataset and with other simultaneously recorded atmospheric and oceanic parameters enabled the characterization of the source regions of particular halocarbons.

Mixing ratios of CH_3Cl and CH_3Br were not significantly affected by the presence of the phytoplankton bloom. CH_3I, CH_2Br_2 and $CHBr_3$ showed pronounced mixing ratio variations, which could be mostly linked to phytoplankton abundance. The temporal variations were similar for all three compounds. However, there was considerable variation in the relative size of the peaks encountered. This was attributed to species specific inhomogeneous phytoplankton emissions, rather than oxidative loss, since the lifetimes of the aforementioned species are long in comparison to transport times. In case of the polybrominated compounds, higher mixing ratios were found closer to the coast, possibly caused by landbased sources like macroalgae or salt marshes.

Within this study a new technique combining satellite derived biomass marker (Chl a) data with back trajectory analysis was applied to analyze the observed halocarbon mixing ratios. Coupled with flux measurements this technique may allow the parameterization of halocarbon emissions according to seawater Chl a concentration. Such methods may be used to obtain more accurate emission maps as input for global models.

1 Introduction

The ocean acts as a huge reservoir for chlorine, bromine and iodine. Volatile organic halogen species (e.g. halocarbons) provide a pathway to transport halogens from the water to the atmosphere. The impact of halocarbons like CH_3Cl and CH_3Br on the ozone budget has been described previously (see sections 1-1.1 and 1-1.2). In this study, additional short-lived compounds were investigated. Due to the relatively short lifetime of CH_3I, CH_2Br_2 and $CHBr_3$ (7, 120 and 26 days, respectively), they mainly affect the boundary layer and tropospheric chemistry. However, deep convection events may occasionally transport them rapidly to the upper layers of the atmosphere.

The global sources of CH_3I, CH_2Br_2 and $CHBr_3$ are dominated by marine contributors (see Table 1.4). The term "ocean", used in most budgets, summarizes myriad physical, chemical and biological processes occurring in the seawater as one net effect. Thus far, studies have shown that that halocarbons like CH_3Cl, CH_3Br, CH_3I, $CHBr_3$ and CH_2Br_2 are emitted from various marine organisms, especially macro[1]- and microalgae[2]. However, their emission levels vary considerably, not only from species to species, but also as a function of environmentally influenced physiological differences such as age, temperature, time of day, nutrition, partial desiccation, grazing, light and tidal movement (Nightingale et al., 1995; Itoh et al., 1997; Ekdahl et al., 1998). Since macroalgae are restricted to the seashore biome, their production influences the concentration in seawater and mixing ratios in air only close to the coast. Thus, while they may have a substantial local impact, on the global scale the contribution of kelp and other macroalgae is negligible for the monohalomethanes (Manley and Dastoor, 1987). However, the production of polyhalogenated bromomethanes by macroalgae is a major contribution to the global budget (Manley et al., 1992). Microalgae i.e. phytoplankton, are not restricted to the coastal zone; rather they are ubiquitous over the entire ocean surface. This is in contrast to macroalgae, which inhabit the ca. 0.5 % of the total oceanic area represented by coastal zones (Tokarczyk and Moore, 1994). Therefore phytoplankton is of great importance to the global flux, even though its net flux per weight unit may be considerably lower.

Halomethanes in the marine environment are not only produced by biological activities (see section 1-3.3 – "Abiotic production"). Abiotic nucleophilic substitution of iodine and bromine with chlorine atoms leads to the formation of CH_3Cl and mixed polyhalomethanes. Using data collected from the Pacific Ocean, it has been estimated that substitution of CH_3I could account for about 15 % of the oceanic CH_3Cl flux to the atmosphere (Moore and Groszko, 1999). Similarly, the contribution of the corresponding CH_3Br reaction was calculated to account for an additional 20 % of the CH_3Cl flux (Moore, 2003).

[1] Fenical, 1974; Lovelock, 1975; Gschwend et al., 1985; Manley and Dastoor, 1987; Nightingale et al., 1995; Laturnus et al., 1995; Manley et al., 1992; Itoh et al., 1997; Ekdahl et al., 1998

[2] Chameides and Davis, 1980; Sturges et al., 1992; Tokarczyk and Moore, 1994; Tait and Moore, 1995; Moore et al., 1996b; Scarratt and Moore, 1996; Scarratt and Moore, 1997; Itoh et al., 1997; Manley and delaCuesta, 1997; Saemundsdottir and Matrai, 1998; Scarratt and Moore, 1999

Moore and Zafiriou (1994) postulated that CH_3I can be formed via a photochemical reaction involving iodine and CH_3 radicals derived from organic matter. This process is inherently dependent on the light intensity. The *in situ* incubation experiments of Richter and Wallace (2004) lead to the conclusion, that up to 50 % of the CH_3I sea-to-air flux in the open ocean results from photochemical production, while in biologically active coastal and upwelling waters, various other production pathways may play a role.
Formation of methyl halides via nucleophilic substitution of DMSP in seawater as postulated by White (1982) and Brinckman et al. (1985), however, was shown to be too slow at ambient temperature to result in significant amounts of CH_3Cl, CH_3Br or CH_3I (Hu and Moore, 1996).

Marine production of halocarbons by whichever process leads to increased concentrations in seawater, which may be released to the atmosphere via sea-air gas exchange. The transport across the sea-air-boundary depends on the concentration of the species in both phases, its solubility and the transfer rate of the particular gas. A measure for the possible extent of exchange of a chemical is the saturation anomaly of the surface ocean at a particular temperature (Moore et al., 1995; Moore, 2000). The rate of exchange is regulated by turbulence at the air-sea interface, which is dependent on wind speed, boundary layer stability, surfactants and bubbles (Wanninkhof, 1992).
The saturation anomaly of CH_3Cl shows a strong dependence on sea surface temperature, with warm waters being usually supersaturated while cooler waters (below 12 °C) are typically undersaturated (Singh et al., 2003; Moore et al., 1996a; MacDonald and Moore, 2007). Overall the ocean is thought to act as a modest source of CH_3Cl supplying a net flux of 300 - 400 Gg CH_3Cl yr^{-1} to the atmosphere (Moore, 2000; Yoshida et al., 2004).
In the global cycle of CH_3Br, the ocean plays an ambiguous role. It is thought to be the single largest source in localized areas but, averaged over the entire ocean, it may act as a small sink ((Lobert et al., 1997; WMO, 2003a). Field measurements suggest that the ocean is a sink for CH_3Br in the oligotrophic regions of the open oceans and a source in coastal and upwelling areas (Singh et al., 1983; Lobert et al., 1995; Lobert et al., 1997).
Butler et al. (2007) found a similar pattern in the oceanic distribution of CH_3I, CH_2Br_2 and $CHBr_3$ combining data of seven cruises from 1994 to 2004. They reported (1) supersaturated surface waters virtually everywhere, all the time, except in regions of substantial mixing with subsurface waters, (2) periodic, extremely high supersaturations near coasts, often in association with beds of attached macroalgae, (3) high supersaturations in equatorial regions and near oceanic divergences and (4) moderate supersaturations in the central gyres.

The importance of the ocean as a possible source becomes evident when its size and productivity are considered. Field et al. (1998) found that although oceanic primary producers represent only 0.2 % of the global autotrophic biomass, about half of the global annual net primary production (NPP) on Earth takes place in the worlds oceans producing 48.5 Pg of C yr^{-1}, compared to 56.4 Pg C yr^{-1} on land. Spatial and seasonal variation of photosynthetic biomass in the oceans varies considerably. It is largely controlled by the availability of light and nutrients like nitrogen and iron. Regions of high oceanic NPP are found in coastal and upwelling regions (Field et al., 1998). Temporary enhanced concentrations of phytoplankton occur in locations with enhanced nutrient availability.

For example, widespread and rapid increases in algae, so-called plankton “blooms”, are observed in the North Atlantic during spring (the aptly named North Atlantic Spring Bloom), in the Eastern Basin Upwelling Zones like the Benguela Upwelling and the Peruvian Upwelling zone as well as in the large-scale Equatorial Upwelling, associated with the equatorial currents. Ocean currents can influence the nutrient supply of blooms and they can also conspire to maintain or restrain blooms due to the advection of water. Fronts may also be marked by locally high levels of phytoplankton, when mixing of two adjacent water masses provides the optimal parameters (nutrients, light, warmth, remnant phytoplankton and enhanced mixing or upwelling) that neither water mass contains alone (Quartly and Srokosz, 2003).

Here we present shipborne measurements of atmospheric CH_3Cl, CH_3Br, CH_3I, CH_2Br_2 and $CHBr_3$ conducted within the Organics over the Ocean modifying Particles in both hemispheres (OOMPH) project. The atmospheric mixing ratios along the MD 158 cruise track crossing the South Atlantic are reported and correlations with other atmospheric and oceanic parameters are examined. The main focus is set on the characterization of emissions from an algae bloom encountered in January/February 2007 off the coast of Argentina. An attempt is made to link variations in the mixing ratios to parameters such as phytoplankton abundance and the abundance of certain phytoplankton species, respectively; by using newly available satellite data based trajectory calculations.

2 Sampling and analysis

2.1 Instrumental

During the MD 158 cruise, air samples were measured *in situ* using GC-MS. The air was drawn from a 10 m mast at the foredeck of the *RV Marion Dufresne* (ca. 20 - 25 m above sea level) to the "wet laboratory", where the instrument was housed. Approximately 80 m of ½" o.d. (1.27 cm) shrouded Teflon sampling line, equipped with a 5 µm Teflon filter was run from the top of the sampling mast to the laboratory, providing a fast flow of sample air for a variety of measurements. Air was pumped through this line at ~ 6 - 8 l min^{-1} resulting in an air residence time on the order of 1 minute.

The GC-MS was equipped with a custom built sampling and cooling device to pre-concentrate chemicals prior to measurement (Gros et al., 2003). This enabled the detection of low-level ambient trace gases. Air was subsampled by the GC-MS from the main sampling line described previously, through a 1/16" (0.159 cm) stainless steel line at 30 ml min^{-1}. The air was dried by a $MgClO_4$ cartridge maintained at 100 °C and the trace gases of interest were then cryogenically trapped (-70 °C, on glass beads in a 1/16" ss tube). The total volume of air subjected to trapping was calculated using the pressure rise in a vacuum canister downstream, over the sampling time of 20 min. On average about 850 ml of air was concentrated. Target compounds were released from the trap by rapidly heating it to 200 °C and passing it onto a separating column (60 m x 0.248 mm x 1µm DB-5 capillary column, J&W Scientific, Agilent Technologies, Palo Alto, CA; USA) and from there to the mass spectrometer for detection (Agilent GC 6890, MS 5973). The temperature program of the GC was as follows: 35 °C for 4 min, heated at 15 °C min^{-1} to 120 °C, held for 3 min, heated at 120 °C min^{-1} to 250 °C, held for 3 min, cooled at 50 °C min^{-1} to 200 °C, held for 0.5 min.
The mass spectrometer was operated in single ion mode (SIM) to achieve maximum sensitivity. The chromatographic parameters were optimized to enable good separation of the halocarbons and a complete run took about 18 minutes. Helium 6.0 carrier gas was additionally purified in a converter tube (Supelco, Bellefonte PA; USA). Between the measurements, the cryotrap was flushed with helium at 200 °C to remove any residual trace compounds and blanks revealed no significant levels of the compounds reported. The measurements were conducted continuously once per hour with one calibration gas measurement every 5 hours.

2.2 Calibration and data quality

Calibrations were performed using a whole air working standard, prepared by filling an aluminum cylinder with ambient marine air using a three stage oil-free piston compressor (RIX industries, Benicia, CA, USA) modified after Mak and Brenninkmeijer (1994). This standard was calibrated subsequent to the cruise by Elliot Atlas (Rosenstiel School of Marine & Atmospheric Science, University of Miami, FL, USA) aligning it to the NCAR scale. The working standard was analyzed every five measurements. The samples in between were calibrated using a virtual standard value, corresponding to the time of the

sample acquisition. This value was obtained, by a linear regression between the adjacent standard gas measurements obtained before and afterwards as a function of acquisition time.
The linearity of the system was confirmed in the range of ambient mixing ratios by measuring a series of seven successively increasing amounts of the calibration gas. The mixing ratio range and the R^2 values of a linear regression (area counts vs. sample volume) are shown in Table 4.1. Generally excellent linearity $R^2 > 0.99$ was observed with the exception of (CH_3I) which was slightly lower ($R^2 = 0.96$).
The detection limit was defined as three times the area of the noise (for the compound specific ion at its specific retention time). To calculate a corresponding mixing ratio, the average sample volume (135 Torr, i.e. 852 ml) was used. Detection limits for all investigated compounds are listed in the Table 4.1.

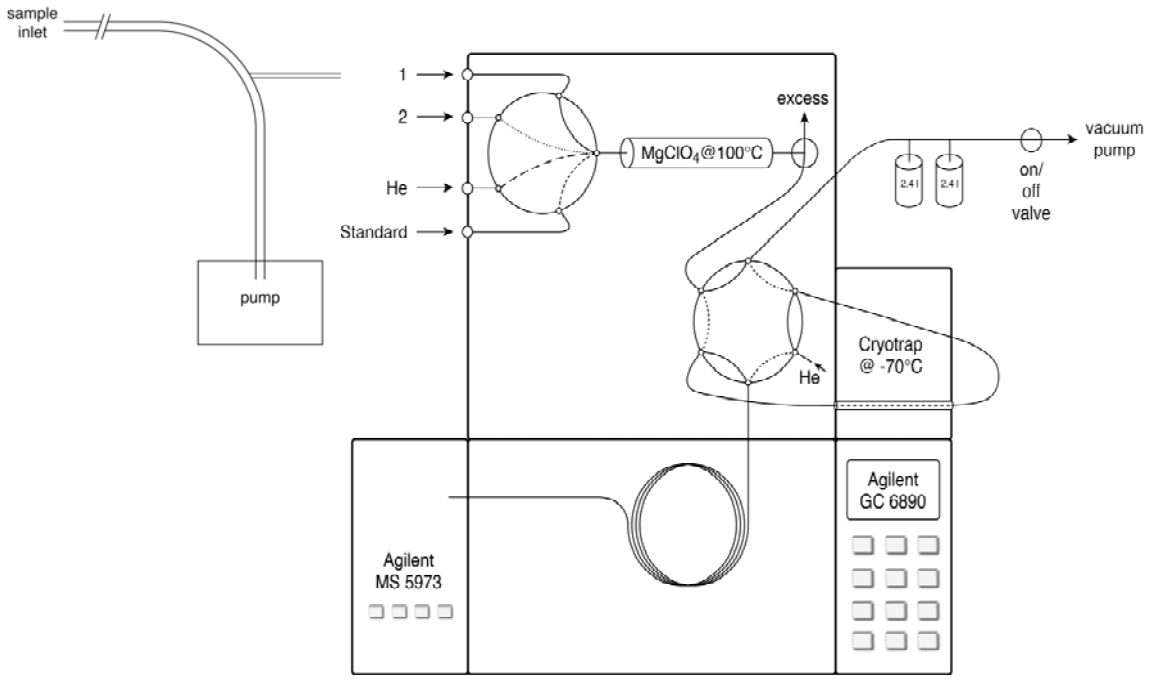

Figure 4.1: A schematic diagram of the *in situ* sampling setup attached to port 1 of the GC-MS inlet system.

The overall uncertainty was calculated by quadratic propagation of error including the calibration gas uncertainty and the measurement uncertainty. The latter is derived by calculating the deviation of the calibration gas measurements from a regression curve which takes into account the loss of detector sensitivity with time. Using this method, all possible errors which occur during the sampling, preconcentration, measurement and data analysis (e.g. statistical noise of the detector, errors arising from manual integration, pressure/sample volume uncertainty, etc.) are included, since they do affect the calibration gas measurements likewise. Therefore the standard deviation of the calibration gas measurements or - in the case of a drifting detector like an MS - the deviation from a sensitivity loss corrected regression line is a good and easily accessible

parameter to describe the measurements uncertainty. As calibration gas measurements are used to determine this parameter, it accounts for the errors corresponding to the peak area of the calibration gas and therefore it is strictly speaking only valid for measurements within the same area range. Since our working standard was ambient air bottled in a remote site at the coast of northern Germany this should be valid for most of the investigated compounds. Very small mixing ratios close to the detection limit will have higher uncertainties.

During this campaign the calibration gas signal did not show a consistent quasi-linear decay, which would be expected of a detector with declining sensitivity. Changing the water trap during the cruise produced pronounced deviations from the expected trend for some compounds. Apparently the water trap took some time to condition and adapt to the ambient air mixing ratios. To avoid misleading results by including rapid changes in the calculation, the deviations were calculated separately for each "water trap interval", omitting the first most probably unconditioned data section directly after the change. For the uncertainty calculation the maximum deviation was used.

Compound	Linearity range /pmol mol^{-1}		R^2	Detection limit / pmol mol^{-1}	Instrumental uncertainty / %	Line Artefact / %	Total Uncertainty / %
CH_3Cl	352	7044	1.000	11.7	2.1	4.4	4.9
CH_3Br	6.1	122	1.000	2.6	5.5	6.5	8.5
CH_2Br_2	0.8	15	0.999	1.1	15.8	N.D.	15.8
$CHBr_3$	74	1481	0.995	0.6	24.9	1.9	24.9
CH_3I	0.2	3.2	0.962	0.5	3.4	0.4	3.4

Table 4.1: Experimental details of the investigated compounds.

2.3 Sampling line artefact test

As stated in the previous section, sampling took place via ~ 80 m of ½" (1.27 cm) o.d. shrouded Teflon tubing fitted with a 5 µm Teflon filter. The residence time within the line was approximately 1 min. Although Teflon is known as a very inert material, over such long lengths there is the possibility that interfering reactions on the surfaces of the inlet occur. Certain chemicals may have been released by the Teflon itself or produced from it by chemical reactions following heating or irradiation with light. Any light induced artefacts were eliminated by shrouding the entire inlet line. Another possible influence on the air sample prior to measurement was through adsorption of gas molecules on the walls of the tubing. Such an adsorption would lead to a smearing of the ambient signal and a tailing of high mixing ratio spikes. Condensation within the sampling line could be neglected because the temperature of the ambient air was colder than the room temperature in the lab most of the time. To exclude a release/adsorption

impact of the tubing on our results tests were in the laboratory on the original tubing employed on the ship.
Various dilutions of a gas mixture with known mixing ratios were sampled with and without the sampling line, i.e. before (OS) and after (MS) the 80 m ½" Teflon line. The Teflon filter and the $MgClO_4$ dryer were not employed, as the gas mixture used was dry. Therefore any effects caused by humidity changes or water adsorption on the inner walls of the tubing could not be reproduced or evaluated by this test. The pump was set to draw air at 6 l min^{-1} as it did on the ship. The calibration gas mixture flow was set to about 10 l min^{-1} and frequently checked during the measurement. Excess flow was allowed to vent. The calibration gas contained all target compounds at about 100 nmol mol^{-1}. To ensure ambient mixing ratio range was covered, three different dilutions were measured (1:200, 1:1250, 1:5000).

Compound	Dilution 1/200 MR /pmol mol^{-1}		Dilution 1/1250 MR /pmol mol^{-1}		Dilution 1/5000 MR /pmol mol^{-1}		Difference ((OS-MS)/OS)) / %
	OS	MS	OS	MS	OS	MS	
CH_3Cl	760.7	727.6	125.0	110.7	34.5	30.4	4.4
CH_3Br	238.3	220.6	39.8	37.3	6.9	6.3	6.5
$CHBr_3$	242.0	235.1	13.7	13.4	2.4	2.8	1.9
CH_3I	772.3	692.0	139.0	128.2	23.7	23.6	0.4

Table 4.2: Mixing ratios of calibration gas mixture sampled with and without 80 m Teflon tubing and the percental difference (grey numbers indicate non ambient concentrations).

The calibration gas did not contain CH_2Br_2, therefore this compound could not be tested. The results generally showed slightly higher values for measurements without the tubing. This implies that the sampling line indeed had an effect on the mixing ratio of chemicals sampled through it. None of the compounds was formed in the tube but a small fraction was lost to the walls. For most compounds, this effect was rather small (< 5 %). CH_3Br showed a decrease of around 6 %. To estimate the importance of this decrease in the mixing ratios it was compared with the measurement uncertainty for the specific compounds (see Table 4.1). For all investigated compounds besides CH_2Cl_2, C_2Cl_4 and $C_6H_5CH_3$ the artefact introduced by the tubing was in the same order of magnitude or lower than the instrumental uncertainty. Its effect was added to the instrumental uncertainty using the quadratic error propagation resulting in the total uncertainty (see Table 4.1).

2.4 Data quality test

Several substances including CH_3I were quantified in canisters filled 2 to 4 times a day during the MD 158 cruise in addition to our online-GC-MS. The analysis of canister air was performed subsequent to the cruise in the laboratory of Elliot Atlas at the Rosenstiel

School of Marine and Atmospheric Sciences, Marine and Atmospheric Chemistry Division, Miami, FL.
The sampling of the canisters took place via a different line (3/8" (0.95 cm) o.d., 80 m shrouded Teflon line). The air was drawn at a higher flow rate through this line (12 l min^{-1}), resulting in a residence time of approximately 30 s. Prior to the sampling the canisters were evacuated to at least 10^{-4} Torr and flushed 5 times and subsequently were pressurized to about 30 psi (2 bar).
Although the air was sampled via different lines and different instruments and calibration gases were used for the quantification, the results of the canister and online samples showed a very good agreement (R = 0.87), establishing the quality of the data set.

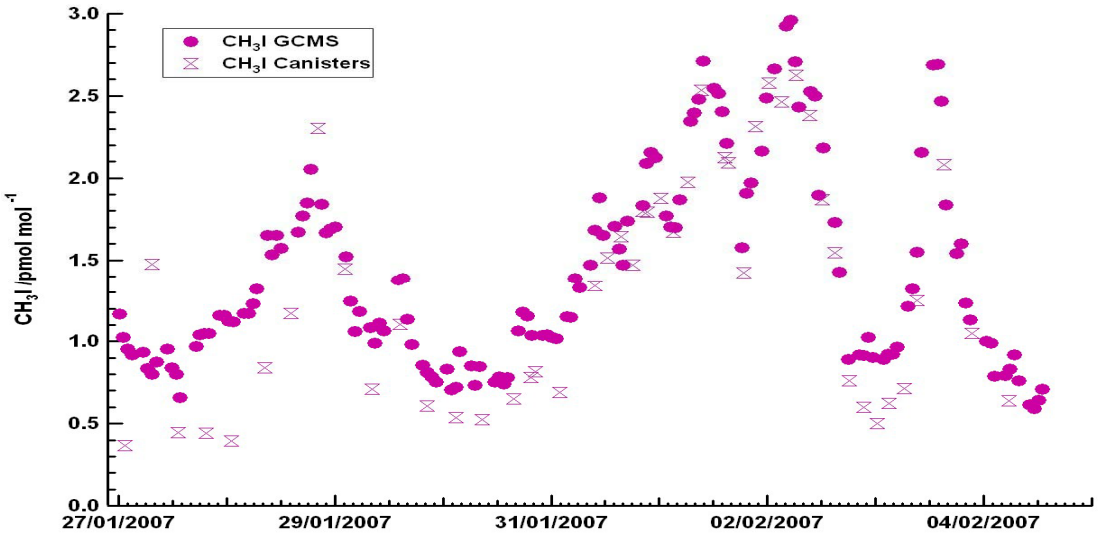

Figure 4.2: Comparison of canister and online-GC-MS data of CH_3I.

2.5 Instrumental details of other relevant instruments

In the course of the data analysis several parameters recorded with other instruments were used for comparison. The salient details of the pertinent instruments are given below:
CO in the gaseous phase was measured every five minutes with a gas chromatograph equipped with a mercuric oxide reduction detector (Trace Analytical, USA) (see Gros et al. (1999) for instrumental details). Air was sampled from the starboard side of the vessel with a 20 m Teflon line (1/4" o.d. (0.64 cm)). The detection limit was 2 nmol mol^{-1} and an overall uncertainty was estimated to about 4 %. Samples were calibrated several times a day against a certified NOAA standard (151.5 nmol mol^{-1}) (Novelli et al., 1994; Masarie et al., 2001).
O_3 was measured every minute with a UV-absorption instrument (Thermo-Electron, model 49C, USA). Air was sampled from the central inlet located at the top of the mast. This type of instrument has shown a good stability and reproducibility (Gros et al., 1998).

The estimated uncertainty is better than 5 %. The instrument used onboard the *RV Marion Dufresne* was not calibrated before the campaign. Therefore a correction was applied to the data based on a comparison with another O_3 analyser performed on a subsequent cruise (Beygi, personal communication, 2008) and calibration of the analyser at the World Calibration Centre for Surface Ozone, Carbon Monoxide and Methane (hosted at Empa, Duebendorf, Switzerland).

DMS was measured by a proton transfer reaction mass spectrometer (PTR-MS). Samples for the PTR-MS were taken from the same inlet line used for GC-MS sampling, extended by ~ 10 m of ¼" o.d. Teflon line at a flow rate of circa 200 ml min^{-1}. The values presented are 10 minute averaged data, which have been filtered for ship contaminated periods. The detection limit varies between 0.2 and 0.8 (avg 0.4) nmol mol^{-1}. The instrumental uncertainty is conservatively estimated to be 20 %.

3. Results and discussion

3.1 Meteorological conditions

The MD 158 cruise began on the 19th of January in Cape Town, South Africa (18.42 °E, 33.91 °S) and ended in Punta Arenas, Chile (70.85 °W, 53.12 °S) on the 5th of February 2007. The *RV Marion Dufresne* crossed the Southern Atlantic Ocean from East to West between approximately 35° - 50 °S, the final section being a North-South leg close to the coast of Argentina (see Fig. 4.3).
The region is dominated by the prevailing strong Westerlies and by successive high and low pressure systems. Cloud cover is usually extensive, caused by warm, moisture-laden air from the tropics encountering cold air over the cold water of the polar oceans. This region of the Southern Ocean is renowned for severe weather and sea conditions, being referred to as the "Roaring Forties" and "Furious Fifties".

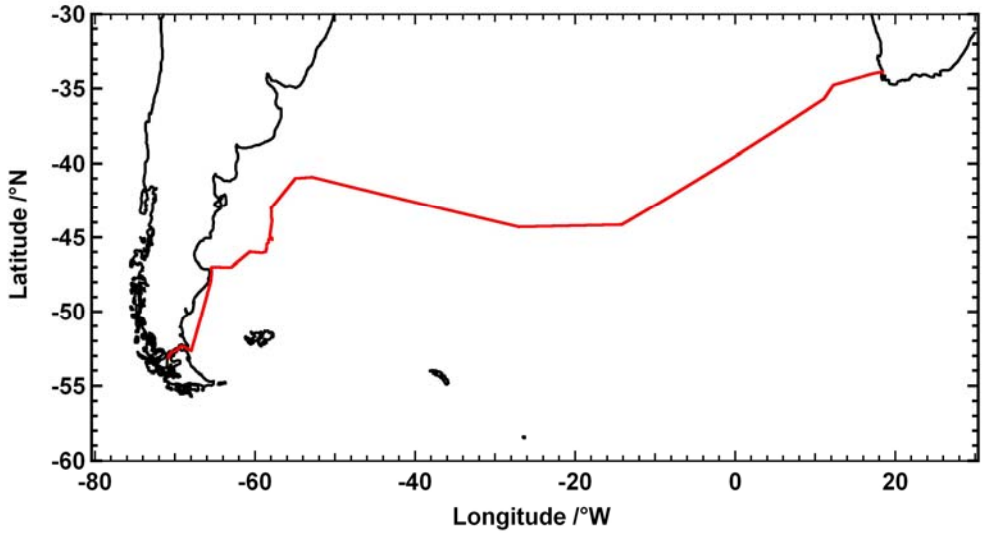

Figure 4.3: Cruise track MD 158.

On the MD 158 cruise, the prevailing wind direction was westerly, with wind speeds varying in strength from virtually windless (Bft 0) up to 25 ms^{-1} (Bft 10). The average wind speed was 9.5 m s^{-1} (Bft 5), corresponding to a fresh breeze. Gale force winds (wind speed > 17 m s^{-1}) occurred frequently.

Meteorological data and models allow back trajectories for the encountered air masses to be calculated. These trajectories show, how an air parcel traveled prior to arrival at the ship (typically 3, 5 or 10 days backwards). Prof. Heini Wernli (University of Mainz, Germany) provided a set of 10-day back trajectories for the MD 158 cruise based on Lagrangian Analysis Tool (LAGRANTO) (Wernli and Davies, 1997; Stohl et al., 2001). A group of 10 trajectories was started every 3 hours within a ± 30 min time interval around the exact ships position. The path of the trajectories was calculated using three-dimensional wind fields from the European Centre for Medium-Range Weather Forecasts (ECMWF). For the analysis, 6 hourly operational global analyses (T799L91) were

complemented by intermediate 3 hourly forecasts interpolated onto a horizontal grid with a resolution of 1° latitude/longitude. The horizontal resolution of the model was 25 km using 91 vertical levels. The computational time step for trajectory calculations was 30 minutes. These trajectories are an important tool in determining the origin and emission history of a given air mass. The trajectories shown in Fig. 4.4 confirm the general westerly wind pattern during the investigated part of the MD 158 cruise.

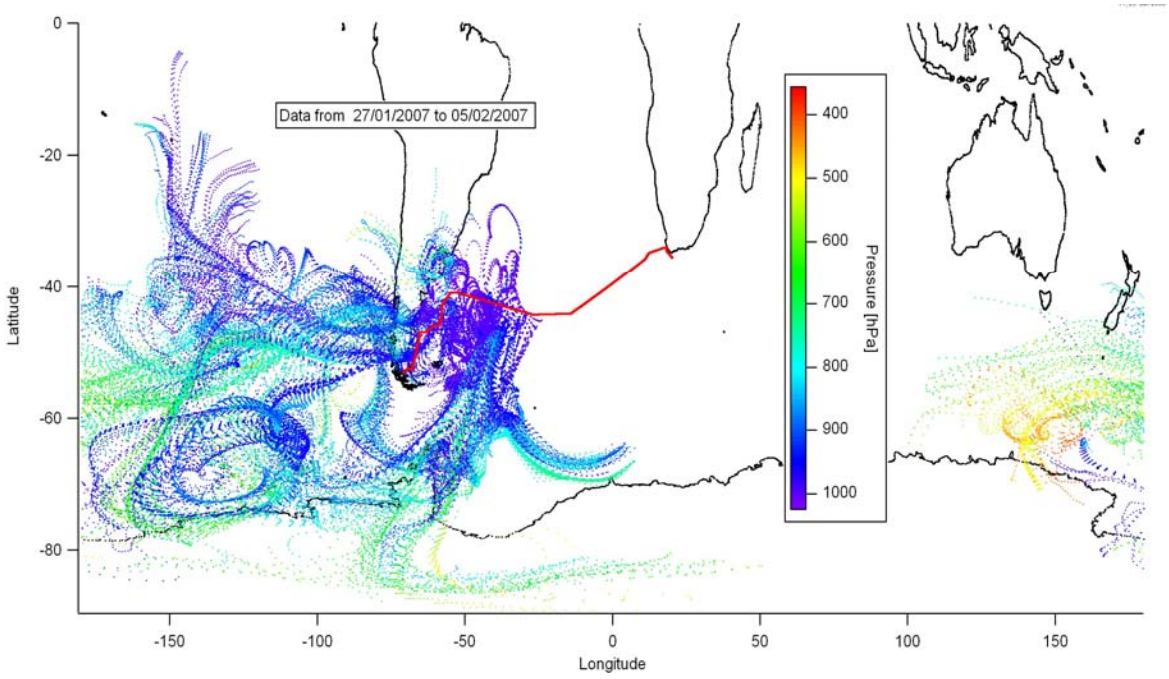

Figure 4.4: Air mass 10-day back trajectories of the cruise track from 27.01. - 05.02.2007. Trajectories were plotted using ITOSA, an IGOR^{TM} based customized program developed at the Max Planck Institute for Chemistry by Dr. Stefanie Wong-Zehnpfennig.

3.2 Oceanographic conditions

The area of the South Atlantic Ocean traversed by MD 158 is not at all homogenous in terms of oceanographic conditions. It can be divided in two sections - the undisturbed open ocean frontal system and a coastal convergence zone off Argentina.
The South Atlantic and Southern Ocean show a pronounced frontal structure. Belkin and Gordon (1996) determined two main frontal zones running mainly east-west, the subtropical frontal zone and the polar frontal zone, which are bordered by the north and south subtropical front, and the subantarctic and polar front, respectively. At the border of these frontal zones, where water masses of different seawater characteristics such as temperature and salinity meet, enhanced biological production may occur.
The Patagonian Shelf off Argentina instigates complex dynamic processes in the ocean involving tides, the confluence of the warm Brazil and the cold Malvinas Current, and the transition zone between the shelf water of various origins and the Malvinas Current water. The Malvinas Current carries cold, fresh and nutrient rich water northward, where it meets the Brazil Current flowing poleward along the continental margin of South America. The confluence, formed by the collision of the two currents, results in an upwelling of water from deeper layers, which transports nutrient-rich water in the euphotic zone and thereby triggers increased phytoplankton growth. South of this confluence region another region of enhanced biological production is to be found, namely the Argentinean shelf-break zone. Although physical processes involved in the shelf break front are poorly understood, *in situ* and remote sensing measurements have shown the high biological productivity of this area (Romero et al., 2006; Signorini et al., 2006).

Since oceanic production of halocarbons is mostly related to biological production or reactions making use of decaying organic material, an overview of the biological activity in the investigated area is of great use. This overview is provided by satellite borne Chl a measurements. Fig. 4.5 shows a map of the biomass marker Chlorophyll a (Chl a) provided by the SeaWiFS Project, NASA/Goddard Space Flight Center and GeoEye. The moderate enhancement of Chl a concentrations, assumed to be phytoplankton abundance, along the southern boundary of the subtropical front is clearly visible as a green band across the South Atlantic. As described previously, this is where colder, nutrient-rich waters of the subantarctic front interact with warmer more stratified waters of the subtropical frontal zone, providing good growing conditions for phytoplankton. In the region of the Brazil-Malvinas confluence close to the Argentinean coast, where due to the convergence of the Brazil and Malvinas current the mixing of warm and cold water masses is even more pronounced, a very significant phytoplankton bloom could be observed.
While satellite derived data give a regional overview, parameters measured *in situ* onboard the *RV Marion Dufresne* provided an instantaneous measurement at the exact time and position of the ship. The phytoplankton abundance and community composition was determined during the cruise via HPLC pigment analysis of 3-hourly collected water samples from the ship's seawater line (7 m below the ship). Samples were filtered on GF/F-filters, rinsed with filtered seawater, immediately frozen at -80 °C and stored until analysis. The analyses were performed by I. Peeken at the IfM-GEOMAR, Kiel,

Germany. Phytoplankton biomass concentrations markedly increased during the cruise as it progressed from East to West, from low values around 0.2 µg Chl a l^{-1} in the oligotrophic Atlantic to 4.5 µg Chl a l^{-1} close to the Argentinean coast. Rapid variations in the phytoplankton biomass from the 28th of January onwards, reflect the complex hydrographic features crossed during this part of the cruise.

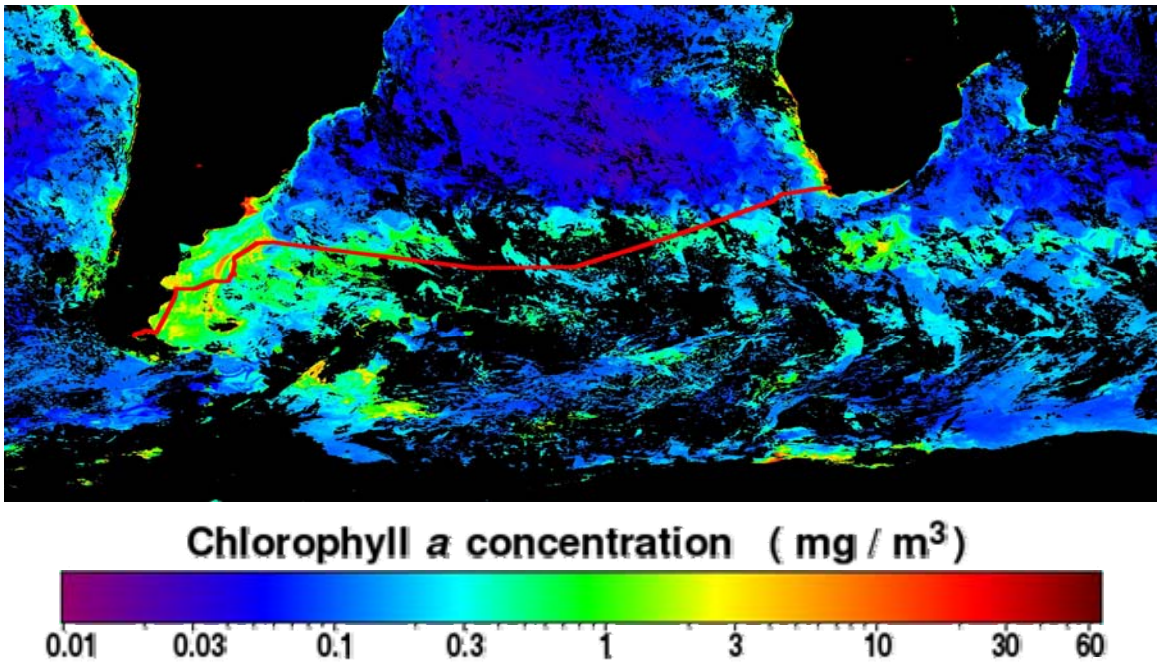

Figure 4.5: Cruise track MD 158 and Chl a in the South Atlantic Ocean from 25.01 - 01.02.2007 (satellite picture provided by the SeaWiFS Project, NASA/Goddard Space Flight Center and GeoEye: http://oceancolor.gsfc.nasa.gov/cgi/level3.pl, downloaded 09.01.2008).

Analysis of further, more specific marker pigments applying CHEMTAX® (Mackey et al., 1996) allowed several algae groups to be distinguished. During the extremely high chlorophyll section close to the Argentinean coast (02.02. 12:00 UTC – 02.02. 19:00 UTC) the phytoplankton bloom was dominated by autotrophic dinoflagellates. A second period of enhanced Chl a at the very end of the cruise (03.02. 10:00 UTC – 03.02. 20:00 UTC) correlated with enhanced diatom abundance. During the other parts of the cruise at moderate Chl a concentrations the background algal community consisted of a mixture of chlorophytes, cyanobacteria, pelagophytes, diatoms, haptophytes and dinoflagellates, with cyanobacteria and chlorophytes being generally most abundant.
Recently, a new approach has been attempted to survey the more species specific pigments from satellites. The PHYSAT classification (Alvain et al., 2005;Alvain et al., 2006) uses an empirically derived relationship between normalized water-leaving radiance at specific wavelengths and abundant phytoplankton species determined via *in situ* measurements to create a global phytoplankton species map from the available satellite data set. The technique uses seven pigments to distinguish between five phytoplankton groups (haptophytes, *Phaeocystis* in particular, diatoms, *Prochlorococcus* and *Synechococcus*-like cyanobacteria). Daily SeaWiFS data (available at the

NASA/GSFC/DAAC homepage) are used to obtain monthly maps of the phytoplankton distribution. If none of the five species dominates the 1°x1°-grid box or unidentified species prevail, the box is left blank. The box is also left blank if the aerosol optical thickness exceeds 0.15.

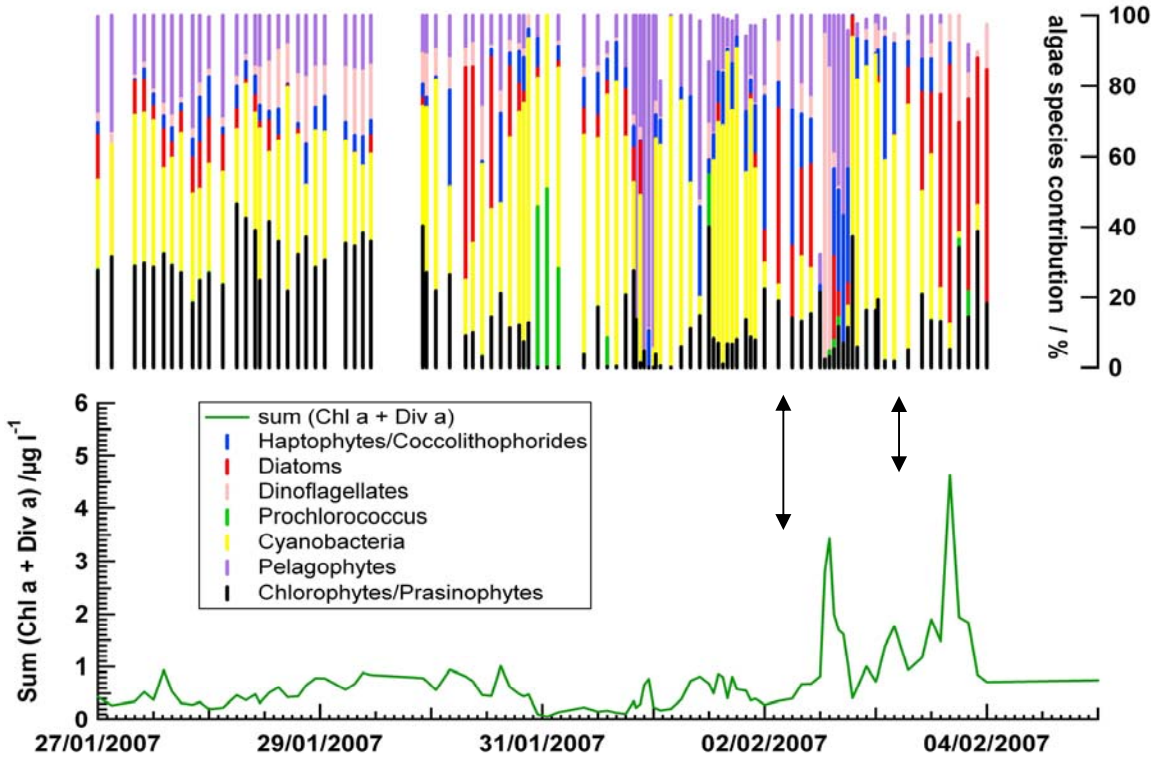

Figure 4.6: Chl a abundance and contributions from specific algae species.

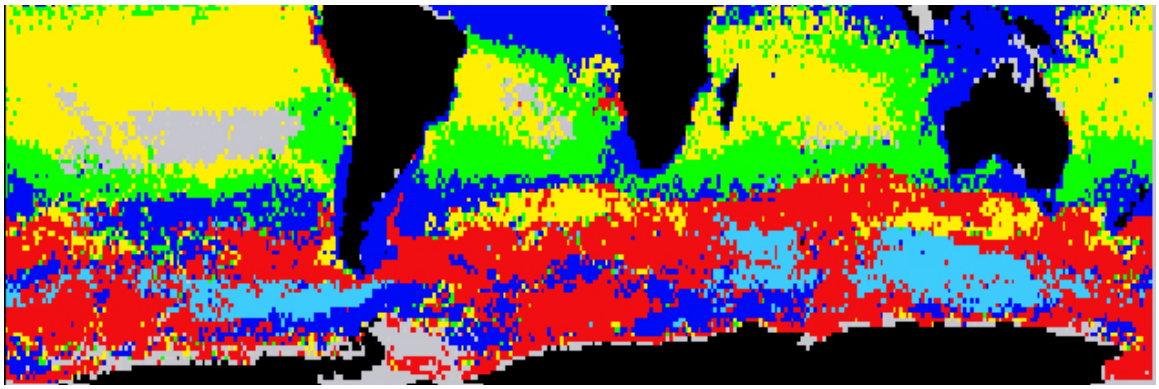

Figure 4.7: PHYSAT January Climatology 1998 - 2007 of the South Atlantic Ocean displaying predominant algae species (blue: haptophytes, light blue: *Phaeocystis*, red: diatoms, green: *Prochlorococcus*, yellow: *Synechococcus*-like picoplankton) provided by S. Alvain, Laboratoire d'Oceanologie et de Geosciences, CNRS-ULCO-USTL, Wimereux, France.

This technique enables us to determine the dominant plankton species not only along the cruise track, but for whole regions of interest (i.e. the region passed by the trajectories (see Fig. 4.4)). Fig. 4.7 shows the predominant plankton species during January as a 10-year average in the Southern Ocean. It demonstrates, that the region crossed by the cruise track is not homogenous in terms of predominant algae species.
Comparison with the *in situ* pigment data along the cruise track revealed a general agreement. However, it needs to be taken into account, that the PHYSAT technique cannot distinguish all phytoplankton groups, and furthermore the phytoplankton classification categories used by marine biologists and the satellite groups are different. For example diatoms and dinoflagellates are both displayed as diatoms in PHYSAT. The general trend of a mixed, cyanobacteria-dominated background community superimposed by a diatom (diatom+dinoflagellate) dominated region along the Malvinas current off Argentina is well captured by the satellite data. However, haptophyte abundance approaching South America seems to be overestimated. On average in January, cyanobacteria dominate the waters north of the subtropical frontal zone. The regions south of the subantarctic front as well as the Brazil-Malvinas confluence seem to be largely dominated by diatoms and haptophytes, in particular by *Phaeocystis*, which is another bloom forming haptophyte. The area in between those frontal zones exhibits various alternating predominant species, i.e. *Prochlorococcus*, diatoms and *Synechococcus*-like picoplankton.

3.3 Halocarbon measurements during MD 158

During the MD 158 cruise, reliable data was obtained from the 27.01. to the 04.02.2007. Depending on the wind direction and the course of the ship, the air at the sampling inlet was occasionally contaminated by the ship's own and other ships emissions for short periods. Although in general the ship was steaming into the prevailing wind, some periods of contamination by stack exhaust occurred. These events were determined according to a filter developed by Zorn et al. (2008) using simultaneously measured aerosol mass spectrometer and relative wind direction data. The contaminated periods are represented by the black and grey areas in Fig. 4.8. In total three (out of 150) samples were affected. A summary of the halocarbon mixing ratios is provided in section 4-3.6 – "Comparison to former studies" (see Table 4.3).

The ambient mixing ratios along the cruise track, sampled at ~ 20 - 25 m above sea level, are shown in Fig. 4.8. It should be noted that the time frame of the data presented covers only the second half of the entire cruise, from the oligotrophic ocean into the intense bloom area.
The CH_3Cl mixing ratios obtained range from 463 to 622 (avg 495, median 491) pmol mol^{-1}, with one outstanding peak on the 1st of February. Less pronounced enhancements were measured around the 29th of January, 2nd and 3rd of February.
CH_3Br mixing ratios show very little variation during the cruise with minimum and maximum values of 5.0 and 8.4 pmol mol^{-1}. Average and median values were 7.2 pmol mol^{-1}. A broad maximum of up to 8.4 pmol mol^{-1} was reached on the 31st of January.
CH_3I showed a clear pattern of several enhanced mixing ratio events. The first peak, in which mixing ratios rose from 0.8 to 2.1 pmol mol^{-1}, was observed on the 28th of January. From the 31st of January to the 2nd of February a period of generally higher mixing ratios followed. Within this time period three separate peaks can be discerned. Towards the end of the cruise a single outstanding peak was observed on the 3rd of February. During the cruise CH_3I mixing ratios ranged from 0.6 to 3.0 (avg 1.4, median 1.2) pmol mol^{-1}.
The last peak in CH_3I on the 3rd of February coincided with a peak in the mixing ratios of CH_2Br_2 and $CHBr_3$, representing their maximum values during the cruise (CH_2Br_2 2.8 pmol mol^{-1}, $CHBr_3$ 15.3 pmol mol^{-1}). The triplet peak pattern (31.01. - 02.02.) observed in CH_3I was found for the brominated compounds as well, although the pattern was less clear. Curiously, the first rise of CH_3I mixing ratios around the 29th of January did not coincide with a peak in either brominated species. Minimum values were close to or at the detection limit (CH_2Br_2 1.0 pmol mol^{-1}, $CHBr_3$ 1.8 pmol mol^{-1}) and the respective average mixing ratios were 1.5 (median 1.5) pmol mol^{-1} for CH_2Br_2 and 5.0 (median 4.6) pmol mol^{-1} for $CHBr_3$.

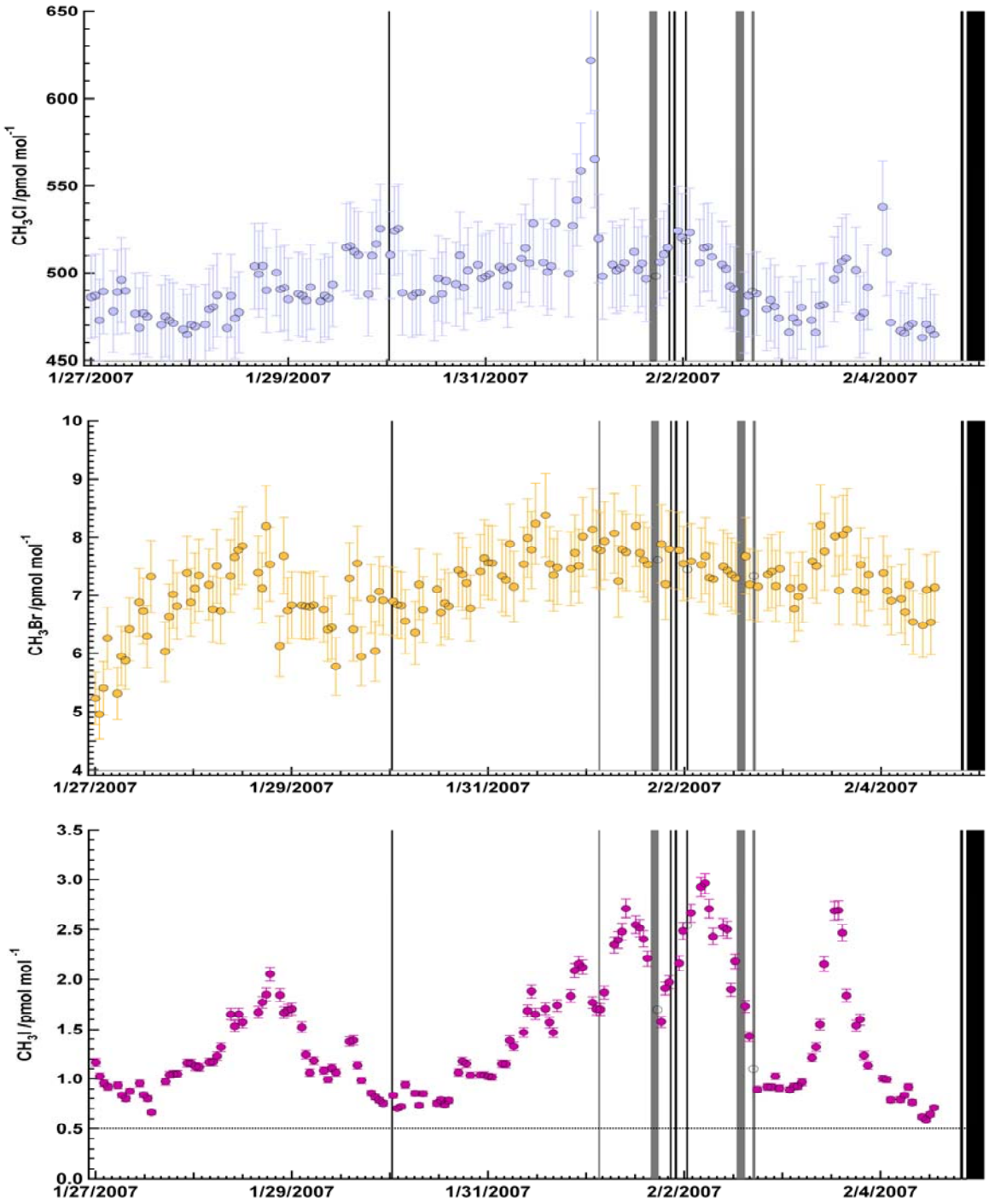

Figure 4.8: Mixing ratios of CH_3Cl, CH_3Br, CH_3I, CH_2Br_2 and $CHBr_3$ vs. time (filled circles mark unpolluted air samples, whereas empty circles represent samples discarded applying the contamination filter). Error bars give the overall uncertainty of the measurements. A dashed horizontal line represents the detection limit, if on scale. Grey and black bars mark pollution events.

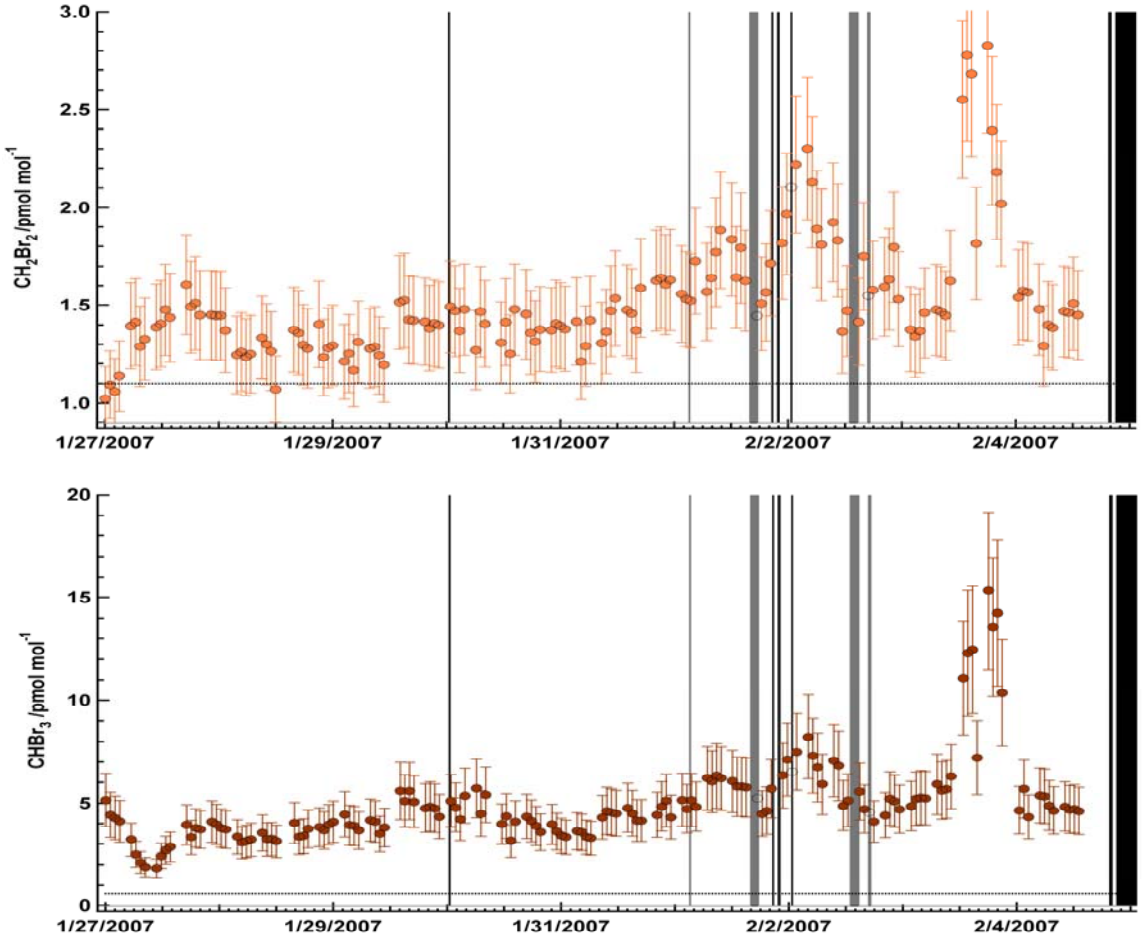

Figure 4.8 continued: Mixing ratios of CH_3Cl, CH_3Br, CH_3I, CH_2Br_2 and $CHBr_3$ vs. time (filled circles mark unpolluted air samples, whereas empty circles represent samples discarded applying the contamination filter). Error bars give the overall uncertainty of the measurements. A dashed horizontal line represents the detection limit, if on scale. Grey and black bars mark pollution events.

3.4 Classification of air masses

Since our measurements were performed in the gas phase, the recent "history" of the air mass needs to be considered to understand variations in mixing ratios. For that purpose back trajectories are a powerful tool. For the second part of the MD 158 cruise, five distinct trajectory patterns are distinguishable. Fig. 4.9 shows one example of each trajectory class.

Class 1: advection from Antarctica, mostly within the marine boundary layer
Class 2: advection from Antarctica crossing the southern tip of South America, mostly within the marine boundary layer
Class 3: advection across the Southern Pacific and Atlantic from various altitudes
Class 4: air masses from free troposphere, subsiding to the boundary layer shortly before measurement
Class 5: back trajectories with undefined directions indicating a change in the weather situation

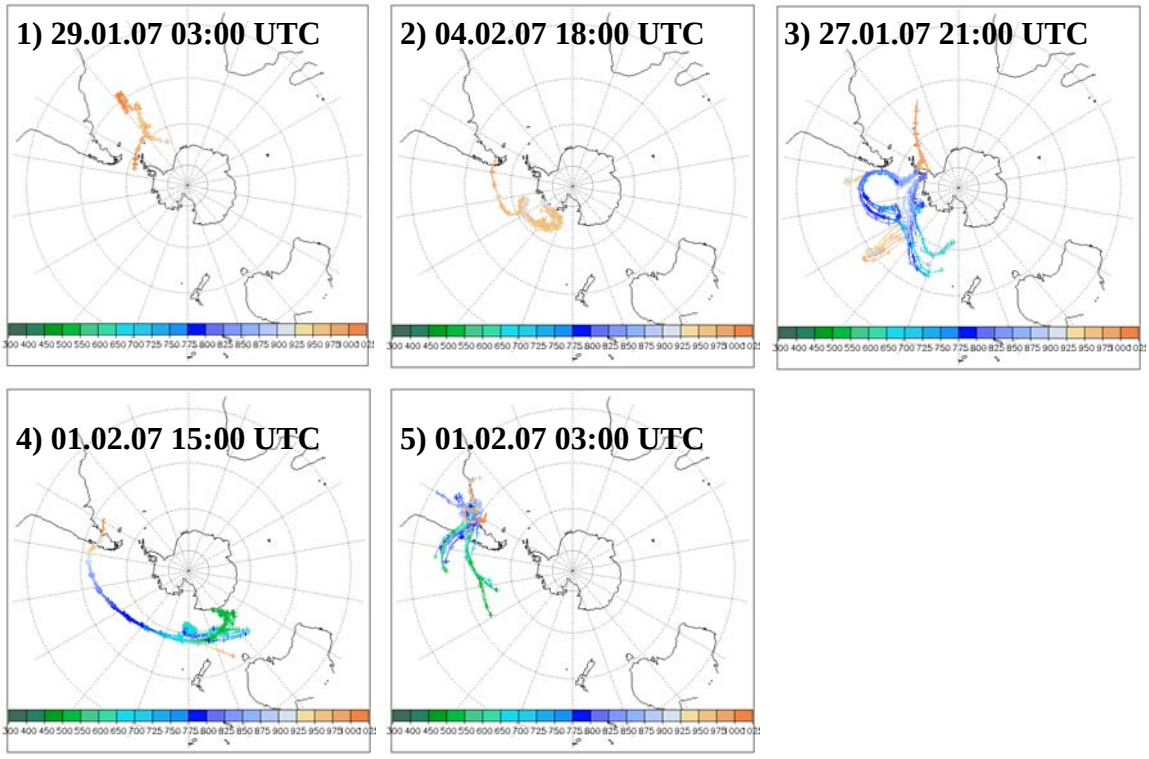

Figure 4.9: Examples for typical trajectories. The colour code indicates the pressure level from dark green (300 hPa) to orange (1025 hPa). Trajectory maps were generated by Prof. Heini Wernli, University of Mainz, Mainz, Germany.

From this classification of air masses according to back trajectories, we may draw some preliminary conclusions on the possible origins of halocarbon mixing ratio peaks. For class 1 and 3 trajectories, the air mass had no terrestrial influence in the past 10 days

besides Antarctica, whereas class 2, 4 and 5 trajectories crossed the southern tip of South America at some point. Therefore for class 1 and 3 trajectories we do not consider terrestrial vegetation or soil as potential sources and assume that variations within these periods are caused by oceanic emissions. This assumption appears reasonable, particularly for very short lived compounds such as CH_3I. For the last part of the cruise most of the back trajectories had some contact with the South American continent (see Fig. 4.10) and influence from terrestrial sources cannot be ruled out. However, during that period the trajectories passed over the biologically active bloom area represented by high Chl a values in the satellite picture (Fig. 4.5), before reaching the ship.

The air mass origin classes are depicted in Fig. 4.10 together with the time series of CH_3I and CH_3Cl data. High and low CH_3I mixing ratios occurred during phases of nearly all trajectory classes. This lack of dependence of mixing ratios on possible contact of air masses with land supports the thesis that this compound is primarily of marine origin.
Higher CH_2Br_2 and $CHBr_3$ mixing ratios appeared during the last part of the cruise. At this time, sampled air fell into trajectory classes 2, 4 and 5, all of which cross the South American continent. A terrestrial influence causing increases in CH_2Br_2 and $CHBr_3$ mixing ratios (e.g. salt marshes or coastal macroalgae) could therefore not be ruled out.
At the time of the highest CH_3Cl mixing ratios, the air mass classification showed a change of air mass origin from class 2 (advection from Antarctica crossing the southern tip of South America, mostly within the marine boundary layer) to class 4 (air masses from free troposphere, subsiding to the boundary layer shortly before measurement), including a period of class 5 (undefined directions) back trajectories. With the help of air mass classification this time could be identified as a period of changing air masses, all of which have been in contact with the South American continent.

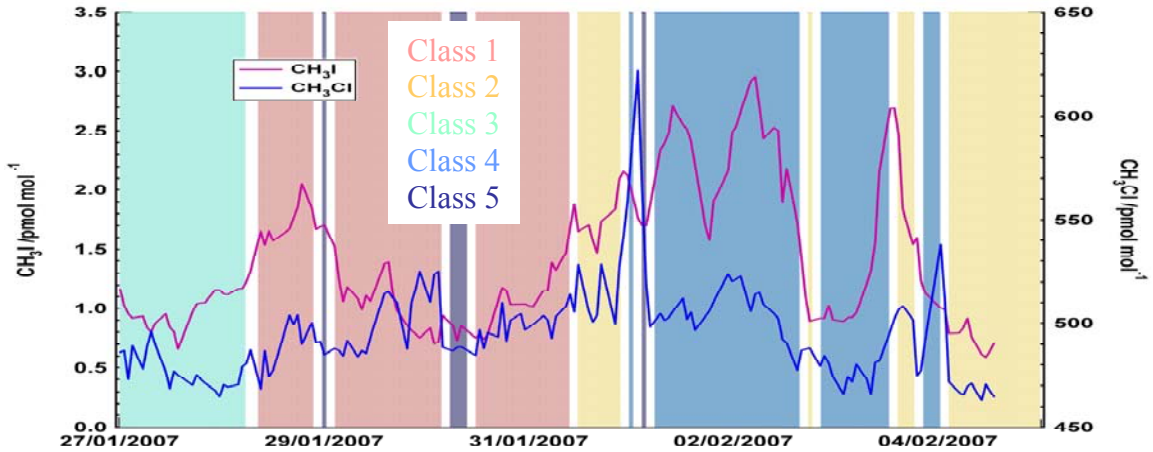

Figure 4.10: CH_3I and CH_3Cl time series and air mass origin corresponding to class 1 to 5.

3.5 The CH_3Cl peak – an isolated anthropogenic signature

More information could be obtained by considering the individual trajectory bundles. The trajectories corresponding to the exact time, when the CH_3Cl peak occurred ran across highly populated areas of the South American continent including the city of Buenos Aires (see Fig. 4.11). The terrestrial origin of the CH_3Cl peak was supported by other parameters measured during the cruise. O_3 as well as CO mixing ratios exhibited a peak at the same time as CH_3Cl (see Fig. 4.12).
Atmospheric CO is a product of incomplete combustion of fossil fuels and biomass and it is formed by oxidation of hydrocarbons. Oceanic and biogenic terrestrial sources play a minor role in the global budget (Khalil et al., 1999). Tropospheric O_3 is formed from volatile organic compounds or CO and nitrogen oxides in the presence of sunlight (see section 1-1.2.1.2 – "Tropospheric ozone"). Therefore high mixing ratios of CO - known to be mainly of anthropogenic origin - accompanied by a large amount of O_3 are indicative of aged, polluted continental air.
This supports the hypothesis, that the enhancement of CH_3Cl mixing ratios was due to a plume of polluted continental air sampled at that particular point of the cruise. Importantly, the absence of any further simultaneous peaks in CO and O_3 indicated, that no further large anthropogenic events were encountered during the cruise. A generally reasonable correlation between CH_3Cl and CO measured in the gas phase ($R = 0.66$), however, suggested similar sources for this species throughout the cruise.

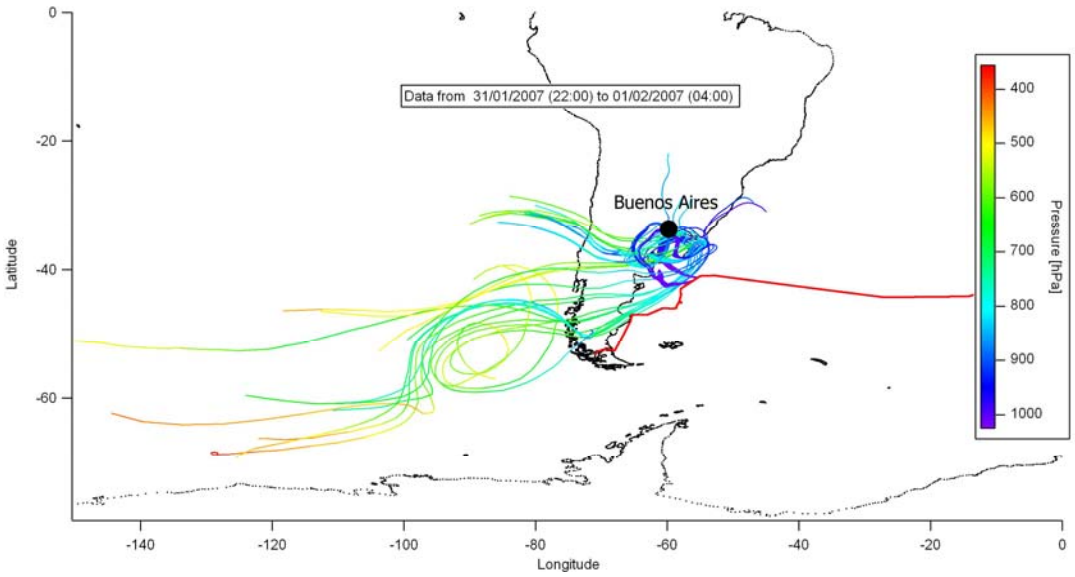

Figure 4.11: Air mass 10-day back trajectories during the time of the CH_3Cl peak. Trajectories were plotted using ITOSA, an IGOR™ based customized program developed at the Max Planck Institute for Chemistry by Dr. Stefanie Wong-Zehnpfennig.

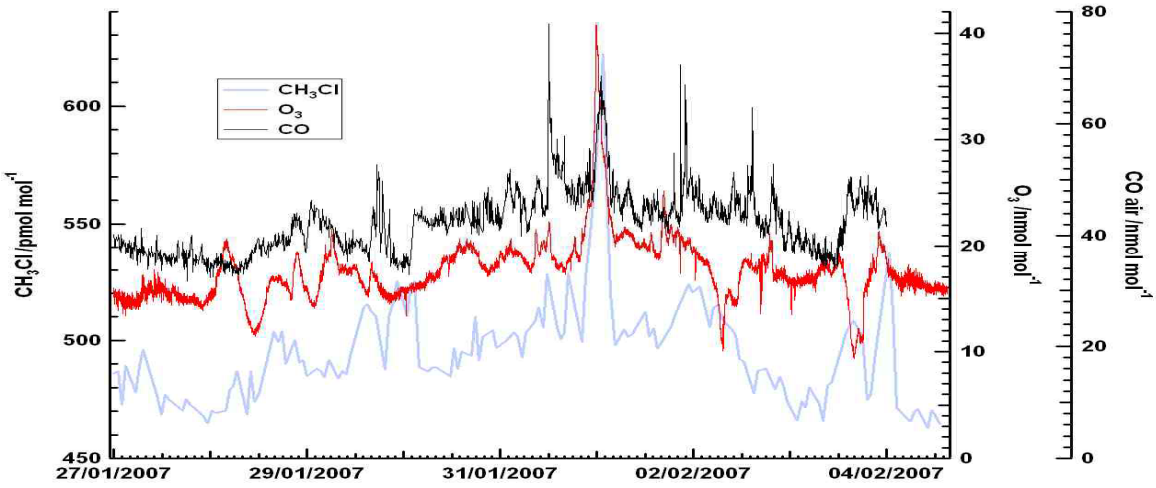

Figure 4.12: Comparison of CH_3Cl, CO and O_3 time series.

3.6 Comparison to former studies

Table 4.3 shows a compilation of mixing ratios obtained in this study as well as southern hemispheric background values and values observed in coastal influenced air masses.
Compared to southern hemispheric coastal background data (Simmonds et al., 2004) the CH_3Cl values obtained in this study appear rather low. The average mixing ratio of 495 pmol mol^{-1} indicates that this cruise was conducted in regions very remote from CH_3Cl sources. The maximum peak of 622 pmol mol^{-1}, identified as emerging from the Buenos Aires region, is a moderate enhancement in comparison to up to 1000 pmol mol^{-1} recorded in biomass burning influenced air (Blake et al., 1996).
The CH_3Br values obtained during the MD 158 cruise fall in the same range as CH_3Br baseline mixing ratios within the southern hemisphere (Simmonds et al., 2004). No high mixing ratio events were recorded. Therefore coastal macroalgae sources (Carpenter et al., 1999) or the phytoplankton species *Phaeocystis*, causing elevated mixing ratios in the North Sea (Baker et al., 1999), seemed to be of minor importance during this cruise.
Average oceanic CH_3I background values vary with latitude and distance from the coast. Chuck et al. (2005) derived mean values of 0.71 pmol mol^{-1} CH_3I over the South Atlantic (36 - 49 °S). These data are in good agreement with the minimum open ocean values of 0.6 pmol mol^{-1} recorded during this study. Substantially elevated mixing ratios in the region of enhanced biological activity (maximum of 3.0 pmol mol^{-1}) appear moderate compared to 10 – 20 pmol mol^{-1} reported from oceanic regions with high biological activity and in air passing by coastal areas covered with macroalgae (Lovelock and Maggs, 1973; Rasmussen et al., 1982; Carpenter et al., 2003).
The average mixing ratio of CH_2Br_2 obtained during this study was 1.5 pmol mol^{-1}. Minimum values of 1.0 pmol mol^{-1} match the reported background data, whereas the maximum values of 2.8 pmol mol^{-1} pointing to enhanced production in the coastal/phytoplankton bloom area compare quite well with mixing ratios reported for coastal influenced air.
The minimum $CHBr_3$ values recorded during MD 158 (1.8 pmol mol^{-1}) come close to the reported oceanic background values. Average $CHBr_3$ mixing ratios (5.0 pmol mol^{-1}) are comparable to 5.4 pmol mol^{-1} reported by Quack and Wallace (2003) for shelf regions. Enhanced values up to 15.3 pmol mol^{-1} towards the end of the cruise indicate increased production. These values come close to values measured in coastal and upwelling influenced air, respectively.

Conclusively, minimum mixing ratios of the investigated halocarbons show general agreement with observed oceanic background values (Simmonds et al., 2004), average CH_3Cl data being even lower than that. CH_3I, CH_2Br_2 and $CHBr_3$ showed mixing ratios elevated above the background values in air masses, which recently passed over oceanic regions exhibiting enhanced biological production. These values were comparable to measurements in coastal/upwelling regions in case of $CHBr_3$ (Carpenter et al., 2003; Quack and Wallace, 2003; Quack et al., 2004; Carpenter et al., 2007; Quack et al., 2007). The CH_3I and CH_2Br_2 enhancement was only moderate compared to values reported from coastal sites (Carpenter et al., 2003; Yokouchi et al., 2005; Quack et al., 2007). Enhanced values recorded during the latter part of the cruise might be attributed to an encountered phytoplankton bloom and/or coastal sources like salt marshes or macroalgae.

Compound	SH oceanic background /pmol mol^{-1}	This study min / pmol mol^{-1}	max / pmol mol^{-1}	Avg / pmol mol^{-1}	Coastal regions / pmol mol^{-1}
CH_3Cl	541.3 [1]	463	622	495	
CH_3Br	7.94 [1]	5.0	8.4	7.2	
CH_2Br_2	0.3 - 1.3 [2]	1.0	2.8	1.5	3.4 - 7.6 [7]
	0.8 - 1.0 [3]				
$CHBr_3$	0.5 - 1.5 [4]	1.8	15.3	5.0	10.9 - 27.2 [8]
	0.7 - 2.1 [5]				25 [9]
CH_3I	0.3 - 0.8 [3]	0.6	3.0	1.4	10 - 20 [10]
	0.7 - 3.8 [6]				

1 Simmonds et al., 2004
2 Yokouchi et al., 2005 and references therein
3 Butler et al., 2007
4 Quack and Wallace, 2003
5 Chuck et al., 2005; Yokouchi et al., 2005; Butler et al., 2007
6 Lovelock and Maggs, 1973; Rasmussen et al., 1982; Happell and Wallace, 1996; Moore and Groszko, 1999; Carpenter et al., 2003
7 Carpenter et al., 2003; Yokouchi et al., 2005; Quack et al., 2007
8 Carpenter et al., 2003; Quack and Wallace, 2003; Quack et al., 2004; Carpenter et al., 2007; Quack et al., 2007
9 Quack and Wallace, 2003
10 Lovelock and Maggs, 1973; Rasmussen et al., 1982; Carpenter et al., 2003

Table 4.3: Comparison of literature and this study's halocarbon mixing ratios.

3.7 Marine sources of halocarbons

In contrast to CH_3Cl, which was shown above to stem from anthropogenic influenced air, other halocarbons investigated in this study originate mostly from marine sources. A comparison with the mixing ratios of DMS, a well known and well investigated compound with almost exclusive oceanic sources, was undertaken to examine its relation to the halocarbons.
DMS mainly results from the enzymatic cleavage of DMSP, which is produced in algal cells. DMSP is found in the cells themselves and exists ubiquitously in the surface sea water (Simo, 2004). It is released mostly through cell autolysis, viral attack and grazing. A fraction of the released DMSP is transformed into DMS by algal or bacterial enzymes (DMSP lyases). This process takes place in free solution, as well as on the surface of particles or in the guts and vascuols of grazers (Simo, 2004). A complex network of biological production and degradation of both DMSP and DMS determines the concentration of DMS in the surface ocean and thereby its flux to the atmosphere. However, there are also abiotic factors influencing the DMS producing communities, e.g. solar radiation, UV spectrum and intensity, wind speed, nutrients and the abundance of coloured dissolved organic matter (CDOM) (Simo (2004) and references therein).

At first we compare the mixing ratio variations of DMS and CH_3I, since the lifetime of both compounds comes closest (DMS: 1.2 d (Putaud et al., 1999), CH_3I: 5 to 7 d (WMO, 2007b). Fig. 4.13 shows CH_3I and DMS mixing ratios as a function of time along the cruise track. DMS was measured by a PTR-MS instrument, while CH_3I was measured with GC-MS, both described in section 4-2 “Sampling and analysis”.

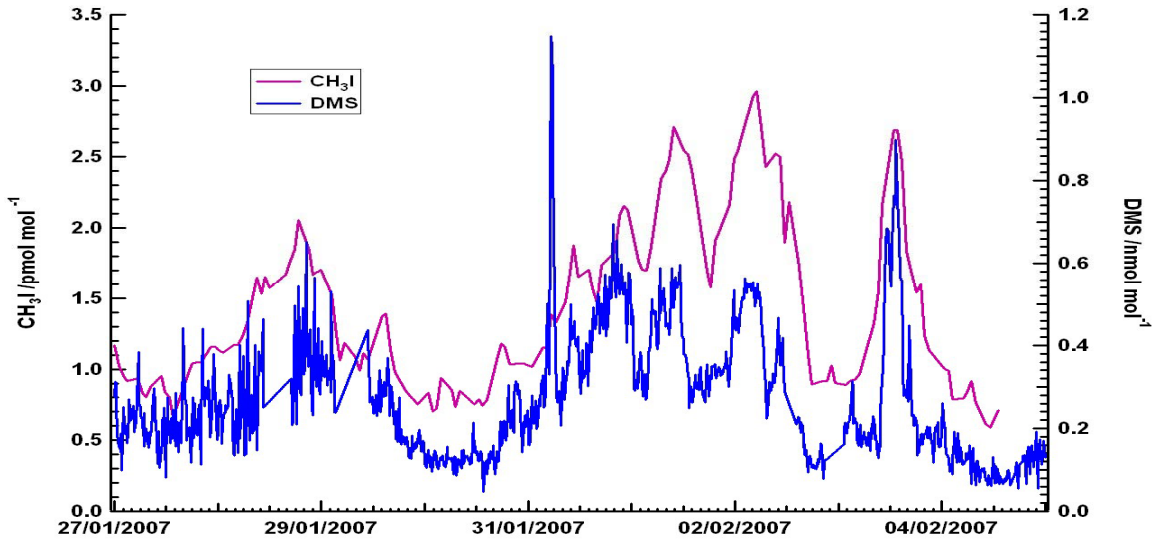

Figure 4.13: Comparison of CH_3I and DMS time series.

The observed correlation of 20 min averaged data of these two compounds is strikingly good (R = 0.71) establishing the marine origin of CH_3I. The two species clearly correlate not only over the broad-scale features but also for the smaller peaks (e.g. the triplet

between 31.01. and 02.02.). The decrease of DMS relative to CH_3I during the second and third peak of the triplet may be caused by the distance between the point of measurement and the source region, which became progressively increased in this period. It should be noted that the time resolution of the CH_3I measurements is hourly while the PTR-MS data is plotted every 10 minutes. Therefore very short features, like the spike in DMS measured by the PTR-MS around 5 o'clock on the 31st of January, were not observed by the GC-MS, which was not collecting sample at the time.

A good correlation between DMS and CH_3I is not observed globally (Yokouchi et al., 2001; Chuck et al., 2005). However, in particular for the Southern Ocean such a correlation has been noted before. Chuck et al. (2005) reported a strong linear relationship of CH_3I with DMS ($R = 0.69$) and $DMSP_p$ ($R = 0.77$) for a subset of their data, i.e. the ADOX Leg 2 data recorded from February to March 1993 in the Southern Ocean east of South Africa. Such good correlation implies that the bulk emission of both compounds stems from the same source or is regulated by the same driving parameters (e.g. phytoplankton, nutrients and/or light abundance).

One possibility of a common production pathway is reported by White (1982), who found that a methyl group transfer from DMSP (a precursor of DMS) to iodide ions leads directly to the production of CH_3I. However, Hu and Moore (1996) reported that the rate of this reaction in seawater was too slow to account for oceanic CH_3I production. This was supported by measurements of Tait and Moore (1995) and Laturnus et al. (1998), who both claim oceanic CH_3I is "unlikely" to be produced by DMSP.
Considering marine sources of CH_3I the abiotic formation from biologic material as investigated in Chapter 3 appears to be of no relevance, since such processes are inhibited by high water content.
Another possible mechanism for co-located release of CH_3I and DMS is the production by phytoplankton via enzymatic processes (Itoh et al., 1997; Simo, 2004). In general, recent studies (Simo, 2004; Vallina et al., 2006;Vallina and Simo, 2007) agree that the global DMS distribution cannot be explained by phytoplankton abundance/activity alone. However, in the Southern Ocean, DMS concentration in the water phase as well as DMS emission fluxes follow the seasonality of the phytoplankton (Vallina et al. (2006) and references therein). Therefore it seems to be suitable to use phytoplankton abundance, i.e. Chl a concentrations, as a proxy for DMS emission in this particular area of the globe. Strong correlations of CH_3I with DMS observed in the very same region (Chuck et al. (2005) and this study) imply that the CH_3I emission is also related to the phytoplankton abundance.

Comparing the *in situ* Chl a measurements along the cruise track with mixing ratios of CH_3I as a model species of halocarbons mainly emitted by marine sources, there seems to be little or no direct correlation between the two parameters (see Fig. 4.14).

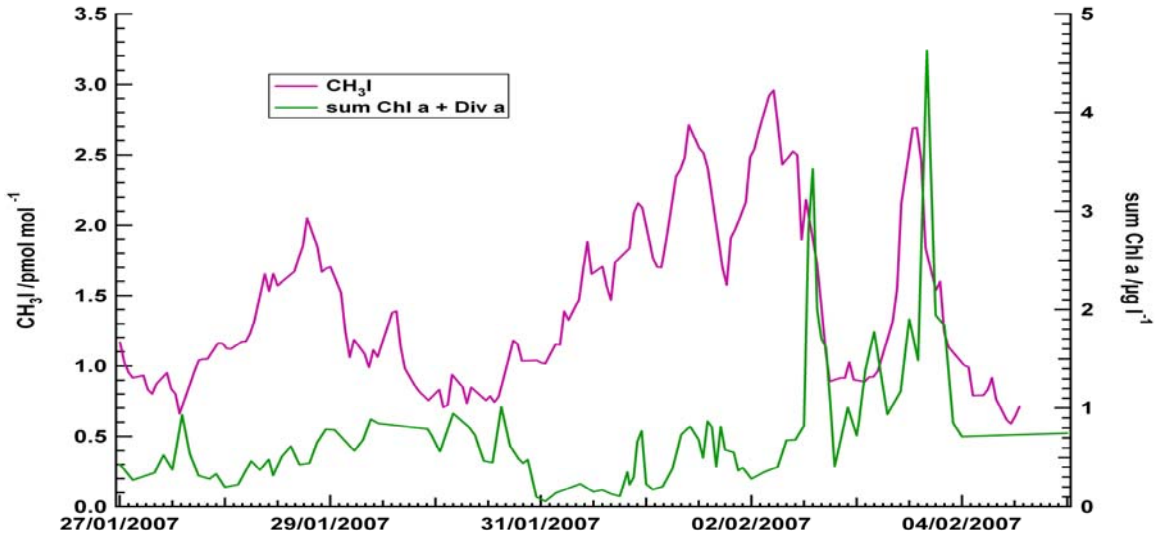

Figure 4.14: Comparison of CH_3I and *in situ* Chl a time series.

However, air and water measurements at the same point are not necessarily directly linked to each other. The emission flux from the water phase (here represented by the aqueous Chl a concentration) is not the only parameter determining the gas phase mixing ratio at the measurements location. Because air movement above the water is usually much faster than the speed of the water mass, and both media do not necessarily move in the same direction, equilibrium in chemical partitioning as might be envisioned by Henry's Law between the two phases is rarely attained. To explain the mixing ratios in the gas phase, physical, biological and chemical processes affecting the air mass along its path to the point of measurement need to be considered. In other words, when a strongly emitting source region is located upwind of the ship, air measurements will show high mixing ratios while water Chl a levels will be low.

Therefore, instead of the *in situ* Chl a point measurement at the ship's position, the average Chl a along the back trajectory would serve as a suitable parameter for comparison to the CH_3I or DMS mixing ratios.
Arnold and Spracklen (2008) have developed a technique to determine time-series of Chl a weighted back trajectories to account for air mass exposure to ocean biology upwind of the ship. One to 9 day kinematic back trajectories initialized from the ships position are calculated from 1.0125-degree resolution ECMWF meteorological fields using the OFFLINE trajectory model (Methven, 1997). The trajectory arrival frequency is one per minute, and positions are stored every 6 hours back along the trajectories. At each position along a back trajectory concentrations of oceanic Chl a are taken from monthly-mean global fields (Level-3 SeaWiFS daily binned observations provided by NASA/GSF/DAAC, degraded to 0.25-degree resolution), provided the air mass stayed in the marine boundary layer ($p < 850$ hPa). An average Chl a exposure is then calculated along each back trajectory, producing a time-series of average Chl a air mass exposure along the ship track.

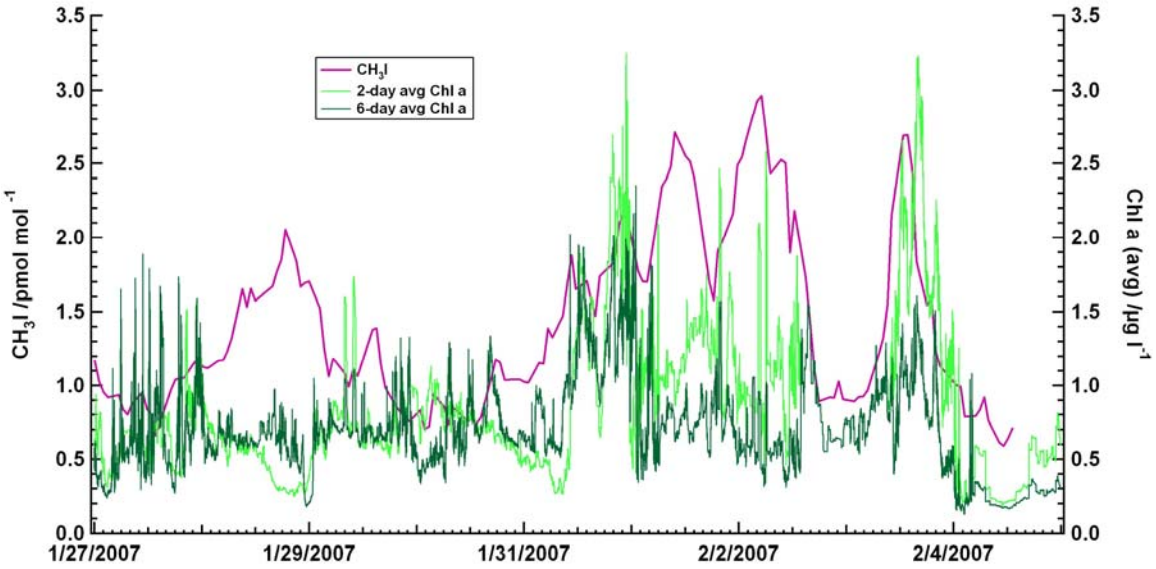

Figure 4.15: Comparison of CH_3I and 2- and 6-day averaged Chl a exposure time series.

Fig. 4.15 shows the CH_3I time series and the average Chl a exposure for the air mass encountered at the ships position along the back trajectory for 2 and 6 days corresponding to the lifetimes of DMS and CH_3I. Compared to Fig. 4.14, which displays the CH_3I against the *in situ* measured Chl a, it is clear that the degree of correlation between CH_3I and the trajectory derived Chl a is improved. The averaged Chl a exposure not only captures the peaks recorded by the *in situ* aqueous Chl a measurements on the 2nd and 3rd of February and the dip in between, but also shows enhanced values during the two days before. In particular the region of the triplet peak in CH_3I (31.01. – 02.02.) during which little chlorophyll was measured *in situ*, the trajectory averaged chlorophyll reproduces the CH_3I pattern. This indicates a source, which is not directly located on the ships track, but that was passed by the encountered air masses some time prior to arrival at the ship. The distance to the high Chl a region from the ship may be estimated from the differences of the ratio of the 2 and 6 day averages.
In general there is much better agreement of the averaged Chl a and CH_3I data than the comparison with *in situ* Chl a showed. However, for the period from the 27. to the 31.01. the averaged Chl a does not follow the CH_3I mixing ratios.
Although this new approach of using Chl a exposure along the back trajectories has proven useful in interpreting this dataset, in particular the region where the ship is approaching the bloom into the wind, it is still not the ideal parameter and number of caveats must be borne in mind when using this new analysis product: Since it does not take into account the process of air-sea exchange at all (with all its influencing parameters, e.g. wind speed, boundary layer stability, surfactants and bubbles) or losses, which might occur in the gas phase. This parameter provides a simple average, without any time/distance weighting of the single constituents.
The satellite Chl a data used for the calculation are monthly mean values. Therefore an event occurring on a very short time scale may not be well represented in the data. Moreover, areas obscured by clouds will not be included in the satellite data. This is of

particular importance in areas with high cloud coverage such as the region investigated during the MD 158 cruise. Generally, in the region of the Southern Ocean there are relatively few *in situ* meteorological measurements. Therefore the wind fields used to calculate the back trajectories may be subject to higher uncertainty. Finally, phytoplankton is not found solely in the open ocean where it alters the colour of the water and is observable by satellites, but it is also found in the polar regions in the snow pack or on sea ice. Since snow and ice are quite opaque and have a high albedo, it is questionable, if reasonable Chl a signals from these regions can be obtained. Each of these points or a combination of them might be the reason, why the first smaller peak of CH_3I and DMS does not appear in the average Chl a exposure trajectory product.

One has to note that the use of marine Chl a as a proxy for DMS and CH_3I emissions respectively, is only valid at high latitudes and in the Southern Ocean, where seasonality of DMS fluxes follow the seasonality of phytoplankton, and in the case of CH_3I solely because it showed a good correlation with DMS. However, in the period sampled over the Southern Ocean the average Chl a of the seawater the air mass was exposed to, serves reasonably well to explain our observed DMS and CH_3I mixing ratios. Likewise enhanced values from the 31.01. to the 02.02. - before the *in situ* Chl a indicated the bloom period - show that CH_3I and DMS emerged from a bloom area upwind the ship.

However, the use of Chl a as an emission proxy must be considered approximate, since algal trace gas release is highly species dependent. Simultaneously enhanced CH_3I and DMS values originating from the bloom area may be linked directly through production by the same phytoplankton species. Stefels et al. (2007) assigned the whole group of phytoflagellates (including haptophytes (*Phaeocystis* among others), several larger prasinophytes and also smaller dinoflagellates) as DMSP producers. In contrast diatoms and prokaryotic picoplankton (including prochlorophytes and cyanophytes e.g. *Synechococcus* and *Trichodesmium*) were found to produce little or no DMSP at all. This is in accordance with Simo (2004), who reported dinoflagellates and *Emiliania huxleyi*, a haptophyte, to be strong DMSP producers. Some of these species, specifically *Phaeocystis* and another haptophyte *Pavlova gyrans*, are also known to produce CH_3I (Itoh et al., 1997; Manley and de la Cuesta, 1997; Baker et al., 1999). Baker et al. (1999) for example reported dramatically increased values of CH_3I as well as CH_3Br during a *Phaeocystis* bloom observed in the North Sea.
According to the *in situ* pigment analysis, the phytoplankton blooms occurring during this cruise consisted mainly of dinoflagellates and diatoms, see section 4-3.2 – "Oceanographic conditions". Haptophytes were only found to be a background community. However, the PHYSAT classification identified haptophytes, in particular *Phaeocystis*, and diatoms as the predominant phytoplankton types in regions the trajectories passed over.
Taking into account the relatively short lifetime of DMS and CH_3I, it seems likely that both DMS and CH_3I were produced locally by the encountered bloom and were advected to the ship. However, an extraordinarily large emission further upwind in regions dominated by other phytoplankton types cannot be excluded.

Other indirect links may exist between biological activity and CH_3I mixing ratios. For instance, Yokouchi et al. (2001) deduced from their observations, that in areas of high biological activity, and therefore high DMS values, there would also be a source of organics that can, in turn, act as source for methyl radicals in seawater. It was further postulated that CH_3I could be produced photochemically from these radicals. Given that high light doses favour the accumulation of DMS in seawater (Vallina and Simo, 2007) and CH_3I is produced photochemically, solar radiation might be the driving parameter for the simultaneous formation.

Conclusively, the good correlation observed in this study region establishes that the regional oceanic sources of CH_3I and DMS in the Southern Ocean, even if not being the same, at least show the same dependence on driving parameters (e.g. phytoplankton, light and organic matter abundance).

Comparing the mixing ratios of other halocarbons investigated within this study to CH_3I it is clear that some, in particular CH_3Cl, have different source distributions.
Fig. 4.16a shows the mixing ratio variation of CH_3I, CH_2Br_2 and $CHBr_3$. From this plot it is clear, that for certain times the agreement between the CH_3I, CH_2Br_2 and $CHBr_3$ was rather good (31.01. - 04.02.), while for other points in time (28. - 29.01.) it was non-existent. For the whole period investigated CH_2Br_2 and $CHBr_3$ showed a pretty good correlation with each other ($R = 0.85$), whereas the correlation between either brominated compound and CH_3I was less pronounced ($CHBr_3$ vs. CH_3I: $R = 0.44$; CH_2Br_2 vs. CH_3I: $R = 0.57$). Similar relationships have been reported previously for gas as well as water phase measurements in various oceanic regions (Schall et al., 1997; Carpenter et al., 2003; Yokouchi et al., 2005; Quack et al., 2007; Zhou et al., 2008). The good correlation of CH_2Br_2 and $CHBr_3$ suggests a common source for these two species.
Since all three compounds follow roughly the average Chl a exposure along the back trajectories (see Fig. 4.16a), a phytoplankton source seems most likely. The differences in mixing ratio variation of CH_3I and the two brominated compounds might be attributed to emission from different phytoplankton species. Maximum $CHBr_3$ and CH_2Br_2 values occurring at the time of the diatom dominated bloom area appear reasonable, since both compounds are known to be emitted by diatoms (Baker et al., 1999). However, additional coastal sources (e.g. coastal macroalgae or salt marshes) can not be ruled out, since the respective air masses passed by the coast of Argentina. The importance of coastal/continental sources was pointed out by simultaneous air and seawater measurements of Quack et al. (2007), which revealed that shelf water emissions from the Mauritanian upwelling region, although quite substantial, accounted just for 10 – 25 % of the high CH_2Br_2 and $CHBr_3$ mixing ratios present in the coastal atmosphere.

When the CH_3Br time series is examined closely, it seems to follow the temporal variations of CH_3I (see Fig. 4.16b), indicating a similar source distribution. However, since the measured atmospheric mixing ratio variation is within the total uncertainty (see Fig. 4.8), this structure cannot be unambiguously interpreted.

In contrast CH_3Cl shows a different pattern of peaks as a function of time (see Fig. 4.16c). A high mixing ratio event at the 01.02. around 01:30 UTC is the most pronounced

feature. A very small increase corresponding to the time of the CH_3I triplet peak (31.01. - 02.02.) and the single peak at the end (03.02.) can be deduced in the data series, but the trends are within the measurement error and hence not significant.

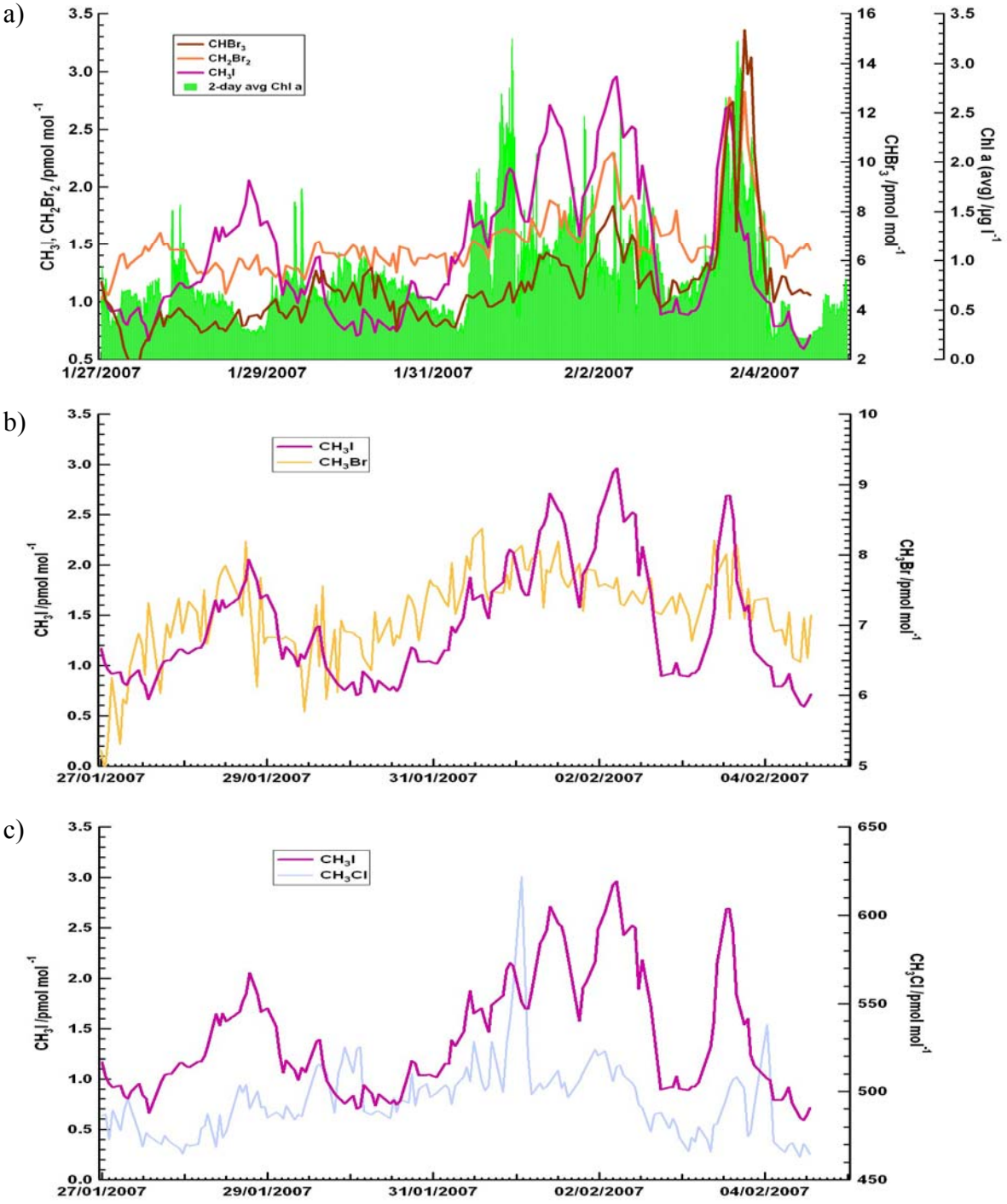

Figure 4.16: A comparison of CH_3I, CH_3Cl, CH_3Br, CH_2Br_2 and $CHBr_3$ mixing ratios.

In conclusion these comparisons revealed that CH_3I, DMS and possibly to a minor extent CH_3Br had the same source regions in the catchment area of the encountered air masses (i.e. mainly Southern Ocean, South Atlantic and South Pacific). CH_2Br_2 and $CHBr_3$ showed a different relative response, but at least for the last part of the cruise (31.01. - 04.02.) the same temporal variation of emission. This was attributed to inhomogeneous species specific phytoplankton emissions, rather than oxidative loss, since the lifetimes of the aforementioned species are long in comparison to transport times.
A reasonable agreement with the average Chl a exposure along the back trajectories suggests a phytoplankton source, although for the last part of the cruise a contribution from coastal sources could not be ruled out. Elevated mixing ratios of CH_3Cl, however, did not originate from oceanic sources, but could be attributed to an air mass influenced by anthropogenic emissions from the Buenos Aires region.

Artificially induced algae blooms have also been used to gauge the effect of enhanced biological production on trace gas emissions. Fertilization experiments, mainly dedicated to monitor the impact of iron fertilization on the productivity of the surface ocean and the associated CO_2 sequestration mitigating climate change (Boyd et al., 2007), have provided an opportunity to study the response of halocarbon emissions from phytoplankton blooms, albeit non-natural. Wingenter et al. (2004) found that CH_3Br during SOFeX 2001was enhanced inside the fertilized patch compared to outside the patch, CH_3I concentration decreased inside the patch and CH_3Cl remained unchanged. In contrast Liss et al. (2005) observed increasing CH_3I concentrations following the iron fertilization during the EisenEx study conducted in the Southern Ocean in November 2000 in the region of the Antarctic Polar Front. $CHBr_3$ was found to decrease inside the iron enriched patch, probably due to enhanced bacterial consumption of this compound. Moore and Wang (2006) observed no clear effect of iron fertilization on methyl halide concentrations up to 13 days after the first iron addition during SERIES 2002. The ambiguous results of several fertilization experiments highlight the complexity of the processes involved due to a large number of parameters influencing the emission of halocarbons.

4 Summary and conclusion

In this study, the impact of a phytoplankton bloom on the emissions of CH_3Cl, CH_3Br, CH_3I, CH_2Br_2 and $CHBr_3$ was investigated. An area of enhanced biological production was encountered in the South Atlantic Ocean in January/February 2007 close to the coast of Argentina. *In situ* pigment analysis allowed determination of the predominant phytoplankton species as dinoflagellates and diatoms. During the open ocean part of the cruise, cyanobacteria dominated the phytoplankton community.

CH_3Cl mixing ratios along the cruise track showed very little variation. The only outstanding event of higher mixing ratios could be attributed to anthropogenic influenced air masses by of simultaneously occurring enhanced O_3 and CO values. Trajectory analysis showed that this event was associated with continental air masses from the region of Buenos Aires. The absence of any further simultaneous peaks in CO and O_3 implied, that no further large anthropogenic events were observed during the cruise. Besides this isolated anthropogenic signature the CH_3Cl values were rather low compared to global background values. A strong contribution from the observed algae bloom is therefore very unlikely.

Mixing ratios of CH_3Br measured during MD 158 varied around 7.2 pmol mol^{-1}, which is close to southern hemispheric background values of 7.9 pmol mol^{-1} CH_3Br reported by Simmonds et al. (2004). Compared to mixing ratios up to 25.5 pmol mol^{-1} recorded during prymnesiophyte blooms (Baker et al., 1999), the effect of the bloom encountered during this cruise on CH_3Br appears negligible.

CH_3I mixing ratios up to 3 pmol mol^{-1} in air masses, which recently passed over oceanic regions exhibiting enhanced biological production, represent a significant elevation compared to global oceanic background values. Lack of correlation of CH_3I levels with land contact suggests this compound is primarily of marine origin. A very good correlation of CH_3I and DMS ($R = 0.71$), a tracer with exclusive oceanic sources, established the marine origin of CH_3I and pointed to similar source regions for the two compounds, which is likely the phytoplankton bloom close to the coast of Argentina. Although it could not be unequivocally proven, the source of both compounds is most probably direct emission from phytoplankton. The regional oceanic production of CH_3I and DMS in the Southern Ocean, even if not due to exactly the same process, at least showed the same dependence on driving parameters (e.g. phytoplankton, light and organic matter abundance).

A direct correlation of CH_3I and *in situ* aqueous phase Chl a, a marker for phytoplankton abundance, could not be observed. However a combination of satellite derived Chl a and back trajectory data - a parameter derived by a new method developed in collaboration with Steve Arnold, University of Leeds, UK - revealed a correlation of the average Chl a exposure along the back trajectory and the atmospheric CH_3I as well as DMS mixing ratios. Enhanced values from the 31.01. to the 02.02., before the *in situ* Chl a indicated the bloom period, show that the halocarbons and DMS respectively were emitted from a bloom area upwind the ship.

Although the link to the average Chl a parameter represents a step forward in the interpretation of gas phase measurements, it is still limited in its ability to explain small-scale features. Incorporating important factors concerning the sea-air gas exchange (in particular the wind speed) and the atmospheric degradation rates of the particular investigated compounds would enhance the suitability of this new analysis method as a proxy for trace gas analysis.

CH_2Br_2 and $CHBr_3$ mixing ratios showed significant variation during the cruise. The average values were consistent with reported mixing ratios for coastal areas (Quack and Wallace, 2003; Carpenter et al., 2003; Yokouchi et al., 2005; Butler et al., 2007). The most pronounced increase in the mixing ratios occurred towards the end of the cruise near the coast of Argentina. Mixing ratios rose up to 2.8 pmol mol^{-1} CH_2Br_2 and 15.3 pmol mol^{-1} $CHBr_3$. Since the back trajectories indicate that air masses encountered by the ship passed over the southern tip of South America, a terrestrial influence (i.e. emission from salt marshes or coastal macroalgae) could not be ruled out. CH_2Br_2 and $CHBr_3$ showed a good correlation ($R = 0.85$) with each other. This is consistent with previous results, reporting similar emission sources for these chemicals (Carpenter et al., 2003; Yokouchi et al., 2005). A correlation of these two compounds with CH_3I resulted in no clear agreement. Only during the last part of the cruise (influenced by the bloom) all three compounds seem to follow the same temporal variation. Variation in the relative size of the peaks was attributed to inhomogeneous species specific phytoplankton emissions, rather than oxidative loss, since the lifetimes of the aforementioned species are long in comparison to transport times.

This study conclusively reveals that mixing ratios of CH_3Cl and CH_3Br were not significantly affected by the phytoplankton bloom occurring off the coast of Argentina in January/February 2007. The emissions of CH_3I, CH_2Br_2 and $CHBr_3$ were increased due to enhanced phytoplankton abundance. Differences in the relative size of the peaks might be due to emissions by different phytoplankton species. However, for the last part of the cruise terrestrial sources (e.g. salt marshes or coastal macroalgae) might have contributed to the higher mixing ratios observed in vicinity of the coast.

The correlation established between satellite derived average Chl a and CH_3I may be used to scale CH_3I emissions from the Southern Ocean used in global models to obtain a more detailed emission map. Such emission maps can be further improved by incorporating parameters influencing the sea-air gas exchange (e.g. wind speed). The PHYSAT classification would allow not only a scaling of the phytoplankton emissions by the Chl a abundance, but permit different emission rates corresponding to different phytoplankton species to be implemented. This information would be very useful, as different plankton species are known to exhibit different specific halocarbon emissions. The phytoplankton distribution, which is likely to change with global temperature, could be assessed by satellite and the emissions of halocarbons implanted in models based on field measurements to run prognostic models for chemistry more accurately.

Conclusion and future perspectives

Halocarbons are of great public and scientific interest since they can act as a carrier for reactive halogens to upper layers of the atmosphere, where they contribute to the chemical depletion of the ozone layer. To be able to estimate feedbacks on future climate scenarios it is crucial to determine current global budgets as precisely as possible and to investigate the dependence of sources and sinks on driving parameters like temperature, solar radiation, soil moisture and plant water content. Since the Montreal Protocol regulates the release of anthropogenic O_3 depleting substances, the relative contribution of naturally produced halocarbons is becoming more important for the budget of stratospheric halogens. An airborne study over the tropical rainforest of Suriname and French Guyana and a shipborne campaign crossing the South Atlantic Ocean at about 40 °S were conducted to investigate the release of halocarbons by the tropical ecosystem as well as from oceanic phytoplankton. Within a laboratory study one possible reaction yielding monohalomethanes was tested with regard to its temperature dependence. The results of this doctoral thesis therefore contribute significantly to the growing body of knowledge on natural halocarbons budgets.

Halocarbon emissions from the tropical rainforest presented in Chapter 2 are not only interesting because the rainforest represents one of the largest and most biodiverse ecosystems, but also because the proximity to the ITCZ means that any emission there will have an enhanced chance of being transported rapidly into the upper troposphere/stratosphere by regionally prevalent deep convection. Several model studies, conducted to gain an improved understanding of the global distribution of CH_3Cl and CH_3Br (Lee-Taylor et al., 2001; Yoshida et al., 2006; Lee-Taylor et al., 1998; Warwick et al., 2006), postulate that CH_3Cl as well as CH_3Br have tropical terrestrial sources. In the case of CH_3Cl there are field studies supporting this thesis (Yokouchi et al., 2002; Scheeren et al., 2003). However, due to sparseness of measurements, the global strength of this source remains poorly quantified.

Halocarbon fluxes derived from samples collected above the tropical forest present the net effect of halocarbon emissions. In reality this net effect is the result of a multitude of processes occurring within the rainforest canopy e.g. emission and/or uptake by soil microbes, fungi, leaves and litter, plants, animals and abiotic reactions. This net flux, based on a large-scale approach, is well suited to extrapolate the rainforests effect to global scale, because it inherently accounts for all possible sources and sinks.

Using the change in mixing ratios with time the air mass spent over the rainforest CH_3Cl and $CHCl_3$ net fluxes from the rainforest to the atmosphere could be obtained. The rainforest ecosystem produced 9.5 (± 3.8 2σ) µg m^{-2} h^{-1} CH_3Cl and 0.35 (± 0.15 2σ) µg m^{-2} h^{-1} $CHCl_3$ during October 2005 (long dry season). No significant trend for CH_3Br could be determined within the limit of detection from these measurements. The tropical vegetation gross source postulated by an inverse model prediction (Warwick et al., 2006) was not observed, and may be being reduced to a very small net flux by concomitant sinks such as soil uptake. Our measurements over the South American rainforest agree with global observations generally, and vertical gradients between the boundary layer and free troposphere appear to be small or absent. This supports the conclusion that the tropical forest ecosystem is not a significant net global CH_3Br source.

The CH_3Cl flux is in good agreement with previously measured fluxes by Yokouchi et al. (2002) and Yokouchi et al. (2007), who reported 5.4 (3.8 - 8) µg CH_3Cl m^{-2} h^{-1} and 12 - 33 µg CH_3Cl m^{-2} h^{-1} for Asian lowland tropical forest, and Scheeren et al. (2003), who derived 7.6 (± 1.8) µg CH_3Cl m^{-2} h^{-1} over Suriname. This suggests that the rainforest ecosystem appears to be a seasonally constant and important CH_3Cl source in the tropics. Extrapolating the flux to the global scale resulted in 1.5 (± 0.6 2σ) Tg CH_3Cl yr^{-1}, which would account for half the additional tropical source postulated by the previous model studies (Lee-Taylor et al., 2001; Yoshida et al., 2006). Since the soil is known to be a sink for CH_3Cl the observed total flux in this study should be considered as lower limit of the possible direct production by plants or plant decay. The global tropical source estimated here is at the lower end of current best estimates but nevertheless would mean that the rainforest is the main global CH_3Cl source.

Regarding the $CHCl_3$ emission we observed a threefold weaker flux than Scheeren et al. (2003). Our lower limit of the global extrapolated flux from the tropical forests is 56 (± 23 2σ) Gg $CHCl_3$ yr^{-1}, about 5 to 10 % of the total global sources. These fluxes may be incorporated in global models to provide an overall net source strength of the rainforest ecosystem. Since these numbers are based on a large-scale approach, local phenomena, which can be problematic for surface sites, tend to be averaged out and a more representative value is obtained.

From the different emission patterns of CH_3Cl and $CHCl_3$ we conclude that these two compounds are probably produced via different mechanisms. According to the literature, $CHCl_3$ is most probably formed by microbial processes in the soil, which depend on temperature and soil moisture, however, there are no clear meteorological differences between March 1998 and October 2005 to explain the flux differences observed. Performing a similar study during the wet season would provide additional information on the soil moisture dependence of the formation pathways and the seasonal variation of the emissions, which could be specifically incorporated in global models.

To obtain a better understanding of the role of the rainforest ecosystem as a possible sink or source of halogenated organic species, more studies on the different tropical biomes are necessary. Furthermore, a more detailed survey of the possible contributors (plants, soil, leaf litter, fungi etc.) would complement the knowledge about the separate sources

and sinks within the tropical rainforest ecosystem. In particular, for prognostic purposes it is necessary to know, how these individual mechanistic contributions change with ambient parameters. If in the future the Earth warms, as it is predicted to do, assessing the change in the effectiveness of the contributions with temperature will be particularly important.

A possible production pathway for methyl halides, namely abiotic formation from dead plant material, was tested with regard to its temperature dependence in a laboratory study (chapter 3). Previous studies (Hamilton et al., 2003; Keppler et al., 2004; Keppler et al., 2005) had established the occurrence and the potential importance of the abiotic formation of CH_3Cl from weathering vegetation for the global budget. The widespread plant component pectin was found to serve as methyl donor (Hamilton et al., 2003). In the aforementioned studies the emission of CH_3Cl from senescent and dead plant material was observed to increase dramatically in strength with temperature (tested up to 350 °C). They concluded, that the postulated abiotic mechanism might not only represent a significant source of CH_3Cl during weathering of plant material, but may also account for CH_3Cl release during biomass burning. In a later study, Keppler et al. (2005) indicated, that the abiotic methylation of chloride in plant and soil organic matter might account for the bulk of CH_3Cl emitted to the atmosphere.

This study was focused on investigating the relevance of the abiotic formation of CH_3Br and CH_3Cl at a range of ambient temperatures. The emissions of dried leaves of several plant species (hay, ash, tomato and saltwort) representative of different terrestrial biomes (grassland, deciduous forest, agricultural areas and coastal salt marshes) and bromide enriched pectin have been monitored over a temperature range from 25 to 50 °C. The observed emission of monohalocarbons was found to be exponentially dependent on temperature; emission rates doubled approximately each 5 °C temperature step. It is noteworthy, that this production took place even at ambient temperature (25 °C). The abiotic nature of the reaction yielding methyl halides was confirmed by its high activation energy calculated via Arrhenius plots. The strength of the emission was found to be additionally dependent on the availability of halides and methoxyl groups within the plant tissue. However, high water content in the plant material was found to inhibit methyl halide emissions.

The conversion efficiency of all investigated samples in the temperature range from 25 to 50 °C was less than 1 % within one day. This leaves a high potential of further release with increasing temperature, especially interesting in light of global warming. However, a similar study by Hamilton et al. (2003) revealed that more substantial increases in conversion efficiency occur at temperatures higher than 175 °C.

The contribution of abiotic formation from vegetation to the global budget will vary geographically as a result of regional differences in both temperature and halide content of terrestrial plants. Maximum emissions are expected for plant material containing high amounts of halogens while decaying under warm and dry conditions. Nevertheless, Hamilton et al. (2003) and Keppler et al. (2005) proposed that abiotic methylation in plants and soil organic matter primarily located in tropical/subtropical areas

(30° N - 30° S) may account for the major global source of CH_3Cl. Thus, a significant part of the CH_3Cl emissions observed over the Suriname rainforest ecosystem might be due to the release from decaying plant material.

If global temperatures increase further, methyl halide emissions by this abiotic mechanism will not only increase due to exponential temperature dependence, but increased occurrence of extreme weather events like heat waves and droughts could cause emission hotspots as plants dry out, and new source regions may emerge in areas where historic wetlands dry out. To gauge these effects, the dependence on the water content of the plant tissue needs to be determined in detail, ideally considering the abiotic emissions under natural conditions.

Another interesting kind of plant, in terms of halocarbons emissions, are marine algae. The ocean is a huge reservoir for halogen ions and its inhabitant micro- and macroalgae may directly or indirectly, via their degradation products, provide a way to transform them into volatile organic halocarbons. Covering more than two third of the Earth's surface the importance of an oceanic source is obvious; in terms of net primary productivity the oceanic and the terrestrial vegetation are comparable. Bearing in mind the observed halocarbon emissions from the rainforest ecosystem, a measurement-based comparison with of halocarbons emission from marine vegetation appears worthwhile.

In a second field campaign, described in Chapter 4, the halocarbon mixing ratios over the South Atlantic Ocean, especially during a phytoplankton bloom encountered off the coast of Argentina in January/February 2007, were investigated, and an attempt was made to link the variations in the mixing ratios to parameters such as the phytoplankton abundance and the abundance of certain phytoplankton species, by using newly available satellite and Chl a data based trajectory products.

Mixing ratios of CH_3Cl and CH_3Br were not significantly affected by the occurrence of the phytoplankton bloom, which was dominated by diatom and dinoflagellate species. The only outstanding event of higher CH_3Cl mixing ratios could be attributed to anthropogenic influenced air masses from the region of Buenos Aires.

CH_3I, CH_2Br_2 and $CHBr_3$ showed pronounced mixing ratio variations, triggered by phytoplankton abundance. Average mixing ratios were substantially elevated compared to oceanic background values. A good correlation ($R = 0.85$) between the two brominated compounds is consistent with being emitted by the same source. For the last part of the cruise (influenced by the bloom) all three compounds seem to follow the same temporal variation. Variation in the relative size of the peaks was attributed to inhomogeneous species specific phytoplankton emissions. Since increased CH_2Br_2 and $CHBr_3$ mixing ratios occurred only towards the end of the cruise near the coast of Argentina, contributions from coastal sources (e.g. salt marshes or macroalgae) could not be ruled out.

A very good correlation of CH_3I and DMS ($R = 0.71$), a tracer for marine bioactivity, established CH_3Is marine origin and indicated similar source regions for the two

compounds, namely the phytoplankton bloom close to the coast of Argentina. Although it could not be unequivocally proven, the source of both compounds is most probably direct emission from phytoplankton. The regional oceanic production of CH_3I and DMS in the Southern Ocean, even if not due to exactly the same process, at least showed the same dependence on driving parameters (e.g. phytoplankton, light and organic matter abundance).

A direct correlation of CH_3I and *in situ* aqueous phase Chl a, a marker for phytoplankton abundance, could not be observed. However a combination of satellite derived Chl a and back trajectory data - a parameter derived by a new method developed in collaboration with Steve Arnold, University of Leeds, UK - revealed a correlation of the average Chl a exposure along the back trajectory and the atmospheric CH_3I as well as DMS mixing ratios. Enhanced CH_3I values in the period 31.01. to 02.02.07, before the *in situ* Chl a indicated the bloom period, showed that the halocarbons and DMS respectively were emitted from a bloom area upwind the ship. The correlation established between satellite derived average Chl a and CH_3I may, in the future, be used to scale CH_3I emissions from the Southern Ocean used in global models to obtain a more detailed emission map.

Although the link to the trajectory related average Chl a parameter represents a big step forward to the interpretation of gas phase measurements, Chl a is restricted to the aqueous phase. Incorporating further important factors into the estimate of halocarbon emissions, in particular, sea-air gas exchange parameters such as wind speed and the atmospheric degradation rates of the particular investigated compounds would enhance the suitability of this new analysis method as a proxy for trace gas analysis. The PHYSAT classification would allow to not just scale the phytoplankton emissions by the Chl a abundance, but also permit different emission rates corresponding to different phytoplankton species to be implemented. This information would be very useful, as different plankton species are known to exhibit different specific halocarbon emissions. The phytoplankton distribution, which is likely to change with global temperature, potentially could be assessed by satellite in real time and the emissions of halocarbons implanted in models based on field measurements to run prognostic models for chemistry more accurately.

In summary, within this study the emission of CH_3Cl and $CHCl_3$ from the rainforest ecosystem in Suriname and French Guyana could be verified for the long dry season in October 2005. Global extrapolations of the derived fluxes revealed the tropical forests to be a minor source of $CHCl_3$ (5 - 10 % of the global sources), but the major contributor to the global budget of CH_3Cl. The estimate of 1.5 ($\pm$ 0.6 2σ) Tg yr^{-1} CH_3Cl helped to narrow down the range of the yet poorly quantified CH_3Cl source from tropical ecosystems. A net source of CH_3Br could not be verified within the limits of detection.
In a second, shipborne field campaign halocarbon emission from the Atlantic Ocean were investigated with special emphasis on the effect of a phytoplankton bloom. CH_3Cl and CH_3Br were found to be not significantly affected by the occurrence of a natural phytoplankton bloom off the coast of Argentina, whereas CH_3I, CH_2Br_2 and $CHBr_3$ showed increased mixing ratios in air masses, which has recently passed over areas of high biological activity within the ocean. A reasonable agreement with the average Chl a

exposure along the back trajectories, derived by a combination of satellite and back trajectory data, points to a common phytoplankton source, although for the last part of the cruise a contribution from coastal sources could not be ruled out.

The abiotic formation process of methyl halides from decaying plant material investigated in chapter 3 may contribute significantly to the emissions from the rainforest, whereas its inhibition by high water content means that it is unlikely to occur within the ocean.

List of tables

List of figures

List of abbreviations

ADOX	Antarctic Deep Outflow eXperiment
AGAGE	Advanced Global Atmospheric Gases Experiment
avg	Average
BB	Biomass Burning
Bft	Beaufort
CDOM	Coloured Dissolved Organic Matter
CFC	ChloroFluoroCarbon
Chl a	Chlorophyll a
CPO	ChloroPerOxidase
CV	Coefficient Variation
DAAC	Distributed Active Archive Center
DMS	dimethyl sulphide
DMSO	dimethyl sulfoxide
DMSP	dimethyl sulfonio propionate
dw	dry weight
ECD	Electron Capture Detector
ECMWF	European Centre for Medium-Range Weather Forecasts
EisenEx	Eisen (iron) Experiment
F	Flux
FT	Free Troposphere
GABRIEL	Guyanas Atmosphere-Biosphere exchange and Radicals Intensive Experiment with the Learjet
GC	Gas Chromatograph
GFD	Gesellschaft für Flugzieldarstellung
GOES	Geostationary Operational Environmental Satellites
GSFC	Goddard Space Flight Center
GWP	Global Warming Potential
H_{ML}	Height of the Mixed Layer
HPLC	High Performance Liquid Chromatography
IAEA	International Atomic Energy Agency
INAA	Instrumental Neutron Activation Analysis
ITCZ	InterTropical Convergence Zone

KNMI	Royal Netherlands Meteorological Institute
LAGRANTO	LAGRAngian ANalysis Tool
LFT	Lower Free Troposphere
MD	Marion Dufresne
ML	Mixed Layer
MMSCl	Methionine Methyl Sulfonium Chloride
MODIS	MODerate resolution Imaging Spectroradiometer
MS	Mass Spectrometer
MS	with tube
NASA	National Aeronautics and Space Administration
NCAR	National Centre for Atmospheric Research
ND	Not Determined
NH	Northern Hemisphere
NIST	National Institute of Standards and Technology
NOAA	National Oceanic and Atmospheric Administration
NPP	Net Primary Production
ODE	Ozone Depletion Event
OOMPH	Organic over the Ocean Modifying Particles in both Hemispheres
OS	without tube
PSC	Polar Stratospheric Cloud
PTFE	PolyTetraFluoroEthylen
PTR-MS	Proton Transfer Reaction Mass Spectrometer
R	alkyl moiety
S/N	signal to noise ratio
SAM	S-adenosyl-L-methionine
SeaWiFS	Sea-viewing Wide Field-of-view Sensor
SERIES	Subarctic Ecosystem Response to Iron Enrichment Study
SH	Southern Hemisphere
SIM	Single Ion Mode
SOFeX	Southern Ocean Iron Experiment
ss	stainless steel
TOL	Time Over Land
UTC	Universal Coordinated Time
UV	ultraviolet
VOC	Volatile Organic Compound
VSLS	Very Short Lived Substance
XRF	X-ray fluorescence
ΔMR	change in mixing ratio

Bibliography

Alvain, S., Moulin, C., Dandonneau, Y., and Breon, F. M.: Remote sensing of phytoplankton groups in case 1 waters from global SeaWiFS imagery, Deep-Sea Research Part I-Oceanographic Research Papers, 52, 1989-2004, 2005.

Alvain, S., Moulin, C., Dandonneau, Y., Loisel, H., and Breon, F. M.: A species-dependent bio-optical model of case I waters for global ocean color processing, Deep-Sea Research Part I-Oceanographic Research Papers, 53, 917-925, 2006.

Andreae, M. O., Atlas, E., Harris, G. W., Helas, G., deKock, A., Koppmann, R., Maenhaut, W., Mano, S., Pollock, W. H., Rudolph, J., Scharffe, D., Schebeske, G., and Welling, M.: Methyl halide emissions from savanna fires in southern Africa, Journal of Geophysical Research-Atmospheres, 101, 23603-23613, 1996.

Andreae, M. O., and Merlet, P.: Emission of trace gases and aerosols from biomass burning, Global Biogeochemical Cycles, 15, 955-966, 2001.

Arnold, S., and Spracklen, D.: manuscript in preparation, 2008.

Asplund, G., Christiansen, J. V., and Grimvall, A.: A Chloroperoxidase-Like Catalyst in Soil - Detection and Characterization of Some Properties, Soil Biology & Biochemistry, 25, 41-46, 1993.

Attieh, J. M., Hanson, A. D., and Saini, H. S.: Purification and Characterization of a Novel Methyltransferase Responsible for Biosynthesis of Halomethanes and Methanethiol in Brassica-Oleracea, Journal of Biological Chemistry, 270, 9250-9257, 1995.

Baker, J. M., Reeves, C. E., Nightingale, P. D., Penkett, S. A., Gibb, S. W., and Hatton, A. D.: Biological production of methyl bromide in the coastal waters of the North Sea and open ocean of the northeast Atlantic, Marine Chemistry, 64, 267-285, 1999.

Barrie, L. A., Bottenheim, J. W., Schnell, R. C., Crutzen, P. J., and Rasmussen, R. A.: Ozone Destruction and Photochemical Reactions at Polar Sunrise in the Lower Arctic Atmosphere, Nature, 334, 138-141, 1988.

Becker, D. A., Anderson, D. L., Lindstrom, R. M., Greenberg, R. R., Garrity, K. M., and Mackey, E. A.: Use of INAA, PGAA, and RNAA to determine 30 elements for certification of an SRM - Tomato Leaves, 1573a, Journal of Radioanalytical and Nuclear Chemistry-Articles, 179, 149-154, 1994.

Belkin, I. M., and Gordon, A. L.: Southern Ocean fronts from the Greenwich meridian to Tasmania, Journal of Geophysical Research-Oceans, 101, 3675-3696, 1996.

Blake, N. J., Blake, D. R., Sive, B. C., Chen, T. Y., Rowland, F. S., Collins, J. E., Sachse, G. W., and Anderson, B. E.: Biomass burning emissions and vertical distribution of atmospheric methyl halides and other reduced carbon gases in the South

Atlantic region, Journal of Geophysical Research-Atmospheres, 101, 24151-24164, 1996.

Blake, N. J., Blake, D. R., Swanson, A. L., Atlas, E., Flocke, F., and Rowland, F. S.: Latitudinal, vertical, and seasonal variations of C-1-C-4 alkyl nitrates in the troposphere over the Pacific Ocean during PEM-Tropics A and B: Oceanic and continental sources, Journal of Geophysical Research-Atmospheres, 108, 2003.

Blake, N. J., Blake, D. R., Wingenter, O. W., Sive, B. C., Kang, C. H., Thornton, D. C., Bandy, A. R., Atlas, E., Flocke, F., Harris, J. M., and Rowland, F. S.: Aircraft measurements of the latitudinal, vertical, and seasonal variations of NMHCs, methyl nitrate, methyl halides, and DMS during the First Aerosol Characterization Experiment (ACE 1), Journal of Geophysical Research-Atmospheres, 104, 21803-21817, 1999.

Bottenheim, J. W., Gallant, A. G., and Brice, K. A.: Measurements of NO_y Species and O_3 at 82° N Latitude, Geophysical Research Letters, 13, 113-116, 1986.

Boyd, P. W., Jickells, T., Law, C. S., Blain, S., Boyle, E. A., Buesseler, K. O., Coale, K. H., Cullen, J. J., de Baar, H. J. W., Follows, M., Harvey, M., Lancelot, C., Levasseur, M., Owens, N. P. J., Pollard, R., Rivkin, R. B., Sarmiento, J., Schoemann, V., Smetacek, V., Takeda, S., Tsuda, A., Turner, S., and Watson, A. J.: Mesoscale iron enrichment experiments 1993-2005: Synthesis and future directions, Science, 315, 612-617, 2007.

Brinckman, F. E., Olson, G. J., and Thayer, J. S.: Biological Mediation of Marine Metal Cycles the Case of Methyl Iodide, Sigleo, a. C. and a. Hattori (Ed.). Marine and Estuarine Geochemistry; International Chemical Congress of Pacific Basin Societies, Honolulu, Hawaii, USA, Dec. 16-21, 1984. Lewis Publishers, Inc.: Chelsea, Mich., USA. Illus. Maps, 227-238, 1985.

Bustan, A., Sagi, M., De Malach, Y., and Pasternak, D.: Effects of saline irrigation water and heat waves on potato production in an arid environment, Field Crops Research, 90, 275-285, 2004.

Butler, J. H.: Atmospheric chemistry - Better budgets for methyl halides?, Nature, 403, 260-261, 2000.

Butler, J. H., King, D. B., Lobert, J. M., Montzka, S. A., Yvon-Lewis, S. A., Hall, B. D., Warwick, N. J., Mondeel, D. J., Aydin, M., and Elkins, J. W.: Oceanic distributions and emissions of short-lived halocarbons, Global Biogeochemical Cycles, 21, 2007.

Campos, M., Nightingale, P. D., and Jickells, T. D.: A comparison of methyl iodide emissions from seawater and wet depositional fluxes of iodine over the southern North Sea, Tellus Series B-Chemical and Physical Meteorology, 48, 106-114, 1996.

Carpenter, L. J., Liss, P. S., and Penkett, S. A.: Marine organohalogens in the atmosphere over the Atlantic and Southern Oceans, Journal of Geophysical Research-Atmospheres, 108, 2003.

Carpenter, L. J., Sturges, W. T., Penkett, S. A., Liss, P. S., Alicke, B., Hebestreit, K., and Platt, U.: Short-lived alkyl iodides and bromides at Mace Head, Ireland: Links to biogenic sources and halogen oxide production, Journal of Geophysical Research-Atmospheres, 104, 1679-1689, 1999.

Carpenter, L. J., Wevill, D. J., Hopkins, J. R., Dunk, R. M., Jones, C. E., Hornsby, K. E., and McQuaid, J. B.: Bromoform in tropical Atlantic air from 25° N to 25° S, Geophysical Research Letters, 34, 2007.

Carpenter, L. J., Wevill, D. J., O'Doherty, S., Spain, G., and Simmonds, P. G.: Atmospheric bromoform at Mace Head, Ireland: seasonality and evidence for a peatland source, Atmospheric Chemistry and Physics, 5, 2927-2934, 2005.

Chameides, W. L., and Davis, D. D.: Iodine - Its Possible Role in Tropospheric Photochemistry, Journal of Geophysical Research-Oceans and Atmospheres, 85, 7383-7398, 1980.

Chuck, A. L., Turner, S. M., and Liss, P. S.: Oceanic distributions and air-sea fluxes of biogenic halocarbons in the open ocean, Journal of Geophysical Research-Oceans, 110, 2005.

Class, T., and Ballschmiter, K.: Chemistry of Organic Traces in Air IX Evidence of Natural Marine Sources for Chloroform in Regions of High Primary Production, Fresenius Zeitschrift Fur Analytische Chemie, 327, 40-41, 1987.

Class, T. H., and Ballschmiter, K.: Chemistry of Organic Traces in Air VIII Sources and Distribution of Bromo- and Bromochloromethanes in Marine Air and Surface Water of the Atlantic Ocean, Journal of Atmospheric Chemistry, 6, 35-46, 1988.

Cohan, D. S., Sturrock, G. A., Biazar, A. P., and Fraser, P. J.: Atmospheric methyl iodide at Cape Grim, Tasmania, from AGAGE observations, Journal of Atmospheric Chemistry, 44, 131-150, 2003.

Colomb, A., Williams, J., Crowley, J., Gros, V., Hofmann, R., Salisbury, G., Klupfel, T., Kormann, R., Stickler, A., Forster, C., and Lelieveld, J.: Airborne measurements of trace organic species in the upper troposphere over Europe: the impact of deep convection, Environmental Chemistry, 3, 244-259, 2006.

Coulter, C., Hamilton, J. T. G., McRoberts, W. C., Kulakov, L., Larkin, M. J., and Harper, D. B.: Halomethane : bisulfide/halide ion methyltransferase, an unusual corrinoid enzyme of environmental significance isolated from an aerobic methylotroph using chloromethane as the sole carbon source, Applied and Environmental Microbiology, 65, 4301-4312, 1999.

Cox, M. L., Sturrock, G. A., Fraser, P. J., Siems, S. T., and Krummel, P. B.: Identification of regional sources of methyl bromide and methyl iodide from AGAGE observations at Cape Grim, Tasmania, Journal of Atmospheric Chemistry, 50, 59-77, 2005.

Cox, M. L., Sturrock, G. A., Fraser, P. J., Siems, S. T., Krummel, P. B., and O'Doherty, S.: Regional sources of methyl chloride, chloroform and dichloromethane identified from AGAGE observations at Cape Grim, Tasmania, 1998-2000, Journal of Atmospheric Chemistry, 45, 79-99, 2003.

Davis, D., Crawford, J., Liu, S., McKeen, S., Bandy, A., Thornton, D., Rowland, F., and Blake, D.: Potential impact of iodine on tropospheric levels of ozone and other critical oxidants, Journal of Geophysical Research-Atmospheres, 101, 2135-2147, 1996.

Dimmer, C. H., Simmonds, P. G., Nickless, G., and Bassford, M. R.: Biogenic fluxes of halomethanes from Irish peatland ecosystems, Atmospheric Environment, 35, 321-330, 2001.

Dvortsov, V. L., Geller, M. A., Solomon, S., Schauffler, S. M., Atlas, E. L., and Blake, D. R.: Rethinking reactive halogen budgets in the midlatitude lower stratosphere, Geophysical Research Letters, 26, 1699-1702, 1999.

Ekdahl, A., Pedersen, M., and Abrahamsson, K.: A study of the diurnal variation of biogenic volatile halocarbons, Marine Chemistry, 63, 1-8, 1998.

Fan, S. M., and Jacob, D. J.: Surface Ozone Depletion in Arctic Spring Sustained by Bromine Reactions on Aerosols, Nature, 359, 522-524, 1992.

FAO: Forestry Paper - 140 "Global Forest Resources Assessment 2000 (FRA 2000)", Food and Agricultural Organization of the United Nations, Rome, Italy140, 1-479, 2001.

Farman, J. C., Gardiner, B. G., and Shanklin, J. D.: Large losses of ozone in Antarctica reveal seasonal ClO_x/NO_x interaction, Nature, 315, 207-210, 1985.

Fenical, W.: Polyhaloketones from Red Seaweed Asparagopsis-Taxiformis, Tetrahedron Letters, 4463-4466, 1974.

Field, C. B., Behrenfeld, M. J., Randerson, J. T., and Falkowski, P.: Primary production of the biosphere: Integrating terrestrial and oceanic components, Science, 281, 237-240, 1998.

Finlayson-Pitts, B. J., and Pitts, J. N.: Chemistry of the Upper and Lower Atmosphere - Theory, Experiments and Applications, Academic Press, San Diego, 1999.

Flowers, T. J., and Yeo, A. R.: Breeding for salinity resistance in crop plants: Where next?, Australian Journal of Plant Physiology, 22, 875-884, 1995.

Frank, H., Frank, W., and Thiel, D.: C_1- and C_2-Halocarbons in soil-air of forests, Atmospheric Environment, 23, 1333-1335, 1989.

Gan, J., Yates, S. R., Ohr, H. D., and Sims, J. J.: Production of methyl bromide by terrestrial higher plants, Geophysical Research Letters, 25, 3595-3598, 1998.

Geen, C. E.: Selected marine sources and sinks of bromoform and other low molecular weight organobromines. MSc Thesis, Oceanography, Dalhousie University, Halifax, 1992.

Goodwin, K. D., North, W. J., and Lidstrom, M. E.: Production of bromoform and dibromomethane by Giant Kelp: Factors affecting release and comparison to anthropogenic bromine sources, Limnology and Oceanography, 42, 1725-1734, 1997.

Graedel, T. E., and Crutzen, P. J.: Chemie der Atmosphäre: Bedeutung für Klima und Umwelt, Spektrum Akademischer Verlag GmbH, Heidelberg, 511 pp., 1994.

Gros, V., Bonsang, B., and Sarda Esteve, R.: Atmospheric carbon monoxide 'in situ' monitoring by automatic gas chromatography, Chemosphere - Global Change Science, 1, 153-161, 1999.

Gros, V., Poisson, N., Martin, D., Kanakidou, M., and Bonsang, B.: Observations and modeling of the seasonal variation of surface ozone at Amsterdam Island: 1994-1996, Journal of Geophysical Research-Atmospheres, 103, 28103-28109, 1998.

Gros, V., Williams, J., van Aardenne, J. A., Salisbury, G., Hofmann, R., Lawrence, M. G., von Kuhlmann, R., Lelieveld, J., Krol, M., Berresheim, H., Lobert, J. M., and Atlas, E.: Origin of anthropogenic hydrocarbons and halocarbons measured in the summertime european outflow (on Crete in 2001), Atmospheric Chemistry and Physics, 3, 1223-1235, 2003.

Gschwend, P. M., Macfarlane, J. K., and Newman, K. A.: Volatile Halogenated Organic-Compounds Released to Seawater from Temperate Marine Macroalgae, Science, 227, 1033-1035, 1985.

Hamilton, J. T. G., McRoberts, W. C., Keppler, F., Kalin, R. M., and Harper, D. B.: Chloride methylation by plant pectin: An efficient environmentally significant process, Science, 301, 206-209, 2003.

Happell, J. D., and Wallace, D. W. R.: Methyl iodide in the Greenland/Norwegian Seas and the tropical Atlantic Ocean: Evidence for photochemical production, Geophysical Research Letters, 23, 2105-2108, 1996.

Harper, D. B.: The global chloromethane cycle: biosynthesis, biodegradation and metabolic role, Natural Product Reports, 17, 337-348, 2000.

Harper, D. B., Buswell, J. A., Kennedy, J. T., and Hamilton, J. T. G.: Chloromethane, Methyl Donor in Veratryl Alcohol Biosynthesis in Phanerochaete-Chrysosporium and Other Lignin-Degrading Fungi, Applied and Environmental Microbiology, 56, 3450-3457, 1990.

Harper, D. B., Hamilton, J. T. G., Ducrocq, V., Kennedy, J. T., Downey, A., and Kalin, R. M.: The distinctive isotopic signature of plant-derived chloromethane: possible application in constraining the atmospheric chloromethane budget, Chemosphere, 52, 433-436, 2003.

Harper, D. B., Hamilton, J. T. G., Kennedy, J. T., and McNally, K. J.: Chloromethane, a Novel Methyl Donor for Biosynthesis of Esters and Anisoles in Phellinus-Pomaceus, Applied and Environmental Microbiology, 55, 1981-1989, 1989.

Harper, D. B., Harvey, B. M. R., Jeffers, M. R., and Kennedy, J. T.: Emissions, biogenesis and metabolic utilization of chloromethane by tubers of the potato (Solanum tuberosum), New Phytologist, 142, 5-17, 1999.

Haselmann, K. F., Ketola, R. A., Laturnus, F., Lauritsen, F. R., and Gron, C.: Occurrence and formation of chloroform at Danish forest sites, Atmospheric Environment, 34, 187-193, 2000a.

Haselmann, K. F., Laturnus, F., Svensmark, B., and Gron, C.: Formation of chloroform in spruce forest soil - results from laboratory incubation studies, Chemosphere, 41, 1769-1774, 2000b.

Helz, G. R., and Hsu, R. Y.: Volatile Chlorocarbons and Bromocarbons in Coastal Waters, Limnology and Oceanography, 23, 858-869, 1978.

Hoekstra, E. J., De Leer, E. W. B., and Brinkman, U. A. T.: Natural formation of chloroform and brominated trihalomethanes in soil, Environmental Science & Technology, 32, 3724-3729, 1998a.

Hoekstra, E. J., Duyzer, J. H., de Leer, E. W. B., and Brinkman, U. A. T.: Chloroform - concentration gradients in soil air and atmospheric air, and emission fluxes from soil, Atmospheric Environment, 35, 61-70, 2001.

Hoekstra, E. J., Verhagen, F. J. M., Field, J. A., De Leer, E. W. B., and Brinkman, U. A. T.: Natural production of chloroform by fungi, Phytochemistry, 49, 91-97, 1998b.

Holton, J. R.: An Introduction to Dynamic Meteorology, 3rd ed., International Geophysics Series, edited by: Dmowska, R., and Holton, J. R., Academic Press, San Diego, 511 pp., 1992.

Hu, H. N., Brown, P. H., and Labavitch, J. M.: Species variability in boron requirement is correlated with cell wall pectin, Journal of Experimental Botany, 47, 227-232, 1996.

Hu, Z. Y., and Moore, R. M.: Kinetics of methyl halide production by reaction of DMSP with halide ion, Marine Chemistry, 52, 147-155, 1996.

ILO, International Chemical Safety Card (ICSC) available at: www.ilo.org/public/english/protection/safework/cis/products/icsc/dtasht/index.htm, 2008.

IPCC: Climate Change 2007: The Physical Science Basis. Contribution of Working Group I to the Fourth Assessment of the Intergovernmental Panel on Climate Change: Annex 4 - Acronyms, IPCC Fourth Assessment Report, edited by: Baede, A. P. M., Cambridge University Press, United Kingdom and New York, NY, USA, 941-987 pp., 2007.

Isidorov, V. A., and Jdanova, M.: Volatile organic compounds from leaves litter, Chemosphere, 48, 975-979, 2002.

Isidorov, V. A., Zenkevich, I. G., and Ioffe, B. V.: Volatile Organic Compounds in the Atmosphere of Forests, Atmospheric Environment, 19, 1-8, 1985.

Itoh, N., Tsujita, M., Takayuki, A., Hisatomi, G., and Higashi, T.: Formation and emission of monohalomethanes from marine algae, Phytochemistry, 45, 67-73, 1997.

Keene, W. C., Khalil, M. A. K., Erickson, D. J., McCulloch, A., Graedel, T. E., Lobert, J. M., Aucott, M. L., Gong, S. L., Harper, D. B., Kleiman, G., Midgley, P., Moore, R. M., Seuzaret, C., Sturges, W. T., Benkovitz, C. M., Koropalov, V., Barrie, L. A., and Li, Y. F.: Composite global emissions of reactive chlorine from anthropogenic and natural sources: Reactive Chlorine Emissions Inventory, Journal of Geophysical Research-Atmospheres, 104, 8429-8440, 1999.

Keppler, F., Eiden, R., Niedan, V., Pracht, J., and Scholer, H. F.: Halocarbons produced by natural oxidation processes during degradation of organic matter, Nature, 403, 298-301, 2000.

Keppler, F., Harper, D. B., Rockmann, T., Moore, R. M., and Hamilton, J. T. G.: New insight into the atmospheric chloromethane budget gained using stable carbon isotope ratios, Atmospheric Chemistry and Physics, 5, 2403-2411, 2005.

Keppler, F., Kalin, R. M., Harper, D. B., McRoberts, W. C., and Hamilton, J. T. G.: Carbon isotope anomaly in the major plant C_1 pool and its global biogeochemical implications, Biogeosciences, 1, 123-131, 2004.

Khalil, M. A. K., Pinto, J. P., and Shearer, M. J.: Atmospheric carbon monoxide, Chemosphere - Global Change Science, 1, ix-xi, 1999.

Khalil, M. A. K., and Rasmussen, R. A.: Atmospheric chloroform, Atmospheric Environment, 33, 1151-1158, 1999a.

Khalil, M. A. K., and Rasmussen, R. A.: Atmospheric methyl chloride, Atmospheric Environment, 33, 1305-1321, 1999b.

Khalil, M. A. K., and Rasmussen, R. A.: Soil-atmosphere exchange of radiatively and chemically active gases, Environmental Science and Pollution Research, 7, 79-82, 2000.

Klick, S.: The Release of Volatile Halocarbons to Seawater by Untreated and Heavy-Metal Exposed Samples of the Brown Seaweed Fucus-Vesiculosus, Marine Chemistry, 42, 211-221, 1993.

Koppmann, R., Czapiewski, K. v., and Komenda, M.: Natural and human induced biomass burining in Africa: an important source for volatile organic compounds in the troposphere, in: Climate Change and Africa, edited by: Low, P. S., Cambridge University Press, 68-78, 2005.

Krejci, R., Strom, J., de Reus, M., Williams, J., Fischer, H., Andreae, M. O., and Hansson, H. C.: Spatial and temporal distribution of atmospheric aerosols in the lowermost troposphere over the Amazonian tropical rainforest, Atmospheric Chemistry and Physics, 5, 1527-1543, 2005.

Laturnus, F., Adams, F. C., and Wiencke, C.: Methyl halides from Antarctic macroalgae, Geophysical Research Letters, 25, 773-776, 1998.

Laturnus, F., Haselmann, K. F., Borch, T., and Gron, C.: Terrestrial natural sources of trichloromethane (chloroform, $CHCl_3$) - An overview, Biogeochemistry, 60, 121-139, 2002.

Laturnus, F., Mehrtens, G., and Gron, C.: Haloperoxidase-Like Activity in Spruce Forest Soil a Source of Volatile Halogenated Organic-Compounds, Chemosphere, 31, 3709-3719, 1995.

Lee-Taylor, J., and Redeker, K. R.: Reevaluation of global emissions from rice paddies of methyl iodide and other species, Geophysical Research Letters, 32, 2005.

Lee-Taylor, J. M., Brasseur, G. P., and Yokouchi, Y.: A preliminary three-dimensional global model study of atmospheric methyl chloride distributions, Journal of Geophysical Research-Atmospheres, 106, 34221-34233, 2001.

Lee-Taylor, J. M., Doney, S. C., Brasseur, G. P., and Muller, J. F.: A global three-dimensional atmosphere-ocean model of methyl bromide distributions, Journal of Geophysical Research-Atmospheres, 103, 16039-16057, 1998.

Lelieveld, J., Butler, T. M., Crowley, J. N., Dillon, T. J., Fischer, H., Ganzeveld, L., Harder, H., Lawrence, M. G., Martinez, M., Taraborelli, D., and Williams, J.: Atmospheric oxidation capacity sustained by a tropical forest, Nature, 452, 737-740, 2008.

Levine, J. G., Braesicke, P., Harris, N. R. P., Savage, N. H., and Pyle, J. A.: Pathways and timescales for troposphere-to-stratosphere transport via the tropical tropopause layer and their relevance for very short lived substances, Journal of Geophysical Research-Atmospheres, 112, Doi:10.1029/2005JD006940, 2007.

Li, H. J., Yokouchi, Y., and Akimoto, H.: Measurement of methyl halides in the marine atmosphere, Atmospheric Environment, 33, 1881-1887, 1999.

Liss, P., Chuck, A., Bakker, D., and Turner, S.: Ocean fertilization with iron: effects on climate and air quality, Tellus Series B-Chemical and Physical Meteorology, 57, 269-271, 2005.

Lobert, J. M., Butler, J. H., Montzka, S. A., Geller, L. S., Myers, R. C., and Elkins, J. W.: A Net Sink for Atmospheric CH_3Br in the East Pacific-Ocean, Science, 267, 1002-1005, 1995.

Lobert, J. M., Keene, W. C., Logan, J. A., and Yevich, R.: Global chlorine emissions from biomass burning: Reactive Chlorine Emissions Inventory, Journal of Geophysical Research-Atmospheres, 104, 8373-8389, 1999.

Lobert, J. M., YvonLewis, S. A., Butler, J. H., Montzka, S. A., and Myers, R. C.: Undersaturation of CH_3Br in the Southern Ocean, Geophysical Research Letters, 24, 171-172, 1997.

Lovelock, J. E.: Natural Halocarbons in Air and in Sea, Nature, 256, 193-194, 1975.

Lovelock, J. E., and Maggs, R. J.: Halogenated Hydrocarbons in and over the Atlantic, Nature, 241, 194-196, 1973.

Lutgens, F. K., and Tarbuck, E. J.: The Atmosphere, 10th ed., edited by: Kaveney, D., Pearson Prentice Hall, Upper Sadle River, New Jersey, 2007.

MacDonald, S., and Moore, R. M.: Seasonal and spatial variations in methyl chloride in NW Atlantic waters, Journal of Geophysical Research-Oceans, 112, 2007.

Mackey, M. D., Mackey, D. J., Higgins, H. W., and Wright, S. W.: CHEMTAX - A program for estimating class abundances from chemical markers: Application to HPLC measurements of phytoplankton, Marine Ecology-Progress Series, 144, 265-283, 1996.

Mak, J. E., and Brenninkmeijer, C. A. M.: Compressed-Air Sample Technology for Isotopic Analysis of Atmospheric Carbon-Monoxide, Journal of Atmospheric and Oceanic Technology, 11, 425-431, 1994.

Manley, S. L., and Dastoor, M. N.: Methyl Halide (CH_3X) Production from the Giant-Kelp, Macrocystis, and Estimates of Global CH_3X Production by Kelp, Limnology and Oceanography, 32, 709-715, 1987.

Manley, S. L., and delaCuesta, J. L.: Methyl iodide production from marine phytoplankton cultures, Limnology and Oceanography, 42, 142-147, 1997.

Manley, S. L., Goodwin, K., and North, W. J.: Laboratory Production of Bromoform, Methylene Bromide, and Methyl Iodide by Macroalgae and Distribution in Nearshore Southern California Waters, Limnology and Oceanography, 37, 1652-1659, 1992.

Manley, S. L., Wang, N. Y., Walser, M. L., and Cicerone, R. J.: Coastal salt marshes as global methyl halide sources from determinations of intrinsic production by marsh plants, Global Biogeochemical Cycles, 20, 2006.

Manley, S. L., Wang, N. Y., Walser, M. L., and Cicerone, R. J.: Methyl halide emissions from greenhouse-grown mangroves, Geophysical Research Letters, 34, 2007.

Masarie, K. A., Langenfelds, R. L., Allison, C. E., Conway, T. J., Dlugokencky, E. J., Francey, R. J., Novelli, P. C., Steele, L. P., Tans, P. P., Vaughn, B., and White, J. W. C.: NOAA/CSIRO Flask Air Intercomparison Experiment: A strategy for directly assessing consistency among atmospheric measurements made by independent laboratories, Journal of Geophysical Research-Atmospheres, 106, 20445-20464, 2001.

McCulloch, A.: Chloroform in the environment: occurrence, sources, sinks and effects, Chemosphere, 50, 1291-1308, 2003.

Methven, J.: Offline trajectories: Calculation and accuracy, Tech. Report 44 , U.K. Univ. Global Modelling Programme, Dept. of Meteorol., University of Reading, Reading, UK., 1997.

Mino, Y., and Yukita, M.: Detection of high levels of bromine in vegetables using X-ray fluorescence spectrometry, Journal of Health Science, 51, 365-368, 2005.

Molina, M. J., and Rowland, F. S.: Stratospheric Sink for Chlorofluoromethanes - Chlorine Atomic-Catalysed Destruction of Ozone, Nature, 249, 810-812, 1974.

Moore, R. M.: The solubility of a suite of low molecular weight organochlorine compounds in seawater and implications for estimating the marine source of methyl chloride to the atmosphere, Chemosphere - Global Change Science, 2, 95-99, 2000.

Moore, R. M.: Marine Sources of Volatile Halocarbons, in: The Handbook of Environmental Chemistry Vol. 3, Part P, edited by: Gribble, G., Anthropogenic Compounds, Springer-Verlag, Berlin Heidelberg, 85-101, 2003.

Moore, R. M., Geen, C. E., and Tait, V. K.: Determination of Henry Law Constants for a Suite of Naturally-Occurring Halogenated Methanes in Seawater, Chemosphere, 30, 1183-1191, 1995.

Moore, R. M., and Groszko, W.: Methyl iodide distribution in the ocean and fluxes to the atmosphere, Journal of Geophysical Research-Oceans, 104, 11163-11171, 1999.

Moore, R. M., Groszko, W., and Niven, S. J.: Ocean-atmosphere exchange of methyl chloride: Results from NW Atlantic and Pacific Ocean studies, Journal of Geophysical Research-Oceans, 101, 28529-28538, 1996a.

Moore, R. M., Gut, A., and Andreae, M. O.: A pilot study of methyl chloride emissions from tropical woodrot fungi, Chemosphere, 58, 221-225, 2005.

Moore, R. M., and Wang, L.: The influence of iron fertilization on the fluxes of methyl halides and isoprene from ocean to atmosphere in the SERIES experiment, Deep-Sea Research Part II-Topical Studies in Oceanography, 53, 2398-2409, 2006.

Moore, R. M., Webb, M., Tokarczyk, R., and Wever, R.: Bromoperoxidase and iodoperoxidase enzymes and production of halogenated methanes in marine diatom cultures, Journal of Geophysical Research-Oceans, 101, 20899-20908, 1996b.

Moore, R. M., and Zafiriou, O. C.: Photochemical Production of Methyl-Iodide in Seawater, Journal of Geophysical Research-Atmospheres, 99, 16415-16420, 1994.

Ni, X. H., and Hager, L. P.: cDNA cloning of Batis maritima methyl chloride transferase and purification of the enzyme, Proceedings of the National Academy of Sciences of the United States of America, 95, 12866-12871, 1998.

Ni, X. H., and Hager, L. P.: Expression of Batis maritima methyl chloride transferase in Escherichia coli, Proceedings of the National Academy of Sciences of the United States of America, 96, 3611-3615, 1999.

Nielsen, J. E., and Douglass, A. R.: Simulation of bromoform's contribution to stratospheric bromine, Journal of Geophysical Research-Atmospheres, 106, 8089-8100, 2001.

Nightingale, P. D., Malin, G., and Liss, P. S.: Production of Chloroform and Other Low-Molecular-Weight Halocarbons by Some Species of Macroalgae, Limnology and Oceanography, 40, 680-689, 1995.

Novelli, P. C., Collins, J. E., Myers, R. C., Sachse, G. W., and Scheel, H. E.: Reevaluation of the NOAA-CMDL Carbon-Monoxide Reference Scale and Comparisons with Co Reference Gases at Nasa-Langley and the Fraunhofer-Institut, Journal of Geophysical Research-Atmospheres, 99, 12833-12839, 1994.

O'Doherty, S., Simmonds, P. G., Cunnold, D. M., Wang, H. J., Sturrock, G. A., Fraser, P. J., Ryall, D., Derwent, R. G., Weiss, R. F., Salameh, P., Miller, B. R., and Prinn, R. G.: In situ chloroform measurements at Advanced Global Atmospheric Gases

Experiment atmospheric research stations from 1994 to 1998, Journal of Geophysical Research-Atmospheres, 106, 20429-20444, 2001.

O'Dowd, C. D., Geever, M., and Hill, M. K.: New particle formation: Nucleation rates and spatial scales in the clean marine coastal environment, Geophysical Research Letters, 25, 1661-1664, 1998.

O'Dowd, C. D., Hameri, K., Makela, J. M., Pirjola, L., Kulmala, M., Jennings, S. G., Berresheim, H., Hansson, H. C., de Leeuw, G., Kunz, G. J., Allen, A. G., Hewitt, C. N., Jackson, A., Viisanen, Y., and Hoffmann, T.: A dedicated study of New Particle Formation and Fate in the Coastal Environment (PARFORCE): Overview of objectives and achievements, Journal of Geophysical Research-Atmospheres, 107, 2002.

O'Dowd, C. D., and Hoffmann, T.: Coastal new particle formation: A review of the current state-of-the-art, Environmental Chemistry, 2, 245-255, 2005.

Oltmans, S. J.: Surface Ozone Measurements in Clean Air, Journal of Geophysical Research-Oceans and Atmospheres, 86, 1174-1180, 1981.

Oltmans, S. J., and Komhyr, W. D.: Surface Ozone Distributions and Variations from 1973-1984 Measurements at the NOAA Geophysical Monitoring for Climatic Change Baseline Observatories, Journal of Geophysical Research-Atmospheres, 91, 5229-5236, 1986.

Platt, U., and Janssen, C.: Observation and role of the free radicals NO_3, ClO, BrO and IO in the troposphere, Faraday Discussions, 100, 175-198, 1995.

Putaud, J. P., Davison, B. M., Watts, S. F., Mihalopoulos, N., Nguyen, B. C., and Hewitt, C. N.: Dimethylsulfide and its oxidation products at two sites in Brittany (France), Atmospheric Environment, 33, 647-659, 1999.

Quack, B., Atlas, E., Petrick, G., Stroud, V., Schauffler, S., and Wallace, D. W. R.: Oceanic bromoform sources for the tropical atmosphere, Geophysical Research Letters, 31, 2004.

Quack, B., Atlas, E., Petrick, G., and Wallace, D. W. R.: Bromoform and dibromomethane above the Mauritanian upwelling: Atmospheric distributions and oceanic emissions, Journal of Geophysical Research-Atmospheres, 112, 2007.

Quack, B., and Wallace, D. W. R.: Air-sea flux of bromoform: Controls, rates, and implications, Global Biogeochemical Cycles, 17, 2003.

Quartly, G., and Srokosz, M.: A plankton guide to ocean physics: Colouring in the currents round South Africa and Madagascar Ocean Challenge, 12, 19-23, 2003.

Rasmussen, R. A., Khalil, M. A. K., Gunawardena, R., and Hoyt, S. D.: Atmospheric Methyl Iodide (CH_3I), Journal of Geophysical Research-Oceans and Atmospheres, 87, 3086-3090, 1982.

Ravindran, K. C., Venkatesan, K., Balakrishnan, V., Chellappan, K. P., and Balasubramanian, T.: Restoration of saline land by halophytes for Indian soils, Soil Biology & Biochemistry, 39, 2661-2664, 2007.

Read, K. A., Mahajan, A. S., Carpenter, L. J., Evans, M. J., Faria, B. V. E., Heard, D. E., Hopkins, J. R., Lee, J. D., Moller, S. J., Lewis, A. C., Mendes, L., McQuaid, J. B., Oetjen, H., Saiz-Lopez, A., Pilling, M. J., and Plane, J. M. C.: Extensive halogen-mediated ozone destruction over the tropical Atlantic Ocean, Nature, 453, 1232-1235, 2008.

Redeker, K. R., Meinardi, S., Blake, D., and Sass, R.: Gaseous emissions from flooded rice paddy agriculture, Journal of Geophysical Research-Atmospheres, 108, 2003.

Reeves, C. E.: Atmospheric budget implications of the temporal and spatial trends in methyl bromide concentration, Journal of Geophysical Research-Atmospheres, 108, doi: 10.1029/2002JD002943, 2003.

Rengasamy, P.: World salinization with emphasis on Australia, Journal of Experimental Botany, 57, 1017-1023, 2006.

Rhew, R. C., Miller, B. R., Vollmer, M. K., and Weiss, R. F.: Shrubland fluxes of methyl bromide and methyl chloride, Journal of Geophysical Research-Atmospheres, 106, 20875-20882, 2001.

Rhew, R. C., Miller, B. R., and Weiss, R. F.: Natural methyl bromide and methyl chloride emissions from coastal salt marshes, Nature, 403, 292-295, 2000.

Rhew, R. C., Teh, Y. A., and Abel, T.: Methyl halide and methane fluxes in the northern Alaskan coastal tundra, Journal of Geophysical Research-Biogeosciences, 112, 2007.

Richter, U., and Wallace, D. W. R.: Production of methyl iodide in the tropical Atlantic Ocean, Geophysical Research Letters, 31, 2004.

Romero, S. I., Piola, A. R., Charo, M., and Garcia, C. A. E.: Chlorophyll-alpha variability off Patagonia based on SeaWiFS data, Journal of Geophysical Research-Oceans, 111, 2006.

Rook, J. J.: Formation of haloforms during chlorination of natural waters, Journal of Water Treatment Examination, 23, 234-243, 1974.

Rook, J. J.: Chlorination Reactions of Fulvic Acids in Natural-Waters, Environmental Science & Technology, 11, 478-482, 1977.

Saemundsdottir, S., and Matrai, P. A.: Biological production of methyl bromide by cultures of marine phytoplankton, Limnology and Oceanography, 43, 81-87, 1998.

Saito, T., and Yokouchi, Y.: Diurnal variation in methyl halide emission rates from tropical ferns, Atmospheric Environment, 40, 2806-2811, 2006.

Saxena, D., Aouad, S., Attieh, J., and Saini, H. S.: Biochemical characterization of chloromethane emission from the wood-rotting fungus Phellinus pomaceus, Applied and Environmental Microbiology, 64, 2831-2835, 1998.

Scarratt, M. G., and Moore, R. M.: Production of methyl chloride and methyl bromide in laboratory cultures of marine phytoplankton, Marine Chemistry, 54, 263-272, 1996.

Scarratt, M. G., and Moore, R. M.: Production of methyl bromide and methyl chloride in laboratory studies of marine phytoplankton II, Marine Chemistry, 59, 311-320, 1997.

Scarratt, M. G., and Moore, R. M.: Production of chlorinated hydrocarbons and methyl iodide by the red microalga Porphyridium purpureum, Limnology and Oceanography, 44, 703-707, 1999.

Schall, C., Heumann, K. G., and Kirst, G. O.: Biogenic volatile organoiodine and organobromine hydrocarbons in the Atlantic Ocean from 42° N to 72° S, Fresenius Journal of Analytical Chemistry, 359, 298-305, 1997.

Scheeren, H. A., Lelieveld, J., Williams, J., Fischer, H., and Warneke, C.: Measurement of reactive chlorocarbons over the Surinam tropical rain forest: indications for strong biogenic emissions, Atmos. Chem. Phys. Discuss., 3, 5469-5512, 2003.

Signorini, S. R., Garcia, V. M. T., Piola, A. R., Garcia, C. A. E., Mata, M. M., and McClain, C. R.: Seasonal and interannual variability of calcite in the vicinity of the Patagonian shelf break (38° S - 52° S), Geophysical Research Letters, 33, 2006.

Simmonds, P. G., Derwent, R. G., Manning, A. J., Fraser, P. J., Krummel, P. B., O'Doherty, S., Prinn, R. G., Cunnold, D. M., Miller, B. R., Wang, H. J., Ryall, D. B., Porter, L. W., Weiss, R. F., and Salameh, P. K.: AGAGE observations of methyl bromide and methyl chloride at Mace Head, Ireland, and Cape Grim, Tasmania, 1998-2001, Journal of Atmospheric Chemistry, 47, 243-269, 2004.

Simo, R.: From cells to globe: approaching the dynamics of DMS(P) in the ocean at multiple scales, Canadian Journal of Fisheries and Aquatic Sciences, 61, 673-684, 2004.

Singh, H. B., Salas, L. J., and Stiles, R. E.: Methyl Halides in and over the Eastern Pacific (40° N - 32° S), Journal of Geophysical Research-Oceans and Atmospheres, 88, 3684-3690, 1983.

Singh, H. B., Tabazadeh, A., Evans, M. J., Field, B. D., Jacob, D. J., Sachse, G., Crawford, J. H., Shetter, R., and Brune, W. H.: Oxygenated volatile organic chemicals in the oceans: Inferences and implications based on atmospheric observations and air-sea exchange models, Geophysical Research Letters, 30, 2003.

Sive, B. C., Varner, R. K., Mao, H., Blake, D. R., Wingenter, O. W., and Talbot, R.: A large terrestrial source of methyl iodide, Geophysical Research Letters, 34, 5, 2007.

Solomon, S., Garcia, R. R., Rowland, F. S., and Wuebbles, D. J.: On the Depletion of Antarctic Ozone, Nature, 321, 755-758, 1986.

Stefels, J., Steinke, M., Turner, S., Malin, G., and Belviso, S.: Environmental constraints on the production and removal of the climatically active gas dimethylsulphide (DMS) and implications for ecosystem modelling, Biogeochemistry, 83, 245-275, 2007.

Stickler, A., Fischer, H., Bozem, H., Gurk, C., Schiller, C., Martinez-Harder, M., Kubistin, D., Harder, H., Williams, J., Eerdekens, G., Yassaa, Y., Ganzeveld, L., Sander, R., and Lelieveld, J.: Chemistry, transport and dry deposition of trace gases in the boundary layer over the tropical Atlantic Ocean and the Guyanas during the GABRIEL field campaign, Atmospheric Chemistry and Physics 7, 3933-3956, 2007.

Stohl, A., Haimberger, L., Scheele, M. P., and Wernli, H.: An intercomparison of results from three trajectory models, Meteorological Applications, 8, 127-135, 2001.

Stolarski, R. S., and Cicerone, R. J.: Stratospheric Chlorine: a Possible Sink for Ozone, Canadian Journal of Chemistry, 52, 1610-1615, 1974.

Sturges, W. T., Cota, G. F., and Buckley, P. T.: Bromoform Emission from Arctic Ice Algae, Nature, 358, 660-662, 1992.

Sturges, W. T., McIntyre, H. P., Penkett, S. A., Chappellaz, J., Barnola, J. M., Mulvaney, R., Atlas, E., and Stroud, V.: Methyl bromide, other brominated methanes, and

methyl iodide in polar firn air, Journal of Geophysical Research-Atmospheres, 106, 1595-1606, 2001.

Tait, V. K., and Moore, R. M.: Methyl-Chloride (CH_3Cl) Production in Phytoplankton Cultures, Limnology and Oceanography, 40, 189-195, 1995.

Teh, Y. A., Rhew, R. C., Atwood, A., and Abel, T.: Water, temperature, and vegetation regulation of methyl chloride and methyl bromide fluxes from a shortgrass steppe ecosystem, Global Change Biology, 14, 77-91, 2008.

Thompson, T. M., Butler, J. H., Daube, B. C., Dutton, G. S., Elkins, J. W., Hall, B. D., Hurst, D. F., King, D. B., Kline, E. S., LaFleur, B. G., Lind, J., Lovitz, S., Mondeel, D. J., Montzka, S. A., Moore, F. L., Nance, J. D., Neu, J. L., Romashkin, P. A., Scheffer, A., and Snible, W. J.: Halocarbons and other atmospheric trace species, in *Climate Monitoring and Diagnostics Laboratory: Summary Report 27 2002-2003*, edited by R.C. Schnell, A.-M. Buggle and R.M. Rosson, 115-135, NOAA/Climate Monitoring and Diagnostics Laboratory, Boulder, Colo. Available: http://www.esrl.noaa.gov/gmd/publications/annrpt27/hats5.pdf, 2004.

Tokarczyk, R., and Moore, R. M.: Production of Volatile Organohalogens by Phytoplankton Cultures, Geophysical Research Letters, 21, 285-288, 1994.

Trigo, R. M., Pereira, J. M. C., Pereira, M. G., Mota, B., Calado, T. J., Dacamara, C. C., and Santo, F. E.: Atmospheric conditions associated with the exceptional fire season of 2003 in Portugal, International Journal of Climatology, 26, 1741-1757, 2006.

Trudinger, C. M., Etheridge, D. M., Sturrock, G. A., Fraser, P. J., Krummel, P. B., and McCulloch, A.: Atmospheric histories of halocarbons from analysis of Antarctic firn air: Methyl bromide, methyl chloride, chloroform, and dichloromethane, Journal of Geophysical Research-Atmospheres, 109, doi:10.1029/2004JD004932, 2004.

Urhahn, T., and Ballschmiter, K.: Chemistry of the biosynthesis of halogenated methanes: C_1-Organohalogens as pre-industrial chemical stressors in the environment?, Chemosphere, 37, 1017-1032, 1998.

Vallina, S. M., and Simo, R.: Strong relationship between DMS and the solar radiation dose over the global surface ocean, Science, 315, 506-508, 2007.

Vallina, S. M., Simo, R., and Gasso, S.: What controls CCN seasonality in the Southern Ocean? A statistical analysis based on satellite-derived chlorophyll and CCN and model-estimated OH radical and rainfall, Global Biogeochemical Cycles, 20, 13, 2006.

Varner, R. K., Crill, P. M., and Talbot, R. W.: Wetlands: a potentially significant source of atmospheric methyl bromide and methyl chloride, Geophysical Research Letters, 26, 2433-2435, 1999.

Vogt, R., Crutzen, P. J., and Sander, R.: A mechanism for halogen release from sea-salt aerosol in the remote marine boundary layer, Nature, 383, 327-330, 1996.

von Glasow, R.: Atmospheric chemistry: Pollution meets sea salt, Nature Geosci, 1, 292-293, 2008a.

von Glasow, R.: Atmospheric chemistry: Sun, sea and ozone destruction, Nature, 453, 1195-1196, 2008b.

von Glasow, R., and Crutzen, P. J.: Tropospheric Halogen Chemistry, in: Treatise on Geochemistry Update 1, edited by: Holland, H. D., and Turekian, K. K., Elsevier Ltd., 1-67, 2007.

von Glasow, R., von Kuhlmann, R., Lawrence, M. G., Platt, U., and Crutzen, P. J.: Impact of reactive bromine chemistry in the troposphere, Atmospheric Chemistry and Physics, 4, 2481-2497, 2004.

Wang, J. X., Li, R. J., Guo, Y. Y., Qin, P., and Sun, S. C.: The flux of methyl chloride along an elevational gradient of a coastal salt marsh, Eastern China, Atmospheric Environment, 40, 6592-6605, 2006.

Wanninkhof, R.: Relationship between Wind Speed and Gas Exchange over the Ocean, Journal of Geophysical Research-Oceans, 97, 7373-7382, 1992.

Warwick, N. J., Pyle, J. A., and Shallcross, D. E.: Global modelling of the atmospheric methyl bromide budget, Journal of Atmospheric Chemistry, 54, 133-159, 2006.

Watling, R., and Harper, D. B.: Chloromethane production by wood-rotting fungi and an estimate of the global flux to the atmosphere, Mycological Research, 102, 769-787, 1998.

Wernli, H., and Davies, H. C.: A Lagrangian-based analysis of extratropical cyclones. I: The method and some applications, Quarterly Journal of the Royal Meteorological Society, 123, 467-489, 1997.

Wever, R., Tromp, M. G. M., Krenn, B. E., Marjani, A., and Vantol, M.: Brominating Activity of the Seaweed Ascophyllum-Nodosum - Impact on the Biosphere, Environmental Science & Technology, 25, 446-449, 1991.

White, R. H.: Analysis of Dimethyl Sulfonium Compounds in Marine Algae, Journal of Marine Research, 40, 529-536, 1982.

WHO: Health Aspect of Air Pollution with Particulate Matter, Ozone and Nitrogen Dioxide, World Health Organization, Bonn, 2003.

Williams, J., Gros, V., Atlas, E., Maciejczyk, K., Batsaikhan, A., Scholer, H. F., Forster, C., Quack, B., Yassaa, N., Sander, R., and Van Dingenen, R.: Possible evidence for a connection between methyl iodide emissions and Saharan dust, Journal of Geophysical Research-Atmospheres, 112, 2007a.

Williams, J., Yassaa, N., Bartenbach, S., and Lelieveld, J.: Mirror image hydrocarbons from Tropical and Boreal forests, Atmospheric Chemistry and Physics, 7, 973-980, 2007b.

Wingenter, O. W., Haase, K. B., Strutton, P., Friedrich, G., Meinardi, S., Blake, D. R., and Rowland, F. S.: Changing concentrations of CO, CH_4, C_5H_8, CH_3Br, CH_3I, and dimethyl sulphide during the Southern Ocean Iron Enrichment Experinments, Proceedings of the national acadamy of sciences of the United States of America, 101, 8537-8541, 2004.

Wingenter, O. W., Kubo, M. K., Blake, N. J., Smith, T. W., Blake, D. R., and Rowland, F. S.: Hydrocarbon and halocarbon measurements as photochemical and dynamical indicators of atmospheric hydroxyl, atomic chlorine, and vertical mixing obtained during Lagrangian flights, Journal of Geophysical Research-Atmospheres, 101, 4331-4340, 1996.

Wingenter, O. W., Wang, C. J. L., Blake, D. R., and Rowland, F. S.: Seasonal variation of tropospheric methyl bromide concentrations: Constraints on anthropogenic input, Geophysical Research Letters, 25, 2797-2800, 1998.

Wishkerman, A., Gebhardt, S., McRoberts, C. W., Hamilton, J. T. G., Williams, J., and Keppler, F.: Abiotic methyl bromide formation from vegetation and its strong dependence on temperature, Environ. Sci. Technol., DOI:10.1021/es800411j, 2008.

WMO: Scientific Assessment of Ozone Depletion: 1998, Chapter 2: Short-Lived Ozone-Related Compounds, Global Ozone Research and Monitoring Project - Report No. 44, World Meteorological Organization, Geneva, Switzerland, 2.1-2.56, 1999.

WMO: Scientific Assessment of Ozone Depletion: 2002, Chapter 1: Controlled Substances and Other Source Gases, Global Ozone Research and Monitoring Project - Report No. 47, World Meteorological Organization, Geneva, Switzerland, 1.1-1.83, 2003a.

WMO: Scientific Assessment of Ozone Depletion: 2002, Chapter 2: Very Short-Lived Halogen and Sulfur Substances, Global Ozone Research and Monitoring Project - Report No. 47 World Meteorological Organization, Geneva, Switzerland, 2.1-2.57, 2003b.

WMO: Scientific Assessment of Ozone Depletion: 2006, Chapter 1: Long-Lived Compounds, Global Ozone Research and Monitoring Project - Report No. 50, World Meteorological Organization, Geneva, Switzerland 1.1-1.63, 2007a.

WMO: Scientific Assessment of Ozone Depletion: 2006, Chapter 2: Halogenated Very Short-Lived Substances, Global Ozone Research and Monitoring Project - Report No. 50, World Meteorological Organization, Geneva, Switzerland, 2.1-2.57, 2007b.

WMO: Scientific Assessment of Ozone Depletion: 2006, Chapter 8: Halocarbon Scenarios, ODPs ans GWPs, Global Ozone Research and Monitoring Project - Report No. 50, World Meteorological Organization, Geneva, Switzerland, 8.1-8.39, 2007c.

WMO: Scientific Assessment of Ozone Depletion: 2006, Twenty questions and answers about the ozone layer: 2006 update, Global Ozone Research and Monitoring Project - Report No. 50, World Meteorological Organization, Geneva, Switzerland, Q.1 - Q.46, 2007d.

Wofsy, S. C., McElroy, M. B., and Yung, Y. L.: Chemistry of Atmospheric Bromine, Geophysical Research Letters, 2, 215-218, 1975.

Worton, D. R., Sturges, W. T., Schwander, J., Mulvaney, R., Barnola, J. M., and Chappellaz, J.: 20th century trends and budget implications of chloroform and related tri-and dihalomethanes inferred from firn air, Atmospheric Chemistry and Physics, 6, 2847-2863, 2006.

Wuosmaa, A. M., and Hager, L. P.: Methyl-Chloride Transferase - a Carbocation Route for Biosynthesis of Halometabolites, Science, 249, 160-162, 1990.

Yang, X., Cox, R. A., Warwick, N. J., Pyle, J. A., Carver, G. D., O'Connor, F. M., and Savage, N. H.: Tropospheric bromine chemistry and its impacts on ozone: A model study, Journal of Geophysical Research-Atmospheres, 110, 2005.

Yokouchi, Y., Hasebe, F., Fujiwara, M., Takashima, H., Shiotani, M., Nishi, N., Kanaya, Y., Hashimoto, S., Fraser, P., Toom-Sauntry, D., Mukai, H., and Nojiri, Y.: Correlations and emission ratios among bromoform, dibromochloromethane, and dibromomethane in the atmosphere, Journal of Geophysical Research-Atmospheres, 110, 2005.

Yokouchi, Y., Ikeda, M., Inuzuka, Y., and Yukawa, T.: Strong emission of methyl chloride from tropical plants, Nature, 416, 163-165, 2002.

Yokouchi, Y., Noijiri, Y., Barrie, L. A., Toom-Sauntry, D., Machida, T., Inuzuka, Y., Akimoto, H., Li, H. J., Fujinuma, Y., and Aoki, S.: A strong source of methyl chloride to the atmosphere from tropical coastal land, Nature, 403, 295-298, 2000.

Yokouchi, Y., Nojiri, Y., Barrie, L. A., Toom-Sauntry, D., and Fujinuma, Y.: Atmospheric methyl iodide: High correlation with surface seawater temperature and its implications on the sea-to-air flux, Journal of Geophysical Research-Atmospheres, 106, 12661-12668, 2001.

Yokouchi, Y., Saito, T., Ishigaki, C., and Aramoto, M.: Identification of methyl chloride-emitting plants and atmospheric measurements on a subtropical island, Chemosphere, 69, 549-553, 2007.

Yoshida, Y., Wang, Y., Shim, C., Cunnold, D., Blake, D. R., and Dutton, G. S.: Inverse modeling of the global methyl chloride sources, Journal of Geophysical Research, 111, doi:10.1029/2005JD006696, 2006.

Yoshida, Y., Wang, Y. H., Zeng, T., and Yantosca, R.: A three-dimensional global model study of atmospheric methyl chloride budget and distributions, Journal of Geophysical Research-Atmospheres, 109, doi:10.1029/2004JD004951, 2004.

Yuita, K.: Overview and Dynamics of Iodine and Bromine in the Environment I Dynamics of Iodine and Bromine in Soil-Plant System, Jarq-Japan Agricultural Research Quarterly, 28, 90-99, 1994.

Zafiriou, O. C.: Reaction of Methyl Halides with Seawater and Marine Aerosols, Journal of Marine Research, 33, 75-81, 1975.

Zhou, Y., Mao, H., Russo, R. S., Blake, D., Wingenter, O., Haase, K. B. A., J., Varner, R. K., Talbot, R., and Sive, B. C.: Bromoform and dibromomethane measurements in the seacoast region of New Hampshire, 2002-2004, Journal of Geophysical Research-Atmospheres, 113, D 08305, 2008.

Zorn, S. R., Drewnick, F., Schott, M., Hoffmann, T., and Borrmann, S.: Characterization of the South Atlantic marine boundary layer aerosol using an Aerodyne Aerosol Mass Spectrometer, Atmospheric Chemistry and Physics Discussion, 8, 4831-4876, 2008.